Treatment of Substitution and Rearrangement Mechanisms of Transition Metal Complexes with Quantum Chemical Methods

François P. Rotzinger*

Institut des Sciences et Ingénierie Chimiques, Ecole Polytechnique Fédérale de Lausanne (EPFL), Station 6, CH-1015 Lausanne, Switzerland

Received September 3, 2004

Contents

François P. Rotzinger is lecturer (Privat-Docent) at the Institut des Sciences et Ingénierie Chimiques of the Ecole Polytechnique Fédérale de Lausanne (EPFL) in Switzerland. He received his diploma in chemistry in 1976 and his Ph.D. degree and the silver medal award in 1980 from the Eidgenössische Technische Hochschule Zürich (ETHZ) in Switzerland. He was a postdoctoral fellow with Professor John F. Endicott at Wayne State University, Detroit (USA), from 1981 to 1982, and with Professor Werner Marty at the Université de Neuchâtel in Switzerland, from 1982 to 1984. Since 1984, he has been a researcher at the Ecole Polytechnique Fédérale de Lausanne (EPFL), where he got his Habilitation in 1994. His research interests include molecular quantum chemical computations of chemical reactions and spectroscopic properties.

1. Introduction

The detailed understanding of chemical reactions still represents a major challenge for experimental as well as theoretical chemists. The enormous progress in both hard- and software allows computations on metal complexes at a sufficiently accurate level to investigate their reactions in solution. The present review focuses on substitution and rearrangement reactions in solution, for which an impressive amount of experimental data is available.[1−7] To limit the extent of the present article, photochemical reactions, redox processes, reactions involving organometallic compounds, being of fundamental importance in catalysis, and classical molecular dynamics simulations, having a limited applicability for transition metal complexes, are not discussed. Reactions in the gas phase and biological or biomimetic systems are not treated either.

The accuracy and the reliability of quantum chemical computations on reaction mechanisms and the conclusions drawn thereof are analyzed. The strengths and limitations of the currently used chemical models and computational techniques are illustrated. Reactivity−electronic structure relationships are presented, whereby the role of the electron configuration of the transition metal ion on the steric course of the reaction and its mechanism is shown.

* E-mail, francois.rotzinger@epfl.ch; fax, ++41 21 693 41 11.

10.1021/cr030715v CCC: $53.50 © 2005 American Chemical Society
Published on Web 04/28/2005

All of the quantum chemical calculations on substitution and rearrangement reactions, published up to the end of June 2004 are included in this review article.

2. Strengths and Limitations of the Current Computational Techniques

Today, two techniques are used for the modeling of reaction mechanisms: (i) molecular dynamics (MD) simulations allowing in principle the treatment of the entire system, the solute and the solvent, and (ii) quantum chemical calculations on clusters involving the reactants, transition states, and intermediates, whereby the bulk solvent is treated usually with continuum models.[8,9] Both techniques have their strengths and limitations. Today, a substitution reaction of a pseudo-octahedral transition metal complex, for example, cannot be modeled "exactly". A survey of classical and quantum chemical methods and their underlying theories was published recently by Erras-Hanauer, Clark, and van Eldik.[9] For a given problem or question, the challenge is to select a method or a combination of methods that produces reliable results.

Electron transfer, rearrangement, or substitution reactions involving transition metal complexes require that the solute is treated with ab initio molecular orbital (MO) methods or density functional theory (DFT). Criteria for the choice of adequate computational techniques and basis sets have been presented in a recent article.[10] Published calculations on reaction mechanisms, and the conclusions based thereon, are analyzed in this review. It will be shown that results and conclusions depend on the computational technique in a more sensitive manner than assumed commonly. The currently applied methods, Hartree−Fock (HF), second-order perturbation theory according to Møller and Plesset (MP2), complete active space self-consistent field (CAS-SCF), and density functional theory (DFT), based on the local density approximation (LDA) or gradient corrected or hybrid functionals, can produce considerably different results for given compounds.[10] Thus, the computational techniques have to be chosen with thought, such that the properties of interest are obtained with the required reliability. Finally, it should be noted that inaccuracies may also arise from too small or unsaturated basis sets.

2.1. Molecular Dynamics (MD) Simulations

The strength of MD simulations is that the solute and the solvent are modeled at finite temperature and that the pathway with the lowest activation free energy ($\Delta G^{\ddagger}$) is sampled. Thermodynamic activation parameters such as $\Delta G^{\ddagger}$, the enthalpy ($\Delta H^{\ddagger}$), or the entropy ($\Delta S^{\ddagger}$) could be computed, but in practice, this is prohibitive today because either (i) a large number of events must be simulated at various temperatures or (ii) free energy profiles must be computed via constrained optimizations at various temperatures, whereby, for each point, the system must be simulated to reach equilibrium.

The system to be computed is very large because of the many solvent molecules, typically at least 500, that are required to avoid artifacts arising from solute−solute interactions. Thus, as limitations, simplifications have to be made to lower the computational labor. In classical MD, the interactions are treated with empirical potentials, on which the result might depend critically. The calculation of the coordination number of the Li^+ ion in aqueous solution is such an illustrative example: with classical MD simulations, coordination numbers of 4−6 have been reported.[11]

An improvement of classical MD simulations is achieved by the treatment of the solute with quantum mechanical (QM) methods, whereby the solvent is modeled classically using molecular mechanics (MM). In such QM/MM approaches, there are approximations for the QM−MM interface and for the MM solvent (as in classical MD). The QM part is usually treated with density functional theory (DFT) or the Hartree−Fock (HF) method, but it is possible to treat electron correlation at a higher level. The effective fragment potential (EFP) method,[12,13] also a QM/MM technique, is described in the next section.

The Car−Parrinello molecular dynamics (CPMD) method[14] is an elegant and popular technique to perform ab initio MD (AIMD) simulations on the basis of DFT. It inherits the approximations and drawbacks of DFT, the nonexact exchange-correlation functional, the approximate treatment of electron correlation, and the inability to describe degenerate, nearly degenerate, or excited electronic states. Its strength is that the entire system, the solute as well as the solvent, is treated quantum chemically, but the size of the system has to be kept relatively small. Today, a metal ion with typically about 50 water molecules is investigated. Another drawback might be the treatment of the counterion as a uniform background charge in periodically repeated systems. Furthermore, only short simulation times, at most about 20 ps, are feasible today. For reactions with high activation barriers, which would require prohibitively long simulation times, the events of interest can be investigated using constrained CPMD.[15,16]

2.2. Cluster Models

In general, the cluster is composed of the reactants and a small number of solvent molecules, typically those being strongly bound to any of the species on the reaction pathway. The smallest possible cluster is composed of the free reactants. For a substitution reaction, for example, this would be the reactant metal complex and the entering ligand. The cluster can be augmented by the addition of strongly bound solvent molecules, for example, those in the second coordination sphere.

The strength of the cluster model (CM) is that "exact" geometries (within the limitations of the model) of the reactants, transition states, intermediates, and products can be computed for a mechanistic pathway of interest, independent of the reactivity of the system. It should be remembered that, currently, MD simulations are feasible for extremely fast reactions only.[8,9] With the CM, any desired pathway can be investigated in a straightforward manner on the basis of MO methods or DFT, whereby systematic

improvements of the computational method, in particular, the treatment of electron correlation, and the basis sets are feasible. If appropriate, computations may also be performed at a semiempirical level. Studies on complex electronic structures and excited states are possible. The solvent can be treated approximately with self-consistent reaction fields (SCRFs),[17−19] the polarizable continuum model (PCM),[20] or the conductor-like screening model (COSMO).[21] Instead of using a continuum model, the solvent molecules can be calculated classically using empirical force fields or the effective fragment potential (EFP) method,[12,13] in which each solvent molecule is described as a fragment with a fixed geometry and potential for interacting with the quantum chemically described solute and the other solvent molecules. The EFP-based QM/MM technique is described in this section because such computations are usually done with a small number of solvent molecules, typically those interacting strongly with the solute. Alternatively, the strongly bound solvent molecules can also be treated quantum chemically, eventually with a smaller basis set. The CM has an excellent expense-to-yield ratio.

With the CM, the treatment of solvation can be improved systematically, and this allows the assessment of the effect of solvation on the property of interest. Ideally, the description of the solvent should be improved incrementally and systematically, until the calculations converge toward the experimental data. This principle was applied in a QM/MM study on $UO_2F_4(OH_2)^{2-}$.[22]

As drawbacks of the CM, the solvent is not treated at a quantum chemical level, and the geometries are optimized at 0 K without consideration of the zero point energy (ZPE), the finite temperature effects, and the entropy, although these corrections can be added subsequently. The thus calculated geometries might differ from those that would be obtained by minimizing $\Delta G^{\ddagger}$ at room temperature, for example. If the geometry at 0 K is significantly different from that based on $\Delta G^{\ddagger}$ at finite temperature, the total energy, the ZPE, the thermal corrections, and the entropy derived from the 0 K geometry may differ considerably from the real values. It just should be remembered that this could be a reason for deviations from experimental data.

The primary result of CM calculations is a total energy difference at 0 K between the reactant(s) and the transition state ($\Delta E^{\ddagger}$) or the reactant(s) and the product(s) or the intermediate (ΔE). Zero point energies (ZPEs), thermal corrections, and entropy terms are not included in $\Delta E^{\ddagger}$ and ΔE. Often, $\Delta E^{\ddagger}/\Delta E$ is used as an *approximation* of $\Delta H^{\ddagger}/\Delta H$ or $\Delta G^{\ddagger}/\Delta G$. Thermodynamic parameters ($\Delta H^{\ddagger}/\Delta H$, $\Delta G^{\ddagger}/\Delta G$, $\Delta S^{\ddagger}/\Delta S$) are available from frequency computations: they are expected to be close to the experimental data, if the solute−solvent interactions are negligible compared with the ZPE and the thermal corrections, and in cases where the solute−solvent contributions cancel *fortuitously*. In metal aqua ions, especially those with a 2+ or a 3+ charge, for example, such interactions, in particular those due to the H-bonds between the first and the second coordination spheres, are strong and non-negligible. Therefore, $\Delta H^{\ddagger}/\Delta H$, $\Delta G^{\ddagger}/\Delta G$, and $\Delta S^{\ddagger}/\Delta S$ data, calculated on the basis of models involving solely the first coordination sphere, cannot be expected to be more reliable than the (approximate) $\Delta E^{\ddagger}/\Delta E$ values. This is the reason why, for such systems, the thermochemical parameters are usually not reported, although they are available from the computed Hessians. For the calculation of thermochemical data, the strongly interacting solvent molecules have to be included into the quantum chemically described cluster. For the remaining weakly interacting solvent, continuum models are appropriate. Furthermore, it should be noted that possibly also the solvent−solvent interactions in proximity of the solute, in the second coordination sphere, for example, might be different from those in the bulk.

2.3. Quantum Chemical Methods

In many cases, quantum chemical calculations on the solute alone are already a demanding task requiring appreciable computational resources. This obliges chemists to make approximations in the treatment of electron correlation and to choose basis sets of a limited size. All of these approximations have to be made with thought, and their consequences should be assessed on well-characterized representative systems. For *transition metal aqua ions*, these problems have been investigated systematically,[10] and the most important findings are presented in the following.

Of utmost importance is the adequate treatment of electron correlation. Thus, in a first step, its nature, only dynamic or static *and* dynamic, has to be determined. This can be done with multireference singles−doubles configuration interaction (MR-SDCI) or, more efficiently, with the recently developed occupation-restricted multiple active space (ORMAS) configuration interaction (CI) method[24] of Ivanic, whereby, in general, the systems are too large to be treated in a single CI calculation. In such cases, the iterative natural orbital method[25] has to be applied. From the population of the natural orbitals (NOs), it can be seen if static electron correlation is present. If so, the NO occupations of the MR-SDCI or ORMAS-CI calculations serve as a basis for the determination of the active space of the CAS-SCF wave function, and the properties can be evaluated with second-order perturbation theories based on CAS-SCF, for example, CASPT2[26,27] or MCQDPT2,[28,29] that take into account static as well as dynamic correlation. If static correlation is absent, MP2 is adequate; today, calculations at higher levels are usually prohibitive for transition metal complexes. In certain cases, simpler methods might also produce correct results due to a cancellation of errors, but the validity of approximate, less demanding methods always needs to be assessed via the comparison with an accurate method.

The computationally fast HF calculations yield reasonable geometries, especially for the H-bonds, and energies of aqua ions with a 2+ and a 3+ charge. If the total energies for different coordination numbers are compared, a slight preference for the higher

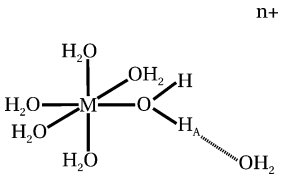

Figure 1. Schematic representation of the water adduct $M(OH_2)_6 \cdot OH_2^{n+}$ exhibiting a single H-bond ($H_A \cdots O$).

number (of about 15−20 kJ/mol) is obtained. For transition metal centers with electron rich subshells, for example, $Cu(OH_2)_2^+$ with a filled 3d shell or η^6-$(C_6H_6)Ru(OH_2)_3^{2+}$ with a filled $4d_\pi$ ("t_{2g}") shell, too long metal−ligand bonds are obtained at the HF level. For these systems, DFT produces significantly better geometries. With HF, metal−oxo bonds, as for example in $VO(OH_2)_5^{2+}$, are too short by at least ~ 0.05 Å due to the neglect of static electron correlation, which arises from the population of σ^*(V=O) and π^*(V=O) MOs by σ(V=O) and π(V=O) electrons. In contrast, with DFT, the H-bonds of aqua ions exhibiting a 3+ charge might be quite unreliable. In $M(OH_2)_6 \cdot OH_2^{3+}$ complexes, in which the water molecule in the second coordination sphere forms a single H-bond to the first sphere (Figure 1), the proton on the water of the first sphere (H_A) is transferred to the water in the second sphere, yielding $M(OH_2)_5OH \cdot H_3O^{3+}$ species. This observation is in line with the known[30,31] limitations of DFT for the treatment of H-bonding and proton transfer reactions. With HF, CAS-SCF, and MCQDPT2, however, the geometries of both species, $M(OH_2)_6 \cdot OH_2^{3+}$ and $M(OH_2)_5OH \cdot H_3O^{3+}$, can be obtained. The currently used functionals may yield incorrect relative strengths (lengths) of weak metal−ligand bonds and H-bonds (which are present in transition states, for example). On the basis of DFT energies, the lower coordination number is preferred for 2+ and 3+ ions (for example, by about 15−75 kJ/mol for BLYP). Consequently, DFT favors also the dissociative (***D/I_d***) substitution mechanisms over the associative ones (***A/I_a***). It is important to note that these limitations are also valid for ab initio molecular dynamics (AIMD) simulations that are based on DFT.

Geometries of complexes with a small permanent dipole moment and neutral ligands can be calculated as free ions (in the gas phase) with an acceptable accuracy.[23,32] If the complex exhibits a sizable permanent dipole moment, that usually arises from the presence of negatively charged ligands, the gas-phase geometries differ considerably from those of the solvated species.[33,34] For such compounds, solvation has to be included for both the geometry optimization and the energy computation, whereby geometry and energy may be computed with different methods.

In certain cases, as in the H-bonding of high-valent aqua ions with H_2O in the second coordination sphere, there are specific and quite strong solute−solvent interactions and, possibly, in the second coordination sphere, also solvent−solvent interactions that differ considerably from those in the bulk. Then, the continuum models cannot be expected to reproduce all of the properties accurately. Such examples are the unavailability of reliable activation entropies for water exchange reactions of transition

Scheme 1. *D* Mechanism

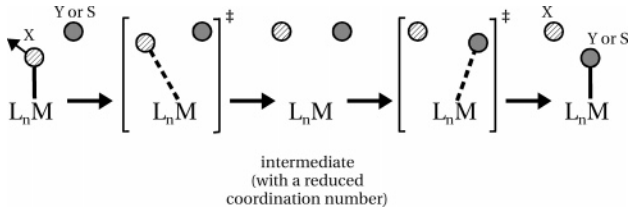

metal hexaaqua ions on the basis of the CM with six or seven H_2O molecules,[23] and inaccurate internal reorganizational energies of electron self-exchange reactions of $V(OH_2)_6^{2+/3+}$, $V(OH_2)_6^{3+/4+}$, $Ru(OH_2)_6^{2+/3+}$, and $Ru(OH_2)_6^{3+/4+}$ couples.[35]

The choice of the basis set is an issue to which, in many studies, the due attention has not been paid. Most of the basis sets for the transition metals were obtained via the optimization of the total energy for the ground state of the neutral atom. In complexes, the electronic state as well as the oxidation state is different from that in the atom. Thus, for an adequate description of the metal center in complexes, it is usually necessary to modify the basis set by adding, for example, d, s, and p functions and/or by uncontracting functions. The unmodified atomic all-electron basis sets of transition metals often give rise to a large basis set superposition error (BSSE), especially when the basis sets of the ligands contain diffuse functions. For basis sets exhibiting effective core potentials (ECPs), the BSSE is much smaller. In practice, the BSSE should be computed for representative compounds, and the basis sets of the metal and the ligands should be modified in order to obtain a small BSSE. It should be noted that a large BSSE can lead, for example, to poor geometries and reaction or activation energies.

The use of too small basis sets on ligand atoms is another source for inaccurate geometries and energies. While polarization functions should be and indeed are used, in general, for second row elements, they are not always absolutely required for first row elements. However, the basis sets of first row elements involved in π bonds or carrying a negative charge have to be supplemented with polarization functions. If, furthermore, anion diffuse functions are required, the basis set of the metal must possibly be adapted to ensure a small BSSE.

As will be shown in the Computational Studies on Reaction Mechanisms section (section 4), quite a few uncertain or incorrect conclusions in the literature are due to the disregard of the above-described criteria for the selection of adequate computational methods and basis sets.

3. Classification of Substitution Mechanisms

3.1. Experimental Criteria

The first classification of substitution mechanisms was proposed by Langford and Gray[36] in 1965. It is based on the detectability of an intermediate formed along the substitution process. In the dissociative (***D***) mechanism (Scheme 1; the charges are omitted for clarity), a ligand (X) is lost from the reactant (L_nMX), leading to an intermediate with a reduced coordina-

Scheme 2. *A* Mechanism

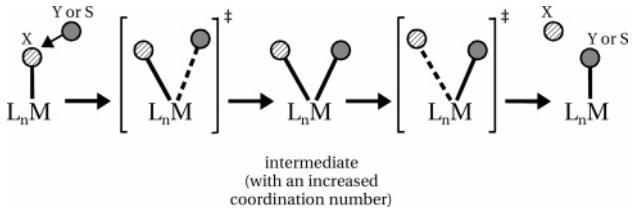

Scheme 3. I_a, *I*, or I_d Mechanism

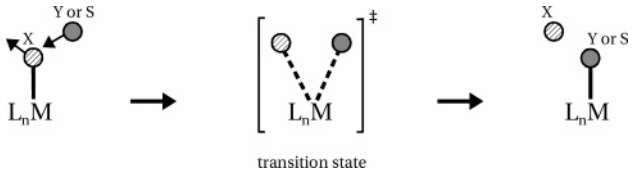

tion number (L_nM). Subsequently, this intermediate reacts with a nucleophile (Y) or a solvent molecule (S) to form the products (L_nMY and L_nMS).

In the associative (***A***) mechanism (Scheme 2), the nucleophile (Y) or a solvent molecule (S) enters the coordination sphere of the reactant (L_nMX), leading to intermediates with an increased coordination number (L_nMXY and L_nMXS), from which the leaving group (X) is lost in a subsequent step.

The ***A*** and ***D*** mechanisms proceed in two steps and involve intermediates with an increased or a decreased coordination number, respectively. Their classification, according to Langford and Gray,[36] is based on experimental evidence for their existence. If the experimental detection of intermediates is not possible, an interchange mechanism (Scheme 3) operates, in which formation of the bond with the entering ligand (Y or S) is concerted with weakening of the bond of the leaving group (X).

In the transition state both the leaving and the entering ligands are bound weakly. If bond formation is more pronounced than bond breaking, the mechanism is called associative interchange ($\boldsymbol{I_a}$), if bond breaking dominates, the dissociative interchange ($\boldsymbol{I_d}$) mechanism operates, and in the interchange (***I***) mechanism, bond formation and breaking occur to the same extent.

The problem with this classification is that the detection of intermediates is a very difficult task, for they are very short-lived and present at extremely low concentrations. Furthermore, the evidence for their existence is indirect. In a few cases, the ***D*** mechanism has been established via experimental evidence for pentacoordinated intermediates. For the ***A*** mechanism, this has not been achieved thus far. In the following, the experiments that supply sound evidence for the existence or the nonexistence of pentacoordinated intermediates are reviewed briefly. These examples are presented because, in almost all substitution reactions, the question whether the stepwise or the concerted mechanism operates is open, although the activation mode, dissociative or associative, is known.

For substitutions on $Fe(CN)_5X^{n-}$ complexes, evidence for the ***D*** mechanism was obtained directly from the rate law.[37−39] In general, however, the rate law does not supply this information. The base hydrolysis of amine complexes of cobalt(III) has been studied extensively during about half of the last century[40] and continues to be investigated[41] with the aim of substantiating the presence or absence of pentacoordinated intermediates in the course of this reaction. To this end, two techniques were used. With the first one, the selectivity of the intermediate toward various nucleophiles and the solvent was measured, and with the second approach, the structure and the site of deprotonation of the pentacoordinated intermediate were probed via reactant−product stereochemistry relationships.

The charge of an intermediate can be determined via the measurement of the product ratio ($[L_nMY]/[L_nMS]$) at variable ionic strength, if the nucleophile (Y) is an anion (the solvent, S, is water).[42−44] The lifetime of the intermediate can be estimated in comparison with the time required for the equilibration of its ion-aggregates with the nucleophile. If the leaving group (X) is charged, a putative pentacoordinated intermediate will have a higher charge than the reactant (which is deprotonated in base hydrolysis reactions), and its ion-aggregation equilibria could be re-established during its lifetime. For the base hydrolysis of $Co(NH_3)_5X^{n+}$ (X = DMSO, NO_3^-, SO_4^{2-}) complexes in the presence of azide as the nucleophile, hexacoordinated intermediates $Co(NH_2)(NH_3)_4X^{(n-1)+}$ (most likely the cis isomer, exhibiting a triplet electronic state and an elongated Co−X bond[45]) are likely to be formed. Their lifetime is longer than that of their ion-aggregation equilibria.[43] Thus, base hydrolysis of $Co(NH_3)_5X^{n+}$ complexes proceeds in two steps, whereby the ligand substitution process occurs at the hexacoordinated intermediate exhibiting a weak Co−X bond. Its substitution mechanism is not known, but it is most likely dissociative, either $\boldsymbol{I_d}$ or ***D***. In contrast, base hydrolysis of $Co(NH_2CH_3)_5X^{n+}$ (X = DMF, Cl^-) complexes leads to a pentacoordinated intermediate $Co(NHCH_3)(NH_2CH_3)_4^{2+}$, whose lifetime is comparable to that of its ion-aggregation equilibria with the nucleophile (azide).[44] This reaction proceeds via the ***D*** mechanism. In both cases, protonation of the amido ligand takes place concerted with or subsequent to product formation.

The alternative way of probing the pentacoordinated intermediate in the course of the base hydrolysis reaction is based on the analysis of reactant−product stereochemistry relationships. Thus, for the base hydrolysis of Co(*mer*-triamine)(diamine)X^{n+} complexes, evidence for the existence of a pentacoordinated intermediate with a trigonal bipyramidal structure, in which the secondary nitrogen of the *mer*-triamine ligand is deprotonated, has been found.[41,46,47]

The above-described examples show that the proof for the existence of an intermediate is a demanding task which, thus far, has been achieved for the ***D*** mechanism only. Due to the lack of experimental evidence for intermediates, most of the substitution reactions would be assumed to follow the $\boldsymbol{I_a}$ or the $\boldsymbol{I_d}$ mechanism according to the criteria[36] of Langford and Gray.

As the activation volume ($\Delta V^{\ddagger}$) for solvent exchange reactions became available, Merbach[48] refined the

classification of substitution mechanisms in 1982. Currently, $\Delta V^{\ddagger}$ is considered to be composed of two terms: the intrinsic component ($\Delta V_{int}^{\ddagger}$), arising from changes in the first coordination sphere, and the electrostrictive one ($\Delta V_{el}^{\ddagger}$), being due to changes in the electrostriction of the solvent. For the exchange of coordinated solvent molecules, $\Delta V_{el}^{\ddagger}$ is often assumed to be negligible,[49] and therefore, the experimental $\Delta V^{\ddagger}$ is supposed to correspond approximatively to its intrinsic component ($\Delta V_{int}^{\ddagger}$). The latter is a straightforward criterion for the attribution of the activation mode:[48] $\Delta V^{\ddagger}$, or more precisely, $\Delta V_{int}^{\ddagger}$, is negative for an associative activation, positive for a dissociative activation, and zero for concerted reactions. For the limiting ***D*** mechanism, $\Delta V^{\ddagger}$ was suggested to be equal to the molar volume increase ($V_S°$) caused by the loss of a water ligand from the first coordination sphere of a hexaaqua ion, whereas, for the ***A*** mechanism, $\Delta V^{\ddagger}$ would be $-V_S°$.[48] $|V_S°|$ is approximately constant, independent of the charge of the metal ion, and amounts to 13.5 ± 1.0 cm^3/mol.[50,51] For the water exchange reaction on $Ti(OH_2)_6^{3+}$, an activation volume of −12.1 ± 0.4 cm^3/mol,[52] close to the limiting value proposed by Swaddle,[50,51] was measured, and it was interpreted to arise from the ***A*** or the "nearly ***A***" mechanism.

Also, these criteria for the classification of the limiting ***A*** and ***D*** mechanisms have their shortcomings because, in the *transition state* for ***A***, the bond with the entering ligand is formed only *partially*[53−55] and, furthermore, the other metal−ligand bonds are elongated to a small extent. Likewise, for ***D***, the bond of the leaving group is broken *partially*, and the other metal−ligand bonds are shortened slightly.[53−55] The limiting $\Delta V^{\ddagger}$ values of ∼13.5 and ∼ −13.5 cm^3/mol are *approximately* valid for the penta- and the heptacoordinated *intermediates*, respectively, but not for the corresponding *transition states*, on which the measured activation volumes are based. This means that $|\Delta V^{\ddagger}|$ is expected to be smaller than $|V_S°|$ because bond formation or bond rupture in the transition state is incomplete. Despite the currently available sophisticated experimental techniques, the attribution of reaction mechanisms, especially the limiting ***A*** and ***D*** cases, remains a difficult and challenging task.

3.2. Theoretical Criteria

The experimental difficulties in the characterization of intermediates called for the application of theoretical methods. Their use for the elucidation of water exchange mechanisms was reviewed by Helm and Merbach[8] and, recently, by Erras-Hanauer, Clark, and van Eldik,[9] who present an extensive description of the various models and computational methods.

In molecular dynamics (MD) simulations, based on empirical as well as quantum chemically calculated potentials (force fields), an intermediate is characterized as a species having a lifetime exceeding the duration of the vibration with which it decays. Typically, this is a metal−ligand stretching mode with frequencies in the range of about 200−500 cm^{-1}, and therefore, an intermediate must be a species with a lifetime of more than about 0.2 ps.

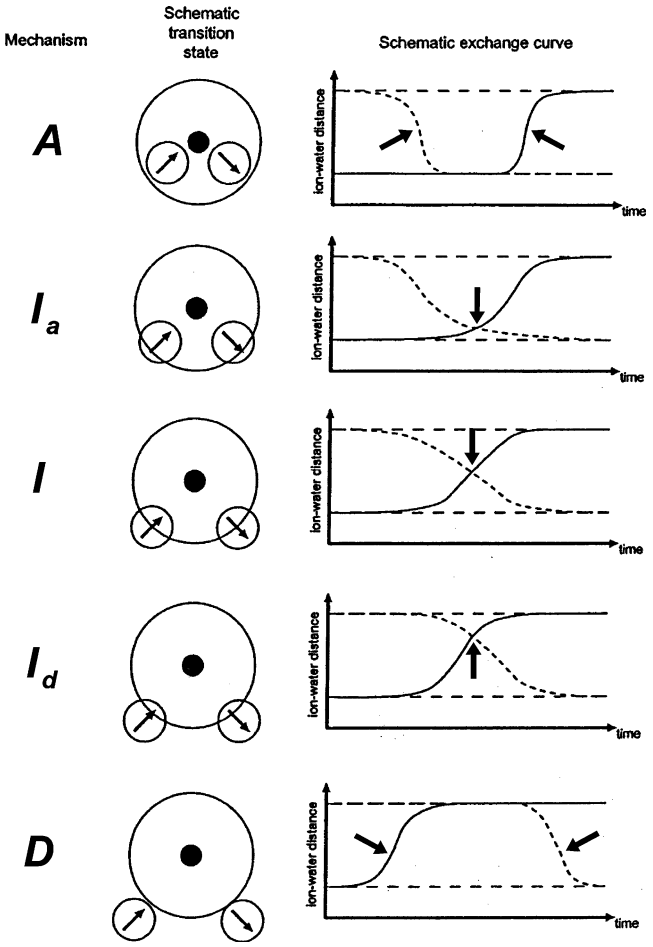

Figure 2. Structural definition of the five exchange processes: first column, exchange mechanism; second column, schematic illustration of the exchanges according to DuCommun and Merbach[56] (for the ***A*** and the ***D*** mechanisms, respectively, the sketches correspond to the hepta- and pentacoordinated intermediates); third column, ion−oxygen distances for ideal exchanges. The locations of transition states are marked with arrows. (Reprinted with permission from ref 11. Copyright 2003 American Chemical Society.)

The attribution of exchange mechanisms on the basis of MD simulations was illustrated by Spångberg et al.[11] (Figure 2). The five classes of mechanisms are given in the first column, a sketch of the transition state with the exchanging ligands[3,8,48,56] is reported in the second column, and in the third column are shown the ion−water distances for the first and second coordination spheres. It should be noted that the sketches for the ***A*** and the ***D*** mechanisms represent the intermediates and not the transition states. The stepwise mechanism operates only if the lifetime of the penta- or heptacoordinated intermediate exceeds ∼0.2 ps. For these two mechanisms, the transition states are located approximately at the inflection points of the ion−water distances (marked with arrows in Figure 2). The transition states for the interchange mechanisms $\boldsymbol{I_a}$, ***I***, and $\boldsymbol{I_d}$ are at the crossing points of the ion−water distances of the incoming and the leaving ligands (also marked with an arrow in Figure 2).

Computations based on the CM contain typically the reactant and the nucleophile. They can be per-

formed with density functional theory (DFT) or ab initio or semiempirical MO methods. A transition state is characterized by a single imaginary frequency in the computed vibrational spectrum, whereas, for an intermediate (as well as for the reactants and the products), all calculated frequencies must be real. Its lifetime can be estimated from the energy difference between the intermediate and its adjacent transition states. The imaginary normal mode represents the reaction coordinate (with which the transition state is formed or decays).

The classification of reaction mechanisms on the basis of computations is straightforward: for the limiting ***A*** or ***D*** mechanism, respectively, an intermediate with an increased or reduced coordination number and a sufficiently long lifetime ($\geq$0.2 ps) must exist. Otherwise, the reactant and the product are connected by a single transition state (or an intermediate with a chemically insignificant lifetime of less than $\sim$0.2 ps), and an interchange mechanism (***I***$_a$, ***I***, or ***I***$_d$) operates. The activation mode, associative (***I***$_a$), concerted (***I***), or dissociative (***I***$_d$), is determined mainly by the bond lengths of the entering and leaving groups in the transition state. One, although crude, qualitative criterion is based on the metal−ligand (M−L) bond length changes, $\Delta\sum_i d_i$(M−L), that take place during the activation process (eq 1).[53,54]

$$\Delta\sum_i d_i(\mathrm{M-L}) = \sum_i d_i(\mathrm{M-L})_{\mathrm{transitionstate}} - \sum_i d_i(\mathrm{M-L})_{\mathrm{reactant}} \quad (1)$$

$\sum_i d_i$(M−L)$_{\mathrm{transitionstate}}$ represents the sum of all metal−ligand bond lengths in the transition state, and $\sum_i d_i$(M−L)$_{\mathrm{reactant}}$ is the sum of the metal−ligand bond lengths in the reactant, whereby, for the ***I***$_d$, ***I***, ***I***$_a$, and ***A*** mechanisms, the distance of the entering nucleophile, located in the second coordination sphere, must be included. As a drawback of this model, $\Delta\sum_i d_i$(M−L) depends on the structure of the reactant−nucleophile adduct, for which several isomers exist (see section 4.2.1). For the thus far studied systems, the sign of $\Delta\sum_i d_i$(M−L), abbreviated as $\Delta\sum$, agrees with that of $\Delta V^{\ddagger}$. This gives a possibility to distinguish the ***I***$_a$ from the ***I***$_d$ mechanism.

Alternatively, $\Delta V^{\ddagger}$ or $\Delta V_{\mathrm{int}}{}^{\ddagger}$ was calculated directly on the basis of the Connolly[57] or PCM[20] volume change for the activation process (Schemes 1−3). $\Delta V^{\ddagger}$ for the water exchange on Al^{3+}, Ga^{3+}, and In^{3+} was computed[55] on the basis of the Connolly volume and a probe radius of 1.40 Å for solvent water. In an empirical approach, the volume of the hydrogen atoms of coordinated water was neglected, and the van der Waals radius of (coordinated) oxygen was scaled by a factor of 1.254 to reproduce the experimental $\Delta V^{\ddagger}$ for Al^{3+} and Ga^{3+}. Thus, for In^{3+}, $\Delta V^{\ddagger}$ values of 4.4 and −5.2 cm^3/mol were estimated for the ***D*** and ***A*** mechanisms, respectively. The same technique was also applied to the estimation of $\Delta V^{\ddagger}$ for the water exchange reaction on $Rh(OH_2)_6{}^{3+}$ and $Ir(OH_2)_6{}^{3+}$.[58]

For the water exchange reaction on $UO_2(OH_2)_5{}^{2+}$ and $UO_2(C_2O_4)OH_2{}^{2-}$,[59] $\Delta V_{\mathrm{int}}{}^{\ddagger}$ was calculated using CPCM volumes, whereby CPCM is the conductor-like version[60,61] of the polarizable continuum model (PCM).[20] For the ***A*** and ***D*** mechanisms, respectively, $\Delta V_{\mathrm{int}}{}^{\ddagger}$ values of −3.0 and +4.9 cm^3/mol were reported for $UO_2(OH_2)_5{}^{2+}$, and values of −6.3 and +4.6 or +4.1 cm^3/mol were reported for $UO_2(C_2O_4)_2OH_2{}^{2-}$. Since the corresponding experimental $\Delta V^{\ddagger}$ values are not available, the accuracy of these data cannot be assessed.

In a reinvestigation[62] of the water exchange reaction on $V(OH_2)_6{}^{2+}$ and $V(OH_2)_6{}^{3+}$ with DFT (B3LYP), $\Delta V_{\mathrm{int}}{}^{\ddagger}$ was computed on the basis of the PCM volumes. For $V(OH_2)_6{}^{2+}$, reacting via the ***I***$_a$ pathway, whereby the nucleophile enters cis to the leaving group, a questionable value for $\Delta V_{\mathrm{int}}{}^{\ddagger}$ of +0.1 cm^3/mol was found on the basis of an incorrect structure[10] for the transition state. For the ***A*** mechanism on $V(OH_2)_6{}^{3+}$, a value of −3.8 cm^3/mol was reported.[62] For exchange reactions, the electrostrictive component ($\Delta V_{\mathrm{el}}{}^{\ddagger}$) is expected to be negligible.[49] Therefore, the error in the calculated $\Delta V_{\mathrm{int}}{}^{\ddagger}$ values is large, greater than about 4 cm^3/mol, and possibly due to the solute−solvent and perhaps also the solvent−solvent interactions in proximity of the solute. These interactions are not taken into account by the CM with only seven water molecules.[23] The limitations of the CM, that is based on the reactants alone, become apparent in the unavailability of accurate $\Delta V_{\mathrm{int}}{}^{\ddagger}$ and $\Delta S^{\ddagger}$ values. An extended CM, in which the *strong* solute−solvent interactions and the solvent−solvent interactions differing considerably from those in the bulk are included, might allow the computation of $\Delta V_{\mathrm{int}}{}^{\ddagger}$ and $\Delta S^{\ddagger}$. Such calculations were performed for the electron self-exchange reactions via the outer-sphere pathway of the $V(OH_2)_6{}^{2+/3+}$, $V(OH_2)_6{}^{3+/4+}$, $Ru(OH_2)_6{}^{2+/3+}$, and $Ru(OH_2)_6{}^{3+/4+}$ couples[35] but not yet for substitution reactions.

4. Computational Studies on Reaction Mechanisms

4.1. Historical Overview of the Application of Quantum Chemical Methods for the Elucidation of Substitution Mechanisms

Prior to 1996, quantum chemical investigations on reaction mechanisms were limited to calculations on reactants, products, and eventually intermediates or species resembling them as models for the transition states. All of these computations were performed for the free species in the gas phase. In 1996, the first gas-phase calculations on transition states for water exchange reactions of transition metal complexes using Hartree-Frock (HF) or complete active space self-consistent field (CAS-SCF) methods were reported.[53] In 1997, similar computations using DFT were published.[63] In 1999, for the water exchange reaction of $Ru(NH_3)_5OH_2{}^{3+}$,[32] hydration was treated with continuum models and electron correlation on the basis of the multiconfigurational quasi-degenerate second-order perturbation theory (MCQDPT2).[28,29] In 2002, the reorganizational energy for outer-sphere electron transfer reactions of transition metal hexaaqua ions was calculated[35] with a model including a quantum chemically described second coordination sphere, whereby the bulk solvent (from the third

sphere on) was treated with the polarizable continuum model (PCM).[20] Electron correlation was computed at the MCQDPT2 level.

In 1997, the coordination number of the Be^{2+} ion was investigated via Car−Parrinello molecular dynamics (CPMD) simulations.[64] The first CPMD computation on a substitution reaction, the hydrolysis of *cis*-$Pt(NH_3)_2Cl_2$,[65] performed with constrained MD[15,16] because of the inertness of the reactant, was reported in 2000. Three years later were published unconstrained CPMD calculations on the water exchange reactions on Ca^{2+} and Sr^{2+}.[66,67]

The first QM/MM study, on the structure and dynamics of the hydrated Ag^+ ion, was also reported in 2003.[68]

4.2. Water Exchange Reactions

4.2.1. Pure Aqua Ions

Apart from a few exceptions, the coordination number of most aqua ions is known today.[69] Still under discussion and investigation are some alkali[70] and alkaline earth[66,71−73] metal ions, the Sc^{3+} ion,[74,75] and the Th^{4+} ion.[76] Since quite recently, the coordination number of Cu^{2+} has been debated,[77−82] whereas that of Cu^+ was unknown but often assumed to be 4. In a recent CPMD study on the Cu^+/Cu^{2+}, Ag^+/Ag^{2+}, and Cu^+/Ag^{2+} electron transfer reactions,[81] a coordination number of 2 was computed for Cu^+. The knowledge of the coordination number is a necessary basis for the elucidation of water exchange mechanisms and for the determination of parameters of electron transfer reactions.

The literature on computations of water exchange reactions involving pure aqua complexes is summarized in Table 1. Most of the abbreviations have been introduced in previous sections; the remaining pertain to the DFT calculations, that were performed with the local density approximation (LDA), exhibiting the Slater exchange[89] and Vosko−Wilk−Nusair correlation (SVWN),[90] the Becke−Lee−Yang−Parr (BLYP),[91−93] the three-parameter hybrid B3LYP,[94−96] the Becke−Perdew (BP),[97,98] the Perdew−Burke−Ernzerhof (PBE),[99] or the Perdew−Wang 1991 (PW91)[100] functional. Only the studies in which the transition states have been optimized without constraints and characterized by a single imaginary frequency are reported in Table 1.

Before computations of transition states for substitution reactions on transition metal complexes were feasible, Åkesson et al.[101] investigated the water exchange mechanism of di- and trivalent transition metal hexaaqua ions with ab initio MO methods (HF and CAS-SCF). They payed the due attention to the basis set superposition error (BSSE) by leaving one s and one p function uncontracted for the 3+ ions, which give rise to a larger BSSE than the 2+ ions. Penta- and heptacoordinated aqua ions, calculated by constrained optimizations, were used as models for the transition states of the dissociative and associative mechanisms, respectively. The hydration energy was estimated using the temperature-dependent Born equation.[102] For the trivalent ions, qualitatively correct mechanistic trends were obtained but, erroneously, all of the divalent ions were found to react dissociatively, although the experimental activation volumes of V^{II} and Mn^{II} are negative. The error is mainly due to the model for the transition state: the heptacoordinated species have a too high energy, and thus, the associative pathways were disfavored with respect to the ***D*** mechanism, for which the energies of the transition state and the intermediate are close.[53,54] Furthermore, for V^{II} and Mn^{II}, the activation energies for the associative and the dissociative activation are close.[23,53,54] The approximation of transition states by intermediates, obtained by constrained optimizations, is at the origin of these incorrect conclusions.

The water exchange reactions on $Pd(OH_2)_4^{2+}$, $Pt(OH_2)_4^{2+}$, and *trans*-$PtCl_2(OH_2)_2^{2+}$ were investigated by Deeth and Elding[103] using relativistic DFT. The transition states for the associative activation were represented by trigonal bipyramidal $Pd/Pt(OH_2)_5^{2+}$ or *trans*-$PtCl_2(OH_2)_3$ species, whose geometries were obtained by constrained optimizations. All of the geometries were optimized for the free ions in the gas phase at the LDA level, and the energies were computed with the BP functional. The hydration energies were estimated using the Born model,[104] or via 18 classically described water molecules surrounding the solute. The activation energy for the water exchange on $Pd(OH_2)_4^{2+}$ via the ***D*** mechanism was also investigated and found to be considerably higher than that of the associative pathway. For the latter, the experimental and calculated activation energies agree. This shows that, for these reactions, the approximate transition states, obtained via constrained geometry optimizations, are adequate models.

Presently, the time of CPMD simulations is of the order of about 20 ps for the current systems involving typically a cation and about 30 to 50 H_2O molecules (Table 1). In a 14 ps simulation of Ca^{2+} in water, two exchange events were observed, whereby $Ca(OH_2)_7^{2+}$ and $Ca(OH_2)_8^{2+}$ were in equilibrium.[66] The lifetime of both species was 1−2 ps.[66] It should be noted that the coordination number of Ca^{2+} in aqueous solution is not established and that in a more elaborate CPMD study, with 54 H_2O molecules and a larger basis set for Ca, in which, however, no exchange events were observed, the coordination number was found to be 6.[72] According to the most recent EXAFS, XANES, and MD-EXAFS studies,[71,73] it is 7.

In a 4 ps CPMD simulation of aqueous Sr^{2+} at room temperature, the coordination numbers of 7 and 8 were observed.[67] The lifetime of $Sr(OH_2)_7^{2+}$ was estimated as ∼1.5 ps on the basis of a single exchange event (at 25 °C).[67] Simulations were also performed at 350 and 600 °C. In the most recent MD-EXAFS study,[73] a coordination number of 8 was reported.

For the water exchange reactions on transition metal hexaaqua ions, investigated with MO methods based on the CM, transition states for the ***A***, $\boldsymbol{I_a}$, and ***D*** mechanisms were found (Table 1). In the transition state for ***A***, the imaginary mode, which is the reaction coordinate, represents the motion of the entering (or leaving) H_2O, while the other six H_2O molecules rearrange slightly (Figure 3). For ***D***, the reaction

Table 1. Water Exchange Reactions of Pure Metal Aqua Ions[a]

	experimental data[b]				quantum chemical computations						
	$\Delta H^{\ddagger}$	$\Delta S^{\ddagger}$	$\Delta G^{\ddagger}$	$\Delta V^{\ddagger}$	model and method[c]	mech	$\Delta E^{\ddagger}$	$\Delta V^{\ddagger}$	d(M···O)[d]	$\Delta\Sigma$	ref
$Ca(OH_2)_{7-8}^{2+}$					CPMD, 31 H_2O (BLYP)						66
$Sr(OH_2)_8^{2+}$					CPMD, 30 H_2O (PBE)						67
$Al(OH_2)_6^{3+}$	84.7	41.6	72.3	5.7	CM, 7 H_2O (HF-GP/HF-GP)	***D***	85.4	5.6	3.16	1.01	55
$Ga(OH_2)_6^{3+}$	67.1	30.1	58.1	5.0	CM, 7 H_2O (HF-GP/HF-GP)	***D***	69.1	4.8	3.11	0.89	55
$In(OH_2)_6^{3+}$	19.2	−96	47.8		CM, 7 H_2O (HF-GP/HF-GP)	***A***	29.1	−5.2	2.78	−1.29	55
					CM, 7 H_2O (HF-GP/HF-GP)	***D***	75.2	4.4	3.44	1.02	55
$Sc(OH_2)_6^{3+}$					CM, 7 H_2O (HF-GP/HF-GP)	***A***	22.3		2.98	−1.11	54
					CM, 7 H_2O (HF-GP/HF-GP)	***D***	>89.5				54
$Ti(OH_2)_6^{3+}$	43.4	1.2	43.0	−12.1	CM, 7 H_2O (HF-GP/HF-GP)	***A***	35.2		2.81	−1.22	53
					CM, 7 H_2O (HF-GP/HF-GP)	***D***	>91.2				53
					CM, 7 H_2O (B3LYP-GP/B3LYP-GP)	***A***	66.1		2.69	−0.96	83
$V(OH_2)_6^{3+}$	49.4	−27.8	57.7	−8.9	CM, 7 H_2O (CAS-SCF-GP/CAS-SCF-GP)	***A***	47.0		2.73	−1.22	54
					CM, 7 H_2O (CAS-SCF-GP/CAS-SCF-GP)	***D***	>93.6				54
					CM, 7 H_2O (B3LYP-GP/B3LYP-GP)	***A***	86.2	−3.8	2.60		62
					CM, 7 H_2O (B3LYP-GP/B3LYP-GP)	***D***	70.7, 82.4, 69.9, 66.9	0.7, 0.8, 2.3, 2.0	2.81, 2.75, 2.90, 2.95		62
					CM, 7 H_2O (B3LYP-GP/B3LYP-PCM)	***A***	46.4	−3.8	2.60		62
					CM, 7 H_2O (B3LYP-GP/B3LYP-PCM)	***D***	91.6, 104.6, 92.0, 96.2	0.7, 0.8, 2.3, 2.0	2.81, 2.75, 2.90, 2.95		62
$V(OH_2)_6^{2+}$	61.8	−0.4	61.9	−4.1	CM, 7 H_2O (HF-GP/HF-GP)	***I_a***	57.9		2.68[e]	−1.18	53
					CM, 6 H_2O (HF-GP/HF-GP)	***D***	58.0		3.63	1.27	53
					CM, 7 H_2O (HF-SCRF/MP2-PCM)	***I_a***	65.5		2.67[e]		23
					CM, 6 H_2O (HF-SCRF/MP2-PCM)	***D***	71.8		3.59		23
					CM, 7 H_2O (B3LYP-GP/B3LYP-GP)	***I***	74.1,[f] 87.4[g]	0.1,[f] −0.3[g]	2.86,[e,f] 2.76[e,g]		62
					CM, 7 H_2O (B3LYP-GP/B3LYP-GP)	***D***	62.8	6.9	3.37		62
					CM, 7 H_2O (B3LYP-GP/B3LYP-PCM)	***I***	72.8,[f] 84.1[g]	0.1,[f] −0.3[g]	2.86,[e,f] 2.76[e,g]		62
					CM, 7 H_2O (B3LYP-GP/B3LYP-PCM)	***D***	86.2	6.9	3.37		62
$Cr(OH_2)_6^{3+}$	108.6	11.6	105.1	−9.6	CM, 7 H_2O (HF-GP/HF-GP)	***I_a***	98.2		2.14[e]	−1.20	54
					CM, 6 H_2O (HF-GP/HF-GP)	***D***	120.9		3.43	1.21	54
					CM, 7 H_2O (HF-SCRF/MP2-PCM)	***I_a***	96.3		2.40[e]	−0.98	84
$Cr(OH_2)_6^{2+}$	∼24−31[h]		∼24−31[h]	4.3[h]	CM, 6 H_2O (HF-GP/HF-GP)	***D***	15.9		3.28	0.74	54
					CM, 7 H_2O (HF-GP/HF-GP)	***I_a***	29.8		2.76[e]	−1.19	54
$Mn(OH_2)_6^{3+}$					CM, 7 H_2O (HF-GP/HF-GP)	***D***	54.1		3.98	0.90	54
					CM, 7 H_2O (HF-GP/HF-GP)	***I_a***	60.7		2.46[e]	−1.17	54
$Mn(OH_2)_6^{2+}$	32.9	5.7	31.2	−5.4	CM, 7 H_2O (HF-GP/HF-GP)	***A***	30.9		2.66	−1.49	54
					CM, 6 H_2O (HF-GP/HF-GP)	***D***	32.4		3.21	0.75	54
					CM, 7 H_2O (HF-GP/HF-GP)	***D***	32.4		3.41	0.93	54
					CM, 7 H_2O (HF-SCRF/MP2-PCM)	***A***	33.0		2.66		23
					CM, 6 H_2O (HF-SCRF/MP2-PCM)	***D***	32.5		3.21		23

Table 1 (Continued)

	experimental data[b]				quantum chemical computations						
	$\Delta H^{\ddagger}$	$\Delta S^{\ddagger}$	$\Delta G^{\ddagger}$	$\Delta V^{\ddagger}$	model and method[c]	mech	$\Delta E^{\ddagger}$	$\Delta V^{\ddagger}$	d(M···O)[d]	$\Delta\Sigma$	ref
$Fe(OH_2)_6^{3+}$	64.0	12.1	60.4	−5.4	CM, 7 H_2O (HF-GP/HF-GP)	***A***	58.8		2.47	−1.35	54
					CM, 7 H_2O (HF-GP/HF-GP)	***D***	>74.8				54
$Fe(OH_2)_6^{2+}$	41.4	21.2	35.1	3.8	CM, 6 H_2O (HF-GP/HF-GP)	***D***	34.8		3.16	0.74	54
					CM, 7 H_2O (HF-GP/HF-GP)	$\boldsymbol{I_a}$	42.3		2.33[e]	−1.52	54
					CM, 6 H_2O (HF-SCRF/MP2-PCM)	***D***	40.9		3.15		23
					CM, 7 H_2O (HF-SCRF/MP2-PCM)	$\boldsymbol{I_a}$	46.5		2.33[e]		23
$Co(OH_2)_6^{2+}$	46.9	37.2	35.8	6.1	CM, 6 H_2O (CAS-SCF-GP/CAS-SCF-GP)	***D***	38.0		3.15	0.78	54
					CM, 7 H_2O (CAS-SCF-GP/CAS-SCF-GP)	***A***	45.9		2.40	−1.50	54
$Ni(OH_2)_6^{2+}$	56.9	32.0	47.4	7.2	CM, 6 H_2O (HF-GP/HF-GP)	***D***	46.9		3.38	1.08	53
					CM, 7 H_2O (HF-GP/HF-GP)	***D***	42.9		3.34	1.00	53
$Cu(OH_2)_6^{2+}$	11.5	−21.8	18.0	2.0	CM, 6 H_2O (HF-GP/HF-GP)	***D***	19.8		3.17	0.73	54
					CM, 7 H_2O (HF-GP/HF-GP)	***D***	17.6		3.12	0.70	54
$Zn(OH_2)_6^{2+}$					CM, 6 H_2O (HF-GP/HF-GP)	***D***	27.3		3.02	0.66	54
					CM, 6 H_2O (B3LYP-GP/B3LYP-GP)	***D***	19.2, 31.0, 17.6, 32.6		2.69 2.90 2.83 3.06	0.37, 0.55, 0.44, 0.72	63
					CM, 7 H_2O (B3LYP-GP/B3LYP-GP)	***D***	28.5		3.03	0.73	63
$Ru(OH_2)_6^{3+}$	89.8	−48.3	104.2	−8.3	CM, 7 H_2O (HF-SCRF/MP2-PCM)	$\boldsymbol{I_a}$	91.8		2.43[e]	−0.97	84
$Ru(OH_2)_6^{2+}$	87.8	16.1	83.0	−0.4	CM, 6 H_2O (HF-SCRF/HF-PCM)	***D***	71.9		3.59	1.25	85
$Rh(OH_2)_6^{3+}$	131	29	122	−4.2	CM, 7 H_2O (HF-SCRF/HF-PCM)	$\boldsymbol{I_a}$	114.8	−3.9	2.70[e]	−0.53	58, 85
					CM, 6 H_2O (HF-SCRF/HF-PCM)	***D***	136.6	6.3	3.46	1.26	58, 85
$Ag(OH_2)_{4-7}^{+}$					QM/MM, 499 H_2O (QM: HF, first coordination sphere)						68
$Ir(OH_2)_6^{3+}$	130.5	2.1	129.9	−5.7	CM, 7 H_2O (HF-SCRF/HF-PCM)	$\boldsymbol{I_a}$	127.9	−3.5	2.74[e]	−0.50	58
					CM, 6 H_2O (HF-SCRF/HF-PCM)	***D***	160.1	5.5	3.49	1.28	58
$Au(OH_2)_{3-7}^{+}$					QM/MM, 499 H_2O (QM: HF, first coordination sphere)						86
$Th(OH_2)_9^{4+}$					CM, 10 H_2O (HF-GP/MP2-GP)	***A***	51.7[i]		3.51	−0.83	87
					CM, 10 H_2O (B3LYP-GP/B3LYP-GP)	***A***	41.4[j]		3.40	−0.87	87
					CM, 10 H_2O (HF-GP/MP2-PCM)	***A***	15.1[k]		3.51	−0.83	87
					CM, 10 H_2O (B3LYP-GP/B3LYP-PCM)	***A***	1.9[l]		3.40	−0.87	87
					CM, 9 H_2O (HF-GP/MP2-GP)	***D***	38.4[i]		3.49	0.64	87
					CM, 9 H_2O (HF-GP/MP2-PCM)	***D***	75.6[k]		3.49	0.64	87
$Th(OH_2)_{10}^{4+}$					CM, 10 H_2O (B3LYP-GP/B3LYP-GP)	***D***	−21.7[j]		3.40	0.35	87
					CM, 10 H_2O (B3LYP-GP/B3LYP-PCM)	***D***	9.0[l]		3.40	0.35	87
					CM, 11 H_2O (B3LYP-GP/B3LYP-GP)	***A***	63.8[j]		3.52	−0.88	87
					CM, 11 H_2O (B3LYP-GP/B3LYP-PCM)	***A***	22.4[l]		3.52	−0.88	87

[a] Units: $\Delta H^{\ddagger}$, $\Delta G^{\ddagger}$, $\Delta E^{\ddagger}$, kJ/mol; $\Delta S^{\ddagger}$, J K^{-1} mol^{-1}; $\Delta V^{\ddagger}$, cm^3/mol; d(M···O), $\Delta\Sigma$, Å. [b] From ref 7, unless noted otherwise. [c] Abbreviations: CPMD, Car-Parrinello MD; CM, cluster model; QM/MM, hybrid quantum mechanical/molecular mechanical calculation. In parentheses is shown the computational level for the geometry/energy: GP, free ions in the gas phase; SCRF, hydration calculated with self-consistent reaction fields; PCM, hydration calculated with the polarizable continuum model. [d] M···O bond length(s) in the transition state. [e] Two symmetry-equivalent M···O bonds. [f] Attack adjacent to the leaving H_2O ligand. [g] Attack adjacent to the H_2O in the trans position of the leaving H_2O ligand. [h] Reference 88. [i] From "E(MP2)" in Table 4 of ref 87. [j] From "E(SCF)" in Table 2 of ref 87. [k] "$\Delta E^{\ddagger}$" in Table 4 of ref 87. [l] From the sum of the "E(SCF)" and "PCM energy" terms in Table 2 of ref 87.

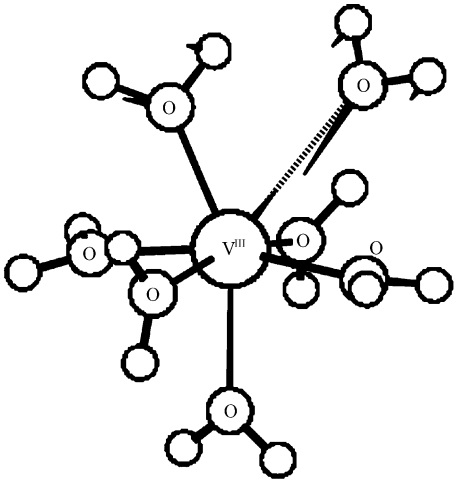

Figure 3. Perspective view of the transition state $[V(OH_2)_6\cdots OH_2^{3+}]^{\ddagger}$ for the ***A*** mechanism (HF geometry).

coordinate represents the motion of the leaving H_2O whereby, depending on the electronic structure of the metal ion, a square pyramidal (Figure 4a) or a trigonal bipyramidal (Figure 4b) intermediate is formed. The latter does not arise from the rearrangement of the square pyramid, but it is generated concerted with the departure of the leaving group. In exchange reactions via an interchange mechanism, the imaginary mode describes the concerted loss and entry of the exchanging ligands (Figure 5). In reactions proceeding with retention of the configuration, the incoming ligand attacks adjacent to the leaving ligand. For the water exchange on $V(OH_2)_6^{2+}$, this pathway (Figure 5a) is more favorable than the stereomobile pathway (Figure 5b), in which the entering ligand attacks adjacent to the ligand trans to the leaving group. As already mentioned, $\Delta\sum$ (eq 1) can be used as a criterion for the distinction of the $\boldsymbol{I_a}$, $\boldsymbol{I}$, and $\boldsymbol{I_d}$ mechanisms.

The failure of finding a transition state for the $\boldsymbol{I_d}$ mechanism should not be taken as evidence against its existence. It should be remembered that all of the presently found transition states for this kind of reactions were obtained on the basis of the CM involving solely the free reactants. According to this simple model, and perhaps also in reality, the H_2O molecules exchanging via the $\boldsymbol{I_d}$ mechanism would form, in addition to two weak M···O bonds, H-bonds with H_2O of the first coordination sphere (Figure 5). For the $\boldsymbol{I_a}$ and $\boldsymbol{I}$ mechanisms, the M···O bonds are sufficiently strong that transition states of the $[M(OH_2)_5\cdots(OH_2)_2^{n+}]^{\ddagger}$ type (Figure 5) can be obtained. The M···O bonds would be weaker for the $\boldsymbol{I_d}$ mechanism, and all of the attempts at computing such transition states lead to species, which are in fact intermediates, with the two "exchanging" H_2O molecules H-bonded to two H_2O molecules of the first coordination sphere (Figure 6) because, in these cases, the H-bonds are much stronger than the rather weak M···O bonds. It remains to be shown whether, with a larger CM involving, for example, a complete quantum chemically described second coordination sphere, transition states for the $\boldsymbol{I_d}$ mechanism can be computed. For water exchange and substitution reactions on amine complexes, transition states for

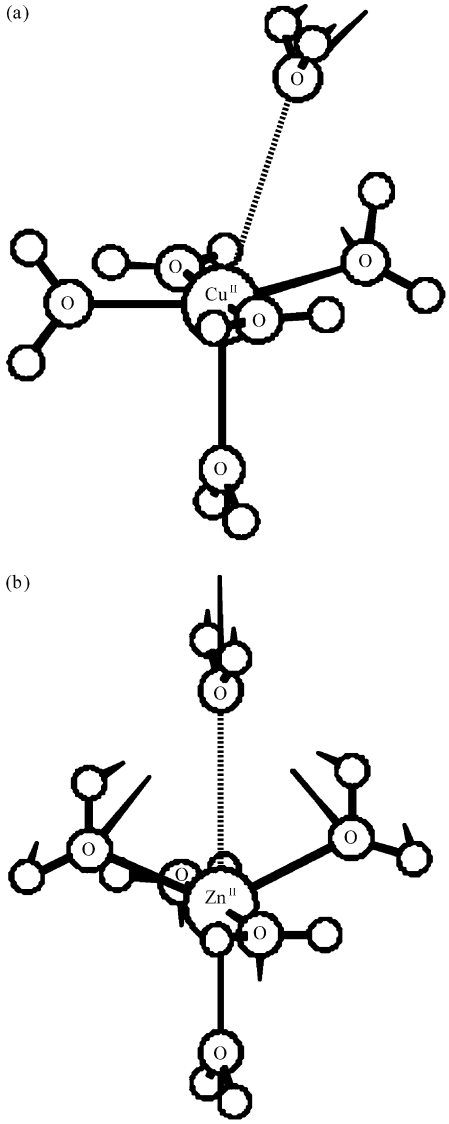

Figure 4. Perspective view of the transition states $[Cu(OH_2)_5\cdots OH_2^{2+}]^{\ddagger}$ (a) and $[Zn(OH_2)_5\cdots OH_2^{2+}]^{\ddagger}$ (b) for the ***D*** mechanism (HF geometries).

the $\boldsymbol{I_d}$ mechanism have been obtained (sections 4.2.2 and 4.5).

The computation of activation energies ($\Delta E^{\ddagger}$) was based on two structures for the water adduct of the reactant, $M(OH_2)_6{\cdot}OH_2^{n+}$: in the first one (Figure 7a),[53,54] the seventh H_2O (which is in the second coordination sphere) is bound to one H_2O of the first coordination sphere via a single H-bond, whereas, in the second structure (Figure 7b),[55,63,83] it forms two H-bonds with two neighboring H_2O molecules of the first coordination sphere. Because of a fortuitous cancellation of errors,[23] the first structure yields activation energies ($\Delta E^{\ddagger}$) closer to $\Delta H^{\ddagger}$ for the gas-phase model whereas, when hydration is included, more accurate $\Delta E^{\ddagger}$ values are obtained on the basis of the second structure.

The activation energies ($\Delta E^{\ddagger}$) reported in Table 1 are differences of total energies with or without zero point energies (ZPEs) and without thermal corrections. In the CM with six or seven H_2O molecules, the solute−solvent interactions are neglected. As already mentioned, their contribution is most likely

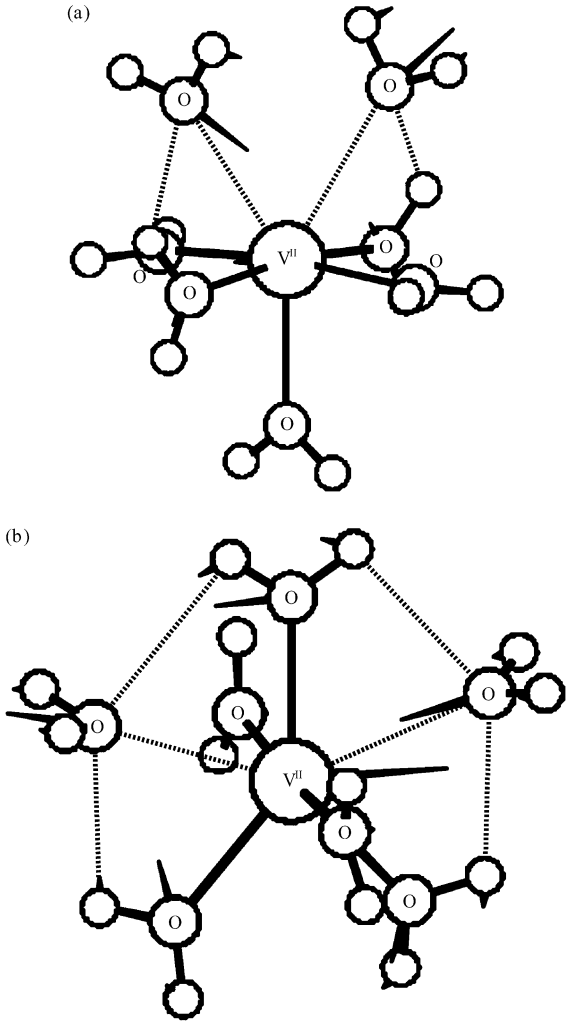

Figure 5. Perspective view of the transition states for the I_a mechanism, $[cis\text{-}V(OH_2)_5\cdots(OH_2)_2{}^{2+}]^{\ddagger}$ (a) and $[V(OH_2)_5\cdots(OH_2)_2{}^{2+}]^{\ddagger}$ (b), respectively, giving rise to stereoretention and stereomobility (HF geometries).

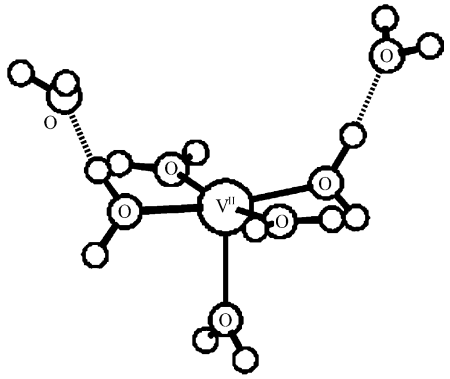

Figure 6. Perspective view of the pentacoordinated intermediate $V(OH_2)_5\cdot(OH_2)_2{}^{2+}$ that is obtained with B3LYP instead of the transition state $[cis\text{-}V(OH_2)_5\cdots(OH_2)_2{}^{2+}]^{\ddagger}$.

larger than those due to the ZPE and the thermal corrections of the free $M(OH_2)_{6/7}{}^{n+}$ species. For this reason, the latter were neglected in most cases. It should be remembered that activation entropies ($\Delta S^{\ddagger}$) based on the CM exhibiting six or seven H_2O molecules must be considered as unreliable because of the neglect of the solute−solvent interactions,[23] whose importance can be perceived in the unavailability of calculated $\Delta S^{\ddagger}$ values being in agreement

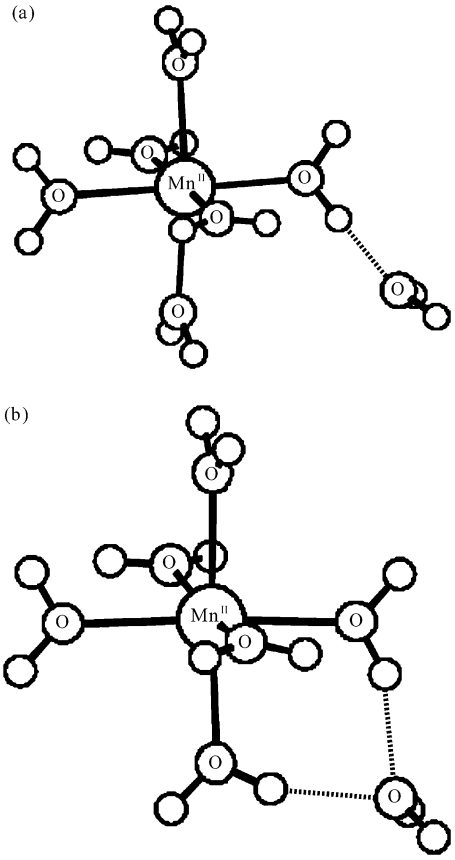

Figure 7. Perspective view of the two isomers for the water adduct, $Mn(OH_2)_6\cdot OH_2{}^{2+}$, in which the seventh H_2O molecule in the second coordination sphere forms one (a) or two (b) H-bonds (HF geometries).

with experiment. In proximity of the metal ion, solvent−solvent interactions might also differ from those in the bulk. Thus, the computation of thermodynamic parameters such as $\Delta H^{\ddagger}$, $\Delta S^{\ddagger}$, or $\Delta G^{\ddagger}$ is a demanding task that would require at least a quantum chemically described second coordination sphere. Such calculations have not been reported thus far for substitution or rearrangement processes.

Before the computational results on the water exchange reactions are analyzed, comments on the basis sets, that are currently used for the transition metals, are appropriate. The HF/CAS-SCF studies on the transition metal aqua ions (Table 1) were performed with the basis sets of Stevens, Krauss, Basch, and Jasien (SBKJ),[105] in which the inner shells are represented by effective core potentials (ECPs) and the valence shells and the semicores by double-ζ and triple-ζ functions. In first-row transition metals, for example, the 3s, 3p, 4s, and 4p shells have double-ζ quality, whereas the 3d shell, represented by six primitives, has triple-ζ quality. For doubly and triply charged aqua ions, the BSSE was shown to be very small.[10] The SBKJ/6-31G(d)[106,107] or SBKJ/6-311G(d)[108] basis sets are of a good quality, and inaccuracies in the HF/CAS-SCF results arise mainly from the neglect of dynamic electron correlation, the approximate or neglected treatment of hydration, and the nonconsideration of the H-bonds between the first and the second coordination spheres.

The B3LYP studies (Table 1) were performed with 6-311G(d)[109,110] or (63311/53/41)[111] basis sets for the

transition metals, whereby the latter were augmented with one p and one d function. The *segmented* 6-311G(d) basis sets were derived from Wachter's *generally contracted* basis sets[109] by reoptimizing the contraction coefficients, but not the exponents, and improving the 3d functions.[110] As Schäfer et al.[111] noted, in good basis sets, both the exponents and the contraction coefficients must be optimized. Thus, results obtained with 6-311G(d) basis sets for the transition metals have to be taken with reservations. The augmented split-valence (63311/53/41) sets are fully optimized, superior to 6-311G(d), but small. Larger, fully optimized basis sets of double-ζ, triple-ζ, or quadruple-ζ valence quality are available[111−113] but, especially the latter, would be unduly demanding for the present investigations. For the first-row transition metals, a fully optimized 6-31G basis set is available[114] which, however, gives rise to a considerable BSSE, unless it is modified in an appropriate manner.[10] For 2+ aqua ions, 6-31G(d,sp) basis sets, having been augmented with one d and one sp function, are adequate.[10] For 3+ aqua ions, the 3s/3p and the 3d functions (of 6-31G) need to be uncontracted,[10] leaving, however, the BSSE still higher than that with the SBKJ basis sets. Doubtless, for the present applications, the computationally efficient SBKJ basis sets are superior over the currently used all-electron basis sets.

The water exchange reactions on the hexaaqua ions of Ti^{3+}, V^{3+}, V^{2+}, and Zn^{2+} were performed with HF or CAS-SCF methods and later with DFT using the B3LYP functional (Table 1). In certain cases, considerable differences can be seen in the geometries and the activation energies as well. The latter are due to the preference of DFT for the lower coordination number as well as the dissociative pathway.[10] Thus, the activation energy for the water exchange on $Ti(OH_2)_6^{3+}$ and $V(OH_2)_6^{3+}$ via the ***A*** mechanism, based on the gas-phase model, is higher with B3LYP than with HF or CAS-SCF. The B3LYP functional also gives rise to a larger error with respect to the experimental $\Delta H^{\ddagger}$ or $\Delta G^{\ddagger}$ values (Table 1). The deficiency of DFT in the description of H-bonds, in particular those of complexes with high valent metal centers, can be seen in the unavailablity[62,83] of the singly H-bonded $Ti(OH_2)_6{\cdot}OH_2^{3+}$ and $V(OH_2)_6{\cdot}OH_2^{3+}$ structures (as in Figures 1 and 7a) with B3LYP.

In their reinvestigation of the water exchange reaction on $V(OH_2)_6^{2+}$, Benmelouka et al.[62] proposed the ***I*** mechanism presumably on the basis of the rather long V···O bonds of 2.858 Å in the transition state and the computed PCM activation volume close to zero (Table 1). The computed data and their interpretation are at variance with the negative experimental $\Delta V^{\ddagger}$ and the two earlier HF studies (Table 1). This incorrect result was obtained with the B3LYP functional and the 6-311G(d)/6-31G(d) basis sets for V and O/H, respectively. It should be noted that, using the B3LYP functional and good all-electron or ECP basis sets for V, it is impossible[10] to obtain the transition state $[cis\text{-}V(OH_2)_5{\cdots}(OH_2)_2^{2+}]^{\ddagger}$ (Figure 5a), but the pentacoordinated intermediate $V(OH_2)_5{\cdot}(OH_2)_2^{2+}$ with two H_2O molecules in the second coordination sphere is obtained instead (resembling the species in Figure 6). The wrong result is due to a fortuitous cancellation of errors. The B3LYP functional does not provide[10] a balanced treatment of the V···O and H···O bonds, and therefore, with appropriate basis sets, the transition state for the $\boldsymbol{I_a}$ mechanism cannot be obtained.[10] With the too small and not fully optimized 6-311G(d) basis set for V, however, a $[cis\text{-}V(OH_2)_5{\cdots}(OH_2)_2^{2+}]^{\ddagger}$ species was obtained because of the combination of an inadequate computational method with a poor basis set for V. This example illustrates that the basis sets, the computational technique, and the model have to be chosen with care and that the results may depend critically on this choice.

Some remarks on the other quantum chemical investigations (Table 1) seem advisable. Due to the small energy difference of 0.5 kJ/mol between $Sc(OH_2)_6^{3+}$ and $Sc(OH_2)_7^{3+}$, it was suggested[54] that hexa- and heptacoordinated species could coexist in aqueous solution. This supposition is wrong because this small energy difference is incorrect and arises from the limitation of HF theory that favors the higher coordination numbers energetically.[10] At the MP2 level, the hexacoordinated species is more stable,[10] in agreement with a recent combined Raman and ab initio MO study.[75]

The geometry and energy of the reactants $Fe(OH_2)_6^{2+}$ and $Co(OH_2)_6^{2+}$ were computed originally[54] with an imposed D_{2h} symmetry. The corresponding species with S_6 symmetry have a slightly lower energy. The reinvestigation[23] of the exchange reaction on $Fe(OH_2)_6^{2+}$ with hydration and electron correlation included was based on the reactant with S_6 symmetry. For $Co(OH_2)_6^{2+}$, the S_6 species is more stable by 1.1 kJ/mol than the D_{2h} one; the activation energy is thus marginally higher, 39.1 kJ/mol.

The coordination number of the aqua ion of Th^{IV} is not yet established. According to EXAFS measurements, it is in the range of 9−11.[115] The water exchange mechanism on $Th(OH_2)_9^{4+}$ and $Th(OH_2)_{10}^{4+}$ was studied with ab initio MO and DFT (B3LYP) methods (Table 1).[87] For the ***A*** mechanism on $Th(OH_2)_9^{4+}$, B3LYP and HF/MP2 gas-phase calculations yielded activation energies differing insignificantly (by ~10 kJ/mol). The corresponding PCM energies are lower. The PCM activation energy for ***D*** is substantially higher. It should be noted that, on the basis of the gas-phase activation energies, the ***D*** mechanism would have been preferred over ***A***. However, there is an error in the computation of the ***D*** mechanism of $Th(OH_2)_{10}^{4+}$, since the SCF energy of the transition state $[Th(OH_2)_9{\cdots}OH_2^{4+}]^{\ddagger}$ with C_{2v} symmetry is *lower* than that of the reactant. The negative $\Delta E^{\ddagger}$ at the B3LYP-GP/B3LYP-GP level might arise from the reactant that is not connected to the transition state, or more likely, the computed species is not a transition state for the ***D*** mechanism. This transition state should have the same structure as that for ***A*** of $Th(OH_2)_9^{4+}$ exhibiting C_1 symmetry. The structural differences, the different symmetries, seem to lie beyond the differences one could expect for the two different computational methods (B3LYP-GP and HF-GP). The calculations on the ***A*** mechanism for $Th(OH_2)_{10}^{4+}$ appear correct, but a

statement about the most favorable mechanism for the water exchange on $Th(OH_2)_{10}^{4+}$ cannot be made (because of the absence of correct data for the ***D*** mechanism). The energy of the intermediate $Th(OH_2)_{11}^{4+}$ was not reported.

In the present examples (Table 1), the geometries depend only slightly on solvation (at the SCRF level at least), but the activation energies are improved considerably upon the treatment of hydration with continuum models.[20] Of course, the inclusion of solvation cannot eliminate the inaccuracies arising form inadequate basis sets or inappropriate computational methods, although the results might also be improved in such cases.

In a recent QM/MM study,[68] the aqua ion of Ag^+ was found to exhibit an average coordination number of 5.4. Tetra- and heptacoordinated species were also found besides the prevailing penta- and hexacoordinated ones. As the authors pointed out,[68] the computed coordination number is higher than the experimental values, which are in the range of 2−4.5. They attributed this difference to the extreme lability and asymmetry of the first coordination sphere and to the fitting of the experimental data to a single species. Another cause might be the QM part of the simulations, which was treated with the HF method that was shown[10] to favor energetically the higher coordination number. Furthermore, the HF method produces longer Ag−O bonds than the MP2 method. For example, this difference is 0.065 Å for $Ag(OH_2)_6^+$ with an imposed S_6 symmetry.[116,117] The too long Ag−O bonds give rise to a weaker repulsion between the H_2O molecules in the first coordination sphere. Thus, the average coordination number might be smaller than 5.4 and closer to the, as the authors noted,[68] possibly not quite correctly interpreted, experimental data. Within the simulation time of 16 ps, 14 H_2O exchanges between the first and the second coordination sphere were observed,[68] and the mean residence time of a first sphere H_2O was estimated as ∼20 ps. The Ag^+ ion is very labile and its structure fluxional. Since stronger Ag−O bonds are obtained with MP2 (and also B3LYP), the residence time might be somewhat longer. In a recent CPMD study[81] based on the BLYP functional, a coordination number of 4 was obtained. Since BLYP tends to favor the lower coordination number, the aqueous Ag^+ ion is most likely four or five coordinate.

In an analogous QM/MM study on Au^+ by Armunanto et al.,[86] an average coordination number of 4.7 was computed. In addition to the prevailing coordination numbers of 4 and 5, some $Au(OH_2)_6^+$ and small amounts of $Au(OH_2)_3^+$ and $Au(OH_2)_7^+$ were predicted to be present in aqueous solution. Water exchange between the first and second hydration shell is faster than that for Ag^+, with the mean residence time of H_2O in the first sphere being ∼5−8 ps. As for Ag^+, the coordination numbers might be overestimated by the treatment of the QM part with the HF method.

4.2.2. Aqua Complexes Containing Ligands Other Than Water

The water exchange reactions on compounds with ligands other than water are summarized in Table 2. First are discussed reactions of complexes exhibiting exclusively neutral ligands, for which the geometries optimized for the free ions (in the gas phase) and with the SCRF model are virtually equal.[32] For the computation of energies, however, hydration needs to be considered.[32] Second, reactions of complexes with anionic ligands are analyzed. For them, hydration has to be included also for the geometry optimization because of the presence of a sizable electric dipole moment that interacts with the (polar) H_2O solvent. Obviously, solvation has to be included in the energy calculations as well. All of these computations were performed on the basis of the smallest possible CM.

Three pathways have been investigated for the water exchange reaction on $Cr(NH_3)_5OH_2^{3+}$: the interchange mechanism for the attack of the nucleophile adjacent to the aqua ligand, which is most favorable; that with the attack opposite to the aqua ligand, being the least favorable; and the dissociative pathway, that is intermediate. According to the calculations, this reaction proceeds via the $\boldsymbol{I_a}$ mechanism with retention of the configuration.

If the five NH_3 ligands are replaced by the bulky NH_2CH_3 ones, the $\boldsymbol{I_a}$ mechanism changes to $\boldsymbol{I_d}$, whose computed activation energy is higher than that for ***D***. Since the activation energies for $Rh(NH_2CH_3)_5OH_2^{3+}$, computed with PCM, were also of a lower accuracy, but underestimated by ∼20 kJ/mol, it was concluded[122] that the PCM might not be perfectly adequate for such systems exhibiting H-bonds (N−**H**···**O**H_2), and hydrophobic interactions (H_2N-CH_3···OH_2). Possibly, not all of the conformations of the NH_2CH_3 ligands correspond to the global minimum, and the nondynamic treatment of the NH_2CH_3 ligands, exhibiting two internal rotations, might be inappropriate. Thus, the higher computed activation energy for $\boldsymbol{I_d}$ in comparison to ***D*** should not be taken as evidence against the existence of $\boldsymbol{I_d}$. The calculation of the $\boldsymbol{I_d}$ pathway was feasible because the N−**H**···**O**H_2 bonds are weaker than the O−**H**···**O**H_2 bonds.

The replacement of the *trans*-NH_3 ligand in $Cr(NH_3)_5OH_2^{3+}$ by the less or more basic OH_2 or NH_2CH_3 ligands, respectively, gives rise to a decrease or increase of the Cr···O bonds of the exchanging H_2O molecules in the transition state.[84] This shows that the basicity of the ligands that do not participate in the substitution process affects the structure of the transition state: the less basic the trans ligand, the stronger the associative character, or alternatively, the higher its basicity, the more it is dissociative. If, in *trans*-$Cr(NH_3)_4(OH_2)_2^{3+}$, the four equatorial NH_3 molecules are replaced by H_2O molecules, the associative character increases, but the effect of the cis ligands is considerably weaker. The replacement of NH_3 in *trans*-$Cr(NH_2CH_3)(NH_3)_4OH_2^{3+}$ by four NH_2CH_3 molecules, on the other hand, gives rise to an increase of the dissociative character. The corresponding experimental $\Delta V^{\ddagger}$ values follow the same trend.[84]

As will be shown (section 5.3), the reactivity of high-spin d^3 and low-spin d^5 systems is similar for electronic reasons. Thus, the water exchange mechanism on $Ru(NH_3)_5OH_2^{3+}$ is virtually equal to that

Table 2. Water Exchange Reactions of Aqua Complexes Also Containing Ligands Other Than Water

	experimental data					quantum chemical computations					
	$\Delta H^{\ddagger}$	$\Delta S^{\ddagger}$	$\Delta G^{\ddagger}$	$\Delta V^{\ddagger}$	ref	model and method[a]	mech	$\Delta E^{\ddagger}$	$\Delta V^{\ddagger}$	$\Delta\Sigma$	ref
$Cr(NH_3)_5OH_2^{3+}$	97.1	0.0	97.1	−5.8	119	CM, 2 H_2O (HF-SCRF/MCQDPT2-PCM)	***I*** $_a$ [b]	106.3		−0.57	84
						CM, 2 H_2O (HF-SCRF/MCQDPT2-PCM)	***I*** $_a$ [c]	138.8		−0.10	84
						CM, 1 H_2O (HF-SCRF/MCQDPT2-PCM)	***D***	118.4		1.25	84
$Cr(NH_2CH_3)_5OH_2^{3+}$	98.5	−17.5	103.7	−3.8	120	CM, 2 H_2O (HF-SCRF/MCQDPT2-PCM)	***I*** $_d$	127.8		0.33	84
						CM, 1 H_2O (HF-SCRF/MCQDPT2-PCM)	***D***	101.5		1.26	84
trans-$Cr(NH_3)_4(OH_2)_2^{3+}$						CM, 3 H_2O (HF-SCRF/MCQDPT2-PCM)	***I*** $_a$	110.0		−0.92	84
trans-$Cr(NH_3)_4(NH_2CH_3)OH_2^{3+}$						CM, 2 H_2O (HF-SCRF/MCQDPT2-PCM)	***I*** $_a$	112.2		−0.36	84
$Ru(NH_3)_5OH_2^{3+}$	91.5	−7.7	93.8	−4.0	121	CM, 2 H_2O (HF-GP/MCQDPT2-GP)	***I*** $_a$ [b]	107.6		−0.84	32
						CM, 2 H_2O (HF-SCRF/MCQDPT2-PCM)	***I*** $_a$ [b]	87.9		−0.82	32
						CM, 2 H_2O (HF-GP/MCQDPT2-GP)	***I*** $_a$ [c]	121.1		−0.45	32
						CM, 2 H_2O (HF-SCRF/MCQDPT2-PCM)	***I*** $_a$ [c]	121.1		−0.49	32
						CM, 1 H_2O (HF-GP/MCQDPT2-GP)	***D***	83.1		1.16	32
						CM, 1 H_2O (HF-SCRF/MCQDPT2-PCM)	***D***	102.8		1.14	32
$Rh(NH_3)_5OH_2^{3+}$	102.9	3.4	101.9	−4.1	119	CM, 2 H_2O (HF-SCRF[d]/MCQDPT2-PCM)	***I***	101.5		0.01	122
						CM, 2 H_2O (HF-SCRF/MCQDPT2-PCM)	***I*** $_d$ [e]	227.9		0.58	122
						CM, 1 H_2O (HF-SCRF/MCQDPT2-PCM)	***D***	126.9		1.21	122
$Rh(NH_2CH_3)_5OH_2^{3+}$	113	37.8	101	1.2	120	CM, 2 H_2O (HF-SCRF/MCQDPT2-PCM)	***I*** $_d$	91.3		0.15	122
						CM, 1 H_2O (HF-SCRF/MCQDPT2-PCM)	***D***	91.2		1.24	122
$TiOH(OH_2)_5^{2+}$						CM, 5 H_2O (B3LYP-GP/B3LYP-GP)	***D***	41.0		0.87	83
						CM, 6 H_2O (B3LYP-GP/B3LYP-GP)	***D***	30.1		0.78	83
cis-$(H_2O)_2Mn^{IV}(OH)_4$						CM, 3 H_2O (B3LYP-GP/B3LYP-COSMO)[f]	***D***	40.2[g]			123
cis-$(H_2O)_2Mn^{IV}(OH)_3Cl$						CM, 3 H_2O (B3LYP-GP/B3LYP-COSMO)[f]	***D***	45.2[g]			123
$Mn^{III}(OH)_3(OH_2)_2$						CM, 3 H_2O (B3LYP-GP/B3LYP-COSMO)[f]	***D***	26.4[g]			123
						CM, 3 H_2O (B3LYP-GP/B3LYP-COSMO)[f]	***A***	>43[g]			123
$Mn^{III}(OH)_2(Cl)(OH_2)_2$						CM, 3 H_2O (B3LYP-GP/B3LYP-COSMO)[f]	***D***	39.7[g]			123
$(H_2O)_2(OH)_2Mn^{IV}(\mu\text{-}O)_2\text{-}Mn^{IV}(OH)_2(OH_2)_2$						CM, 5 H_2O (B3LYP-GP/B3LYP-COSMO)[f]	***D***	36.0[g]			123
CpRu[(*R*)-Binop-F]OH_2^+	50.6	10.2	47.5	4.8	124	CM, 1 H_2O (PW91-GP/PW91-GP)	***D***	57.1[g]			124
						CM, 1 H_2O (PW91-GP/PW91-PCM)	***D***	57.0[g,m]			124
						CM, 2 H_2O (PW91-GP/PW91-GP)	***I*** $_d$	68.6[g]			124
						CM, 2 H_2O (PW91-GP/PW91-PCM)	***I*** $_d$	77.1[g,m]			124
CpRu[(*R*)-Binop-F]OH_2^+	79.1[n]	95.6[n]	50.7[n]	11.6[n]	124	CM, 1 H_2O (PW91-GP/PW91-GP)	*n*	66.8[g]			124
						CM, 1 H_2O (PW91-GP/PW91-PCM)	*n*	48.0[g,m]			124
$ThOH(OH_2)_9^{3+}$						CM, 9 H_2O (B3LYP-GP/B3LYP-GP)	***D*** [h]	−23.4[i]		0.53	87
						CM, 9 H_2O (B3LYP-GP/B3LYP-PCM)	***D*** [h]	2.8[j]		0.53	87
						CM, 9 H_2O (B3LYP-GP/B3LYP-GP)	***D*** [k]	−17.5[i]		0.55	87
						CM, 9 H_2O (B3LYP-GP/B3LYP-PCM)	***D*** [k]	3.8[j]		0.55	87

Table 2 (Continued)

	experimental data					quantum chemical computations					
	$\Delta H^{\ddagger}$	$\Delta S^{\ddagger}$	$\Delta G^{\ddagger}$	$\Delta V^{\ddagger}$	ref	model and method[a]	mech	$\Delta E^{\ddagger}$	$\Delta V^{\ddagger}$	$\Delta\Sigma$	ref
$UO_2(OH_2)_5^{2+}$	26	−40	38		125	CM, 5/6 H_2O (HF-GP/MP2-GP)	***I*$_d$**				125
						CM, 5 H_2O (HF-GP/MP2-GP)	***D***	37.0		0.66[l]	59
						CM, 5 H_2O (HF-CPCM/MP2-CPCM)	***D***	59.2	4.9	0.95[l]	59
						CM, 6 H_2O (HF-GP/MP2-GP)	***I***	38.1		−1.30[l]	59
						CM, 6 H_2O (HF-CPCM/MP2-CPCM)	***A***	18.7	−3.0	−1.29[l]	59
						CM, 6 H_2O (HF-GP/MP2-GP)	***D***	45.7		0.41[l]	59
						CM, 6 H_2O (HF-CPCM/MP2-CPCM)	***D***	74.0	4.6	0.58[l]	59
$UO_2(OH_2)_5^{+}$						CM, 6 H_2O (HF-GP/MP2-CPCM)	***D***	36.4			126
$UO_2(C_2O_4)_2OH_2^{2-}$						CM, 1 H_2O (HF-GP/MP2-GP)	***D***	20.6	4.6	0.49[l]	59
						CM, 1 H_2O (HF-GP/MP2-CPCM)	***D***	53.8	4.6	0.49[l]	59
						CM, 2 H_2O (HF-GP/MP2-GP)	***D***	21.3	4.1	0.71[l]	59
						CM, 2 H_2O (HF-GP/MP2-CPCM)	***D***	56.3	4.1	0.71[l]	59
						CM, 2 H_2O (HF-GP/MP2-GP)	***A***	28.8	−3.5	−2.51[l]	59
						CM, 2 H_2O (HF-GP/MP2-CPCM)	***A***	11.7	−3.5	−2.51[l]	59
$UO_2F_4(OH_2)^{2-}$						CM, 2 H_2O (HF-CPCM/MP2-CPCM)	***D***	39.2	4.7		127
						CM, 2 H_2O (HF-CPCM/MP2-CPCM)	***I***	49.5	0.5		127
						CM, 1 H_2O (HF-CPCM/MP2-CPCM)	***D***	26.1	1.8		127
$NpO_2(OH_2)_5^{2+}$						CM, 6 H_2O (HF-CPCM/MP2-CPCM)	***A***	30.0			126
						CM, 6 H_2O (HF-CPCM/MP2-CPCM)	***D***	70.0			126
$AmO_2(OH_2)_5^{2+}$						CM, 6 H_2O (HF-GP/MP2-CPCM)	***A***	>22.6			126
						CM, 6 H_2O (HF-GP/MP2-CPCM)	***D***	>67.7			126

[a] Abbreviations: CM, cluster model. In parentheses is shown the computational level for the geometry/energy: GP, free ions in the gas phase; SCRF, hydration calculated with self-consistent reaction fields; (C)PCM, hydration calculated with the (conductor-like) polarizable continuum model. [b] Attack of the entering H_2O adjacent to the leaving H_2O. [c] Attack of the entering H_2O adjacent to the NH_3 trans to the leaving H_2O. [d] The same geometry was obtained for the transition state $[cis\text{-}Rh(NH_3)_5\cdots(OH_2)_2^{3+}]^{\ddagger}$ at the CAS-SCF-SCRF level. [e] Reaction via the lowest electronic triplet state. [f] For a protein environment, $\epsilon = 4$. [g] $\Delta G^{\ddagger}$. [h] The H_2O ligand cis to OH^- is leaving. [i] From "*E*(SCF)" in Table 2 of ref 87. [j] From the sum of the "*E*(SCF)" and "PCM energy" terms in Table 2 of ref 87. [k] The H_2O ligand trans to OH^- is leaving. [l] The U=O bond length changes are not considered. [m] In acetone. [n] Rocking motion of the Cp ligand.

on $Cr(NH_3)_5OH_2^{3+}$: the ***I*$_a$** pathway with retention of the configuration is most favorable, whereas that with stereomobility, involving the attack of the incoming H_2O opposite to the leaving H_2O, is the least favorable. The data in Table 2 show that the gas-phase activation energies are inaccurate and that hydration has to be included to obtain agreement with experiment.

The water exchange reaction on $Rh(NH_3)_5OH_2^{3+}$ proceeds via the ***I*** mechanism with retention of the configuration. Computations on the stereomobile pathway were not feasible for the low-spin (singlet) electron configuration, but for the lowest triplet state, a transition state for ***I*$_d$** could be computed. Its activation energy (Table 2) is enormously high due to the spin change, and the dissociative character is due to the elongation of bonds arising from the formation of the triplet state, which requires the promotion of one electron from a nonbonding orbital into an antibonding one. The ***I*** mechanism is more favorable than ***D***. For $Rh(NH_2CH_3)_5OH_2^{3+}$, both dissociative pathways, ***I*$_d$** and ***D***, were available, as for Cr^{III}, and their activation energies ($\Delta E^{\ddagger}$) are equal but somewhat too low compared with $\Delta H^{\ddagger}$. Also in this case, the calculations cannot be used for the distinction of the ***I*$_d$** from the ***D*** mechanism. The Rh···O bond lengths in the transition state for the ***I*** mechanism, $[cis\text{-}Rh(NH_3)_5\cdots(OH_2)_2^{3+}]^{\ddagger}$, are longer than those in the corresponding Cr^{III} and Ru^{III} species because of the additional electron in the d_β level (section 5.3). Since the experimental activation volumes for $Ru(NH_3)_5OH_2^{3+}$ and $Rh(NH_3)_5OH_2^{3+}$ are equal (Table 2) and because the intrinsic components of $\Delta V^{\ddagger}$ are greater for Rh^{III} than for Ru^{III} (due to the

different Rh···O and Ru···O bond lengths in the transition state), the respective electrostrictive components have to be different as well, whereby $\Delta V_{el}^{\ddagger}$ for Rh^{III} is smaller. This could be taken as an indication that $\Delta V_{el}^{\ddagger}$ might not always be zero or constant for similar reactions.

All of these water exchange reactions on amine and aqua complexes of Cr^{III}, Ru^{III}, and Rh^{III} proceed with retention of the configuration, and the pertinent reasons will be discussed later (section 5.4).

Water exchange on $TiOH(OH_2)_5^{2+}$ proceeds via the ***D*** mechanism, whereby the water ligand trans to OH^- is eliminated most readily (due to the trans effect). In this reactant, involving an anion bound to a cation, there is a sizable permanent electric dipole moment that interacts with the solvent. Thus, the geometries and energies computed with B3LYP on the basis of the gas-phase model might be inaccurate: for such systems, hydration has to be included for the calculation of both geometry and energy.

Lundberg et al.[123] modeled water exchange reactions on mono- and dimeric Mn^{III} and Mn^{IV} centers in order to understand the reactivity of manganese compounds in biological systems. The geometries were optimized for the free ions (in the gas phase), and the energies were computed with COSMO, whereby a dielectric constant of 4 was used to mimic the protein environment. The ***D*** pathway is most favorable for all of these reactions. For $Mn^{III}(OH)_3(OH_2)_2$, the ***A*** mechanism is feasible but unfavorable by >16 kJ/mol (the transition state was not computed, but the hexacoordinated intermediate was). The tetracoordinated trihydroxy−aqua Mn^{III} species was predicted to be more stable than the corresponding pentacoordinated diaqua Mn^{III} species. This could be incorrect, since DFT, also with the B3LYP functional, favors the lower coordination number systematically.[10] In $Mn^{IV}(OH)_2(Cl)(OH_2)_2$, the substitution of OH^- by H_2O was also investigated. It involves first a H^+ transfer from an aqua ligand to the leaving hydroxide. This reaction is assisted by a H_2O molecule in the second coordination sphere and has a barrier of 21.8 kJ/mol. Subsequently, this H_2O molecule is exchanged via the ***D*** mechanism.

In the $[(H_2O)_2(HO)_2Mn^{IV}]_2(\mu\text{-}O)_2$ dimer were modeled[123] the exchange of a H_2O trans to the μ-O bridge and the substitution of one μ-O ligand by H_2O. The latter reaction proceeds in a sequence of many steps involving protonation and opening of one μ-O bridge. The exchange of the μ-OH bridge in $(H_2O)(OH)_3(Cl)Mn^{IV}(OH)Ca^{II}(OH)(OH_2)_4$ and the exchange of the terminal oxyl radical in $[(terpy)(H_2O)Mn^{IV}(\mu\text{-}O)_2Mn^{IV}(O^{\bullet})(terpy)]^{3+}$ were also investigated.

The computations[87] on the water exchange reaction on $ThOH(OH_2)_9^{3+}$ are incorrect, since the B3LYP gas-phase energies (that are based on B3LYP gas-phase geometries) of the transition states [*cis/trans*-$ThOH(OH_2)_8\cdots OH_2^{3+}]^{\ddagger}$ are lower than those of the reactant. Furthermore, as already mentioned, gas-phase geometries of hydroxy complexes of Th^{IV} are most likely inaccurate. From the reported data,[87] it is questionable whether the coordination number of the hydroxy complex is 10.

In a combined experimental and quantum chemical study, Alezra et al.[124] synthesized the $CpRu((R)\text{-Binop-F})(OH_2)^+$ complex and investigated its water exchange reaction and the equivalencing of the two diastereotopic P donor atoms of the Binop-F ligand by variable-temperature and variable-pressure NMR. Furthermore, they modeled these reactions quantum chemically by optimizing the geometries of the free ions in the gas phase using the PW91 functional. The energies were computed for PCM acetone, also with PW91. In good agreement with experiment, they computed $\Delta G^{\ddagger}$ for the ***D***-activated water exchange process and the rocking motion of the Cp ligand (Table 2). Furthermore, they calculated a third transition state, claimed to be that for the $\boldsymbol{I_d}$ mechanism. The inspection of the imaginary mode (species H in Table 5, ref 124) shows that one H_2O molecule is virtually immobile, that the other one moves as for the ***D*** mechanism (B in Table 5, ref 124), and that the Cp ligand performs the rocking motion (D in Table 5, ref 124). To be the transition state for $\boldsymbol{I_d}$ would require that the imaginary mode describes a concerted motion of *both* H_2O molecules, as, for example, in $[cis\text{-}V(OH_2)_5\cdots(OH_2)_2^{2+}]^{\ddagger}$ (Figure 5a). The "$\boldsymbol{I_d}$ transition state" is most likely that for the loss of H_2O (***D*** mechanism) occurring concerted with the equivalencing of the diastereotopic P donors of Binop-F; the other H_2O looks just like an immobile spectator.

In a first article, Farkas et al.[125] reported a variable-temperature ^{17}O NMR study on the water exchange reaction on $UO_2(OH_2)_5^{2+}$. They measured $\Delta H^{\ddagger}$ and $\Delta S^{\ddagger}$, but $\Delta V^{\ddagger}$ was not available (Table 2). To attribute the exchange mechanism, they resorted to the model[101] in which the transition states are approximated by species with increased or decreased coordination numbers, whereby their geometries were computed with constraints (see beginning of section 4.2.1). This model was known[53,54] to favor the dissociative mechanism, since it had predicted erroneously a dissociative exchange mechanism for $V(OH_2)_6^{2+}$ and $Mn(OH_2)_6^{2+}$. Furthermore, the chosen computational methods, geometry optimizations at the HF level and energy computations with MP2, are inadequate, as can be seen by the large error in the U=O and U−O bond lengths of $UO_2(OH_2)_5^{2+}$: the former are too short by 0.11 Å and the latter too long by 0.15 Å. The MP2 energies are questionable due to the presence of static electron correlation (see below).

In a second study on $UO_2(OH_2)_5^{2+}$ from the same laboratory,[59] a better model[53,54] was used, and hydration was included using CPCM in both the geometry optimizations and the energy computations. Also, these results are not free of doubts because the same quantum chemical methods as in the first study have been applied. In $UO_2(OH_2)_5^{2+}$, there is static electron correlation, arising from the population of σ^*(M=O) and π^*(M=O) MOs by σ(M=O) and π(M=O) electrons as in $VO(OH_2)_5^{2+}$.[10] Such systems require[10] CAS-SCF or the improved CAS-SCF based second-order perturbation theory, such as CASPT2[26,27] or MC-QDPT2.[28,29] Due to the neglect of static correlation

Table 3. Substitution Reactions

reaction	experimental data					quantum chemical computations				
	$\Delta H^{\ddagger}$	$\Delta S^{\ddagger}$	$\Delta G^{\ddagger}$	$\Delta V^{\ddagger}$	ref	model and method[a]	mech	$\Delta E^{\ddagger}$	$\Delta\Sigma$	ref
$Cr(NH_3)_5Cl^{2+} + H_2O \rightarrow Cr(NH_3)_5OH_2^{3+} + Cl^-$	93	−29	102	−10.6	133, 134	CM (HF-SCRF/HF-PCM)	I_a	112.5	−0.93	135
$Co(NH_3)_5Cl^{2+} + H_2O \rightarrow Co(NH_3)_5OH_2^{3+} + Cl^-$	93	−44	106	−9.9	136, 137	CM (HF-SCRF/HF-PCM)	I_d	129.0	−0.15	135
$Co(NH_3)_5NCS^{2+} + H_2O \rightarrow Co(NH_3)_5OH_2^{3+} + SCN^-$						CM (HF-SCRF/HF-PCM)	I_d	152.9	2.07	33
$Co(NH_3)_5SCN^{2+} + H_2O \rightarrow Co(NH_3)_5OH_2^{3+} + SCN^-$			112.7		138	CM (HF-SCRF/HF-PCM)	I_d	119.6	1.84	33
cis-$Pd(NH_3)_2Cl_2 + H_2O \rightarrow$ *cis*-$Pd(NH_3)(OH_2)Cl_2 + NH_3$						CM (MP2-GP/CCSD(T)-GP)	I_a	77	−0.28	139
cis-$Pd(NH_3)_2Cl_2 + H_2O \rightarrow$ *cis*-$Pd(NH_3)_2(OH_2)Cl^+ + Cl^-$						CM (MP2-GP/CCSD(T)-GP)	I_a	76	−0.17	139
cis-$Pd(NH_3)(OH_2)Cl_2 + H_2O \rightarrow$ *cis*-$Pd(OH_2)_2Cl_2 + NH_3$						CM (MP2-GP/MP2-GP)	I_a	115	−0.75	139
cis-$Pd(NH_3)(OH_2)Cl_2 + H_2O \rightarrow$ *cis*-$Pd(NH_3)(OH_2)_2Cl^+ + Cl^-$						CM (MP2-GP/MP2-GP)	I_a	95	−0.88	139
cis-$Pd(NH_3)(OH_2)Cl_2 + H_2O \rightarrow$ *trans*-$Pd(NH_3)(OH_2)_2Cl^+ + Cl^-$						CM (MP2-GP/MP2-GP)	I_a	118	−0.93	139
cis-$Pd(NH_3)_2(OH)Cl + H_2O \rightarrow$ *cis*-$Pd(NH_3)(OH_2)(OH)Cl + NH_3$						CM (MP2-GP/MP2-GP)	I_a	92	−0.76	139
cis-$Pd(NH_3)_2(OH)Cl + H_2O \rightarrow$ *trans*-$Pd(NH_3)(OH_2)(OH)Cl + NH_3$						CM (MP2-GP/MP2-GP)	I_a	115	−0.56	139
cis-$Pd(NH_3)_2(OH)Cl + H_2O \rightarrow$ *cis*-$Pd(NH_3)_2(OH_2)(OH)^+ + Cl^-$						CM (MP2-GP/MP2-GP)	I_a	92	−0.90	139
trans-$Pd(NH_3)_2Cl_2 + H_2O \rightarrow$ *trans*-$Pd(NH_3)(OH_2)Cl_2 + NH_3$						CM (MP2-GP/CCSD(T)-GP)	I_a	99	−1.07	139
trans-$Pd(NH_3)_2Cl_2 + H_2O \rightarrow$ *trans*-$Pd(NH_3)_2(OH_2)Cl^+ + Cl^-$						CM (MP2-GP/CCSD(T)-GP)	I_a	91	−1.04	139
trans-$Pd(NH_3)(OH_2)Cl_2 + H_2O \rightarrow$ *trans*-$Pd(OH_2)_2Cl_2 + NH_3$						CM (MP2-GP/MP2-GP)	I_a	133	−1.04	139
trans-$Pd(NH_3)(OH_2)Cl_2 + H_2O \rightarrow$ *cis*-$Pd(NH_3)(OH_2)_2Cl^+ + Cl^-$						CM (MP2-GP/MP2-GP)	I_a	123	−0.88	139
trans-$Pd(NH_3)_2(OH)Cl + H_2O \rightarrow$ *cis*-$Pd(NH_3)(OH_2)(OH)Cl + NH_3$						CM (MP2-GP/MP2-GP)	I_a	140	−0.89	139
trans-$Pd(NH_3)_2(OH)Cl + H_2O \rightarrow$ *trans*-$Pd(NH_3)_2(OH_2)(OH)^+ + Cl^-$						CM (MP2-GP/MP2-GP)	I_a	126	−0.86	139
$PtCl_4^{2-} + H_2O \rightarrow Pt(OH_2)Cl_3^- + Cl^-$	87.9	−33	97.9		140	CM (BP-COSMO/BP-COSMO)	I_a	93.9[d]		141
$Pt(NH_3)Cl_3^- + H_2O \rightarrow$ *trans*-$Pt(NH_3)(OH_2)Cl_2 + Cl^-$	62.8	−126	100.0		140	CM (BP-COSMO/BP-COSMO)	I_a	105.0[d]		141
$Pt(NH_3)Cl_3^- + H_2O \rightarrow$ *cis*-$Pt(NH_3)(OH_2)Cl_2 + Cl^-$	83.7	−38	95.0		140	CM (BP-COSMO/BP-COSMO)	I_a	107.1[d]		141
$Pt(OH_2)Cl_3^- + H_2O \rightarrow$ *cis*-$Pt(OH_2)_2Cl_2 + Cl^-$	83.7	−46	97.5		140	CM (BP-COSMO/BP-COSMO)	I_a	107.3[d]		141
$Pt(OH_2)Cl_3^- + H_2O \rightarrow$ *trans*-$Pt(OH_2)_2Cl_2 + Cl^-$	100.4	−50	115.5		140	CM (BP-COSMO/BP-COSMO)	I_a	122.2[d]		141
$PtCl_4^{2-} + NH_3 \rightarrow Pt(NH_3)Cl_3^- + Cl^-$	66.9	−92	94.6		140	CM (BP-COSMO/BP-COSMO)	I_a	89.8[d]		141
$Pt(NH_3)Cl_3^- + NH_3 \rightarrow$ *trans*-$Pt(NH_3)_2Cl_2 + Cl^-$	75.3	−75	95.8		140	CM (BP-COSMO/BP-COSMO)	I_a	99.1[d]		141
$Pt(NH_3)Cl_3^- + NH_3 \rightarrow$ *cis*-$Pt(NH_3)_2Cl_2 + Cl^-$	66.9	−75	89.5		140	CM (BP-COSMO/BP-COSMO)	I_a	89.7[d]		141
cis-$Pt(NH_3)_2Cl_2 + H_2O \rightarrow$ *cis*-$Pt(NH_3)(OH_2)Cl_2 + NH_3$						CM (MP2-GP/CCSD(T)-GP)	I_a	121	−0.24	139
cis-$Pt(NH_3)_2Cl_2 + H_2O \rightarrow$ *cis*-$Pt(NH_3)_2(OH_2)Cl^+ + Cl^-$	83.7	−59	101.3		140	CM (BP-COSMO/BP-COSMO)	I_a	109.7[d]		141
	87.0	−36	97.0	−9.5	142, 143	CPMD,[b] 35 H_2O (BLYP)	I_a	∼88		65
cis-$Pt(NH_3)_2Cl_2 + NH_3 \rightarrow Pt(NH_3)_3(OH_2)^{2+} + Cl^-$	75.3	−63.0	94.1		140	CM (BP-COSMO/BP-COSMO)	I_a	100.4[d]		141
						CM (mPW1PW91-GP/mPW1PW91-GP)[c]	I_a	98.9[d]		144
						CM (mPW1PW91-SCRF/mPW1PW91-PCM[e])[c]	I_a	100.9[d]		144
						CM (MP2-GP/CCSD(T)-GP)	I_a	110	−0.46	139
						CM (mPW1-GP/mPW1-GP)[c]	I_a	95.9		145
						CM, 10 H_2O (mPW1-GP/mPW1-GP)[c]	I_a	101.6		145

Table 3 (Continued)

reaction	experimental data $\Delta H^{\ddagger}$	$\Delta S^{\ddagger}$	$\Delta G^{\ddagger}$	$\Delta V^{\ddagger}$	ref	quantum chemical computations model and method[a]	mech	$\Delta E^{\ddagger}$	$\Delta\Sigma$	ref
cis-$Pt(NH_3)_2(OH_2)Cl^+ + H_2O \rightarrow$ *cis*-$Pt(NH_3)_2(OH_2)_2^{2+} + Cl^-$	83.7	−46.0	97.5		140	CM (BP-COSMO/BP-COSMO)	I_a	116.0[d]		141
						CM (mPW1PW91-GP/mPW1PW91-GP)[c]	I_a	153.0[d]		144
						CM (mPW1PW91-SCRF/mPW1PW91-PCM[e])[b]	I_a	135.0[d]		144
cis-$Pt(NH_3)(OH_2)Cl_2 + H_2O \rightarrow$ *cis*-$Pt(OH_2)_2Cl_2 + NH_3$						CM (MP2-GP/CCSD(T)-GP)	I_a	126	−0.69	139
cis-$Pt(NH_3)(OH_2)Cl_2 + H_2O \rightarrow$ *cis*-$Pt(NH_3)(OH_2)_2Cl^+ + Cl^-$						CM (MP2-GP/CCSD(T)-GP)	I_a	119	−0.84	139
cis-$Pt(NH_3)(OH_2)Cl_2 + H_2O \rightarrow$ *trans*-$Pt(NH_3)(OH_2)_2Cl^+ + Cl^-$						CM (MP2-GP/CCSD(T)-GP)	I_a	123	−0.92	139
cis-$Pt(NH_3)_2(OH)Cl + H_2O \rightarrow$ *cis*-$Pt(NH_3)(OH_2)(OH)Cl + NH_3$						CM (MP2-GP/CCSD(T)-GP)	I_a	128	−0.75	139
cis-$Pt(NH_3)_2(OH)Cl + H_2O \rightarrow$ *trans*-$Pt(NH_3)(OH_2)(OH)Cl + NH_3$						CM (MP2-GP/CCSD(T)-GP)	I_a	127	−0.54	139
cis-$Pt(NH_3)_2(OH)Cl + H_2O \rightarrow$ *cis*-$Pt(NH_3)_2(OH_2)(OH)^+ + Cl^-$	92	−75	115		142	CM (MP2-GP/CCSD(T)-GP)	I_a	109	−0.91	139
trans-$Pt(NH_3)_2Cl_2 + H_2O \rightarrow$ *trans*-$Pt(NH_3)(OH_2)Cl_2 + NH_3$						CM (MP2-GP/CCSD(T)-GP)	I_a	141	−1.04	139
trans-$Pt(NH_3)_2Cl_2 + H_2O \rightarrow$ *trans*-$Pt(NH_3)_2(OH_2)Cl^+ + Cl^-$	92	−26	100		142	CM (MP2-GP/CCSD(T)-GP)	I_a	123	−1.00	139
	79.5	−46	93.3		140	CM (BP-COSMO/BP-COSMO)	I_a	106.6[d]		141
trans-$Pt(NH_3)(OH_2)Cl_2 + H_2O \rightarrow$ *trans*-$Pt(OH_2)_2Cl_2 + NH_3$						CM (MP2-GP/CCSD(T)-GP)	I_a	156	−1.03	139
trans-$Pt(NH_3)(OH_2)Cl_2 + H_2O \rightarrow$ *cis*-$Pt(NH_3)(OH_2)_2Cl^+ + Cl^-$						CM (MP2-GP/CCSD(T)-GP)	I_a	142	−0.78	139
trans-$Pt(NH_3)_2(OH)Cl + H_2O \rightarrow$ *cis*-$Pt(NH_3)(OH_2)(OH)Cl + NH_3$						CM (MP2-GP/CCSD(T)-GP)	I_a	160	−0.77	139
trans-$Pt(NH_3)_2(OH)Cl + H_2O \rightarrow$ *trans*-$Pt(NH_3)_2(OH_2)(OH)^+ + Cl^-$						CM (MP2-GP/CCSD(T)-GP)	I_a	123	−0.75	139
trans-$Pt(NH_3)_2Cl_2 + NH_3 \rightarrow Pt(NH_3)_3Cl^+ + Cl^-$	41.8	−138	82.8		140	CM (BP-COSMO/BP-COSMO)	I_a	91.6[d]		141
$Pt(NH_3)_3Cl^+ + H_2O \rightarrow Pt(NH_3)_3(OH_2)^{2+} + Cl^-$	75.3	−75	97.9		140	CM (BP-COSMO/BP-COSMO)	I_a	114.1[d]		141
$Pt(NH_3)_3Cl^+ + NH_3 \rightarrow Pt(NH_3)_4^{2+} + Cl^-$	71.1	−63	90.0		140	CM (BP-COSMO/BP-COSMO)	I_a	94.6[d]		141
$Pt(en)Cl_2 + H_2O \rightarrow Pt(en)(OH_2)Cl^+ + Cl^-$	85	−42	98	−9.2	143, 146	CM (MP2-GP/MP2-GP)		103[d]		147
$Pt(en)(OH_2)Cl^+ + H_2O \rightarrow Pt(en)(OH_2)_2^{2+} + Cl^-$	34	−209	96		146	CM (MP2-GP/MP2-GP)		144[d]		147
						CM (MP2-GP/MP2-PCM)		108[d,f]		148
						CM (MP2-GP/MP2-PCM)		99[d,f]		148
$Pt(dien)Cl^+ + H_2O \rightarrow Pt(dien)(OH_2)^{2+} + Cl^-$						CM (mPW1PW91-GP/mPW1PW91-GP)[c]	I_a	123.1[d]		144
						CM (mPW1PW91-SCRF/mPW1PW91-PCM[e])[c]	I_a	108.7[d]		144
$UO_2(OH_2)_5^{2+} + HF \rightarrow UO_2F(OH_2)_4^+ + H_3O^+$	38	−12	42		149	CM (B3LYP-GP/B3LYP-GP)		∼34		150

[a] Abbreviations: CM, cluster model involving, unless noted otherwise, solely the reactants. In parentheses is shown the computational level for the geometry/energy: GP, free ions in the gas phase; SCRF, hydration calculated with self-consistent reaction fields; PCM, hydration calculated with the polarizable continuum model; COSMO, hydration calculated with the conductor-like screening model. [b] Constrained CPMD calculations.[15,16] [c] mPW1PW91 or mPW1 is the PW91 functional, modified according to Adamo and Barone.[151] [d] $\Delta G^{\ddagger}$. [e] The self-consistent isodensity version of the PCM was used. [f] The reaction was investigated starting from two isomers for the water adduct $Pt(en)Cl_2 \cdot OH_2$.

in the geometry optimizations, the U=O bonds are too short, and this error is opposite to the common error in the U−O bonds, which are too long, as are all of the M−O bonds of aqua ions. BLYP and B3LYP yield good U=O and U−O bond lengths,[128] but the H-bonds between H_2O molecules in the first and the second coordination sphere are expected to be too short.[10] Hence, it remains to be shown whether DFT is suitable for the geometry optimizations of such H-bonded systems. The single-reference MP2 energies are not appropriate either, also because of static electron correlation. For MP2 to be appropriate, the zeroth-order (Hartree−Fock) wave function must be a good approximation and, therefore, the perturbation must be small. If static correlation is present, this condition is not fulfilled. Most preferably, the energies should be evaluated using CAS-SCF based second-order perturbation theory.[10]

Table 4. Rearrangements

reaction	experimental data $\Delta H^{\ddagger}$	$\Delta S^{\ddagger}$	$\Delta G^{\ddagger}$	$\Delta V^{\ddagger}$	ref	quantum chemical computations model and method[a]	mech	$\Delta E^{\ddagger}$	$\Delta\Sigma$	ref
(i) Linkage Isomerizations										
$Co(NH_3)_5\mathbf{S}CN^{2+} \rightarrow Co(NH_3)_5\mathbf{N}CS^{2+}$			106.9		33	CM (HF-SCRF/HF-PCM)	***I***	108.6	0.06	33
						CM (HF-GP/HF-GP)	$\boldsymbol{I_a}$	143.1	−0.40	33
$Co(NH_3)_5\mathbf{S}CN{\cdot}OH_2^{2+} \rightarrow Co(NH_3)_5\mathbf{N}CS{\cdot}OH_2^{2+}$						CM (HF-SCRF/HF-PCM)	***I***	105.4	−0.02	33
$Co(NH_3)_5\mathbf{S}CN^{2+} \rightarrow Co(NH_3)_5{\cdot}NCS^{2+}$						CM (HF-GP/HF-GP)	***D***	269.1	2.33	33
						CM (HF-SCRF/HF-PCM)	***D***	139.5	2.98	33
$Co(NH_3)_5\mathbf{O}NO^{2+} \rightarrow Co(NH_3)_5\mathbf{N}O_2^{2+}$						CM (B3LYP-GP/B3LYP-GP)	$\boldsymbol{I_a}$	143.5	−0.64	34
	91.6	−17	96.7	−6.7	154	CM (B3LYP-PCM/B3LYP-PCM)	$\boldsymbol{I_a}$	107.9	−0.10	34
	102[b]	−7[b]	104[b]		155	CM (B3LYP-PCM/B3LYP-PCM)	$\boldsymbol{I_a}$	118[b,c]		34
	106[d]	0[d]	106[d]		153	CM (B3LYP-PCM/B3LYP-PCM)	$\boldsymbol{I_a}$	126[c,d]		34
reaction 9	70.2	23.1	63.3		154	CM (HF-CPCM/MP2-CPCM)	$\boldsymbol{I_d}$	63		157
						CM (HF-GP/MP2-GP)	$\boldsymbol{I_d}$	48		157
reaction 10 (mechanism A)						CM (HF-GP/MP2-CPCM)	$\boldsymbol{I_d}$	∼90		157
reaction 10 (mechanism B)						CM (HF-CPCM/MP2-CPCM)	$\boldsymbol{I_a}$	38		157
						CM (HF-GP/MP2-CPCM)	$\boldsymbol{I_a}$	28		157
reaction 10 (mechanism C)						CM (HF-GP/MP2-CPCM)		39[e]		157
(ii) cis−trans Isomerization										
cis-$Cu(NH_2CH_2COO)_2 \rightarrow$ *trans*-$Cu(NH_2CH_2COO)_2$						CM (G3′-GP/G3′-GP[f])		33.1		156
(iii) Rearrangement of Pentacoordinated Species										
reaction 11 ($Cr(NH_3)_5^{3+}$)						CM (HF-SCRF/MCQDPT2-PCM)		21.3	0.04	84
						CM (CAS-SCF-SCRF/MCQDPT2-PCM)		230[g]	0.01[g]	84
reaction 11 ($Cr(NH_2CH_3)_5^{3+}$)						CM (HF-SCRF/MCQDPT2-PCM)		22.1	0.04	84
reaction 11 ($Cu(OH_2)_5^{2+}$)						CPMD, 50 H_2O (BLYP)				77

[a] Abbreviations: see footnote *c* of Table 1 and footnote *a* of Tables 2 and 3. [b] In acetone. [c] Energy based on the gas-phase geometry. [d] In tetrahydrofuran. [e] Activation energy based on the highest lying transition state with respect to the reactant. [f] G3′: modified G3 method, G3(MP2)-$B3_{LanL2DZ}$. [g] Via the lowest doublet state of the trigonal bipyramidal transition state.

The methodology (MP2-CPCM energies based on HF-CPCM geometries) introduced in this $UO_2(OH_2)_5^{2+}$ study[59] was applied to a variety of other UO_2^{2+} reactions (Tables 2 and 3). For this reason, and to be thorough, the authors should have assessed the reliability of their approximations, that is, the neglect of static electron correlation in both the geometry optimizations and the energy computations. Errors in the energies may cancel (fortuitously) or not, and this needs to be verified. As shown[10] for other quantum chemical studies on metal aqua ions, inappropriate computational methods gave rise to incorrect conclusions and statements.

It is quite unusual that a different exchange mechanism was found, when hydration effects were included: on the basis of the gas-phase model, the ***I*** mechanism was obtained, whereas, with hydration, the ***A*** mechanism was found,[59] which is proposed to be the water exchange pathway for $UO_2(OH_2)_5^{2+}$,

Table 5. Transition Metal Ions Exhibiting a Pronounced Preference for the Square Pyramidal Geometry

metal ion	electron config	steric course of substitution reactions of the corresponding (pseudo-) octahedral complexes
V^{II}, Cr^{III}	high-spin d^3	retention of the configuration
Fe^{III}	low-spin d^5	stereomobile, if a trigonal bipyramid with a sextet state lying close to the doublet ground state of the square pyramid exists
Ru^{III}	low-spin d^5	retention of the configuration
Fe^{II}, Co^{III}	low-spin d^6	stereomobile, if a trigonal bipyramid with a quintet state lying close to the singlet ground state of the square pyramid exists
Ru^{II}, Rh^{III}, Ir^{III}	low-spin d^6	retention of the configuration
Ni^{II}	high-spin d^8	retention of the configuration

since its activation energy is lower than that for the ***D*** pathway.

Also in their second article, Vallet et al.[59] investigated the water exchange reaction on $UO_2(C_2O_4)_2OH_2^{2-}$ theoretically. Since HF-CPCM geometry optimizations were too demanding, they computed the MP2-CPCM energies for the gas-phase HF geometries. As for $UO_2(OH_2)_5^{2+}$, the ***A*** mechanism was predicted to be favored over ***D***. However, at the MP2-CPCM level, the intermediate with an increased coordination number, $UO_2(C_2O_4)_2(OH_2)_2^{2-}$, was found to be slightly more stable than the reactant $UO_2(C_2O_4)_2OH_2 \cdot OH_2^{2-}$. The replacement of four H_2O molecules by two $C_2O_4^{2-}$ ions, strong electron donors, is expected to *destabilize* the intermediate with a higher coordination number rather than stabilize it. With the reservation that ΔE is not equal to ΔG, this might be an additional indication for the inadequacies in the computations discussed above, in particular the inappropriate treatment of static electron correlation. Furthermore, for all of the species exhibiting a permanent dipole moment, hydration should have been included for the geometry optimizations, whereby a less demanding method than CPCM could have been used. As will be shown in the following, these most likely inappropriate computational methods are also at the origin of other incorrect or inconsistent results on reactions of the UO_2^{2+} ion.

The water exchange mechanism of $UO_2F_4(OH_2)^{2-}$ was also investigated by Vallet et al.[127] Hydration was treated with CPCM for the geometry optimizations and the energy computations (Table 2). Again, static electron correlation was neglected, which is responsible for too short U=O bonds and an unknown accuracy of the computed activation energies. Because of the unavailability of experimental data, the energies should have been computed with a method whose accuracy has been assessed, and the effect of the approximate geometries on the total energies should have been estimated. The ***D*** mechanism was favored over ***I***, possibly because of the repulsion of the water ligand by the negatively charged UO_2F_4 core. This result is opposite to that for the $UO_2(C_2O_4)_2OH_2^{2-}$ ion, exhibiting the same charge, which was predicted (see above) to undergo water exchange via the ***A*** mechanism. It is an open question whether the diametrical difference in the exchange mechanisms of $UO_2F_4(OH_2)^{2-}$ and $UO_2(C_2O_4)_2OH_2^{2-}$ is real or whether it is an artifact arising from inappropriate computational methods.

In their most recent study, Vallet et al.[126] reported quantum chemical calculations on the water exchange reaction on $UO_2(OH_2)_5^{+}$, $NpO_2(OH_2)_5^{2+}$, and $AmO_2(OH_2)_5^{2+}$ (Table 2), which were based on their usual approximations. For U^{V}, only the ***D*** mechanism could be computed, whereas, for Np^{V} and Am^{VI}, the ***A*** mechanism is favored over ***D***.

4.3. Ammonia Exchange Reactions

Rode and co-workers investigated the solvation of Cu^{2+} and Ag^{+} in ammonia with QM/MM MD simulations.[129,130] At the HF/MM level, Cu^{2+} is six coordinated (98% $Cu(NH_3)_6^{2+}$) with two short and four long Cu−N bonds of 2.05 and 2.17 Å, respectively. The ammonia exchange reaction proceeds via the I_d mechanism, and the mean residence time of an NH_3 ligand is 32 ps.[129] A lower coordination number was obtained on the basis of B3LYP/MM computations: the prevailing species (64%) is pentacoordinated with two short and three longer bonds. The $Cu(NH_3)_5^{2+}$ ion undergoes NH_3 exchange via the ***A*** mechanism; the residence time of NH_3 in the first coordination sphere is 10 ps.[129] Ammonia exchange on Cu^{2+} is faster than water exchange because of the "inverse" 2 + 4 or 2 + 3 Jahn−Teller structure.[129]

Since the HF method tends to overestimate coordination numbers, whereas DFT underestimates them,[10] the coordination number of Cu^{2+} as well as its ammonia exchange mechanism cannot be considered as established. If the "true" coordination number lies between the extremes of HF/MM and B3LYP/MM, $Cu(NH_3)_6^{2+}$ would exchange via the ***D*** mechanism because of the presence of significant amounts of $Cu(NH_3)_5^{2+}$.

According to HF/MM calculations by Armunanto et al.,[130] Ag^{+} is tetrahedral with Ag−N bond lengths of 2.54 Å, which are longer by >0.2 Å than the experimental values.[131,132] Since HF tends to overestimate metal−ligand bond lengths of electron-rich metal ions,[10] DFT might yield shorter Ag−N bonds which, possibly, are in better agreement with experiment. In contrast to the corresponding aqua ion (section 4.2.1), the ammine complex has a well-defined, quite inert coordination sphere.[130]

4.4. Fluoride Exchange Reactions

The fluoride exchange process on $UO_2F_5^{3-}$ was investigated[127] together with the water exchange on $UO_2F_4(OH_2)^{2-}$ (section 4.2.2). The direct fluoride exchange (reaction 2)

$$UO_2F_5^{3-} + \mathbf{F}^- \rightarrow UO_2(\mathbf{F})F_4^{3-} + F^- \qquad (2)$$

and the exchange via hydrolysis, followed by the substitution of water by fluoride, (reactions 3 and 4) were considered.

$$UO_2F_5^{3-} + H_2O \rightarrow UO_2F_4(OH_2)^{2-} + F^- \qquad (3)$$

$$UO_2F_4(OH_2)^{2-} + \mathbf{F}^- \rightarrow UO_2(\mathbf{F})F_4^{3-} + H_2O \qquad (4)$$

The geometries were optimized at the HF level for the free and the hydrated ions (using CPCM), and the energies were calculated for the free and the hydrated ions with HF and MP2 methods. Due to the importance of H-bonding of F^- with H_2O, the ***D*** mechanism for reaction 2 was computed on the basis of $UO_2F_5 \cdot (OH_2)_n^{3-}$ clusters with $n = 0$, 1, and 2. The respective $\Delta E^{\ddagger}$ values are 93.1, 74.9, and 73.1 kJ/mol (MP2-CPCM level). The two-step process (reactions 3 and 4) was investigated starting from $UO_2F_5 \cdot OH_2^{3-}$. For reaction 3, proceeding via the interchange mechanism, $\Delta E^{\ddagger} = 70.5$ kJ/mol was obtained. On the basis of the long U···F bond in the transition state, the authors attributed the I_d mechanism to this reaction.[127] It should be noted, however, that $\Delta\Sigma$ is slightly negative, −0.37 Å (if changes in the U=O bond lengths are neglected), and that $\Delta V_{CPCM}^{\ddagger}$ is only

Scheme 4[a]

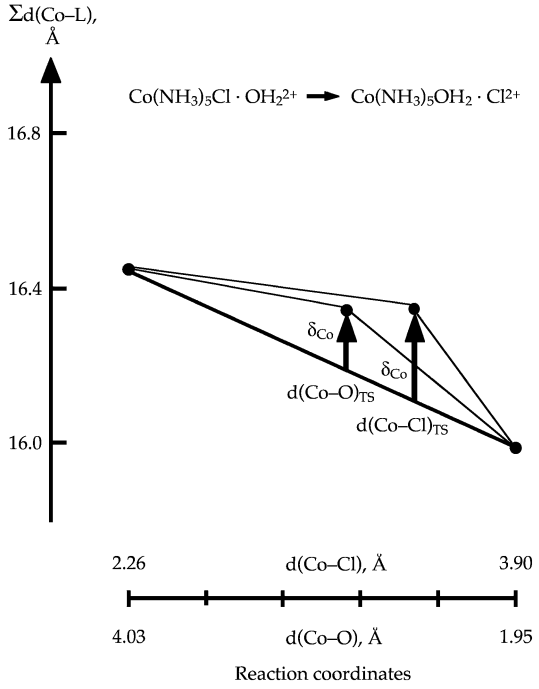

[a] Reprinted with permission from ref 135. Copyright 1999 American Chemical Society.

Scheme 5[a]

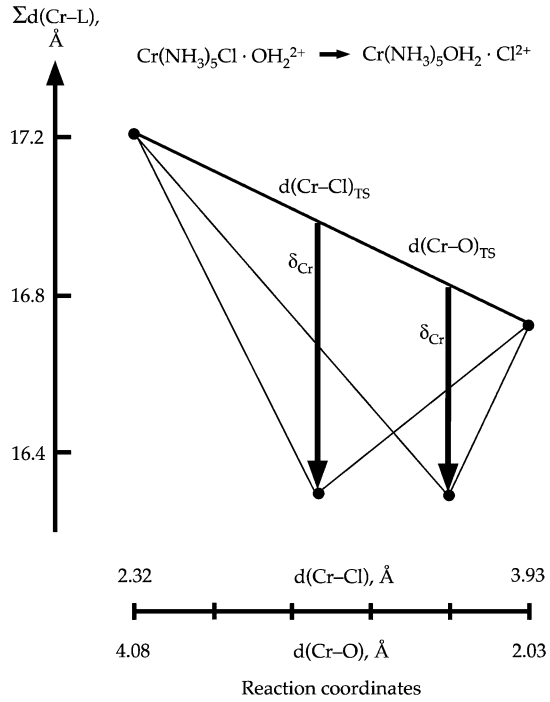

[a] Reprinted with permission from ref 135. Copyright 1999 American Chemical Society.

slightly positive, 1 cm^3/mol. On this basis, the ***I*** mechanism, eventually with a weak associative (on the basis of $\Delta\sum$) or a weak dissociative character (on the basis of $\Delta V_{CPCM}^{\ddagger}$), should not be ruled out for reaction 3. Since the reaction energy for 3 is 11.2 kJ/mol (Supporting Information of ref 127), the activation energy for reaction 4 is 59.3 kJ/mol. Hence, the direct pathway and the two-step fluoride exchange pathway have similar computed activation energies.

The authors preferred the ***D*** mechanism because this reaction would then involve the same intermediate as the water exchange on $UO_2F_4(OH_2)^{2-}$ (section 4.2.2). Also for this study, the effect of the negligence of static electron correlation on the geometries and the total energies is unknown.

4.5. Ligand Substitution Reactions

The activation volumes for the aquation (substitution by water) of $Co(NH_3)_5Cl^{2+}$ and $Cr(NH_3)_5Cl^{2+}$ are quite similar (Table 3), although the water exchange reactions on the respective aqua pentaammine complexes proceed via the $\boldsymbol{I_d}$ and the $\boldsymbol{I_a}$ mechanisms. In these aquations, the mechanistically diagnostic intrinsic activation volume ($\Delta V_{int}^{\ddagger}$) is masked by the electrostrictive ($\Delta V_{el}^{\ddagger}$) component as well as the reaction volume ($\Delta V°$). More than 25 years ago, Swaddle and co-workers[134,137] showed experimentally why the substitution mechanism is $\boldsymbol{I_d}$ for Co^{III} and $\boldsymbol{I_a}$ for Cr^{III}. The computations[135] on the two aquation reactions corroborate in a straightforward way Swaddle and co-workers' finding. Taking either the Co−Cl or the Co−O distance as a reaction coordinate, the $\sum(Co-L)_{TS}$ parameter at the transition state is greater than $\sum(Co-L)_{TS}$ for a hypothetically fully concerted ***I*** mechanism (Scheme 4). Likewise, for Cr^{III}, $\sum(Cr-L)_{TS}$ is smaller than $\sum(Cr-L)_{TS}$ for a hypothetically fully concerted ***I*** mechanism (Scheme 5). The difference in the reactivities of Co^{III} and Cr^{III} is due to their different number of 3d electrons (section 5.3).

All of the geometry optimizations were performed at the HF-SCRF level, since the gas-phase geometries of these compounds, which exhibit a sizable permanent dipole moment, are inaccurate.[135] The distinction of the present substitution mechanisms on the basis of $\sum(M-L)_{TS}$ requires predominantly reliable M−Cl and M−O bond lengths whereby, if hydration is neglected, the M−Cl bonds are too short. The energies, calculated at the HF-PCM level, are only qualitatively correct because dynamic as well as static electron correlation was neglected. In this case, they anyway are not useful for the distinction of reaction mechanisms.

The aquation of $Co(NH_3)_5SCN^{2+}$ (Table 3) is a minor parallel reaction of the S → N linkage isomerization (section 4.6.1). The aquation of its product, $Co(NH_3)_5NCS^{2+}$, was investigated for the comparison of the structures and energies of the transition states $[Co(NH_3)_5\cdots(\mathbf{S}CN)(OH_2)^{2+}]^{\ddagger}$ and $[Co(NH_3)_5\cdots(\mathbf{N}CS)(OH_2)^{2+}]^{\ddagger}$. As for $Co(NH_3)_5Cl^{2+}$, these two aquations proceed via the $\boldsymbol{I_d}$ mechanism. $[Co(NH_3)_5\cdots(\mathbf{N}CS)(OH_2)^{2+}]^{\ddagger}$ is slightly more stable (by 4.3 kJ/mol) than $[Co(NH_3)_5\cdots(\mathbf{S}CN)(OH_2)^{2+}]^{\ddagger}$: this shows that the (for low-spin Co^{III}) more nucleophilic N-end of SCN^- has an effect on the stability of the transition state. All of the three transition states for the $\boldsymbol{I_d}$ mechanism exhibit two weak bonds and are similar.

The first hydrolysis step of *cis*-$Pt(NH_3)_2Cl_2$ was investigated by Carloni et al.[65] using constrained CPMD (Table 3).[15,16] For each point, the Pt^{II} complex with 35 H_2O molecules in a periodically repeated box was simulated on the basis of the BLYP functional for ~1 ps; the computed activation energy agrees with

experiment. In a second set of calculations, they studied "cisplatin"−DNA interactions.

About one year later, Zang et al.[144] investigated the two hydrolysis steps of *cis*-$Pt(NH_3)_2Cl_2$ and the hydrolysis of $Pt(dien)Cl^+$ for the free and the hydrated ions. They assessed the performance of a variety of functionals and basis sets, whereby the mPW1PW91[151] functional was found to yield the best geometries for these systems. The geometries are sensitive to hydration, and so are the activation and reaction energies with the exception of the energies for the first hydrolysis step of *cis*-$Pt(NH_3)_2Cl_2$. The computed activation entropies deviate quite strongly from the experimental values, most likely because, as noted earlier,[23] in the present minimum CM, the solute−solvent interactions are not included.

Cooper and Ziegler[141] investigated the hydrolysis, ammoniolysis, and anation reactions of the experimentally well-studied[152] square-planar $Pt(OH_2)_x(NH_3)_y$-Cl_{4-x-y}^{x+y-2} complexes, which proceed via a direct and a solvent-assisted pathway. The relativistic DFT computations (with the BP functional) were performed for the free and the hydrated species using COSMO. The authors noted[141] that, although the reactions proceed via the $\boldsymbol{I_a}$ mechanism, the activation is dominated by bond breaking. The $\Delta H^{\ddagger}$ and $\Delta G^{\ddagger}$ values calculated on the basis of the free species in the gas phase deviate strongly from experiment.[141] They made the interesting observation that $\Delta G^{\ddagger}$ based on the hydrated species is more accurate than $\Delta H^{\ddagger}$ and $\Delta S^{\ddagger}$ because of a compensation between enthalpic and entropic effects arising from weak interactions, changes in solvent−solvent hydrogen bonding, and Coulomb interactions with the counterion, which are neglected in the model.[141] Changes in solute−solvent interactions are likely to contribute as well.

Burda et al.[139] studied recently the hydration of cis and trans dichloro-diammine complexes of Pd^{II} and Pt^{II} (Table 3): the geometries were optimized for the free ions (in the gas phase) at the MP2 level, and most energies were computed with CCSD(T), also for the free ions. The authors were apparently not aware of the various computations[33,135,141,144] on substitutions of anions (Table 3), in particular those of Pt^{II}, in which hydration was treated with continuum models, and that the model they used had been introduced about 8 years ago. It should be remembered that geometries and energies of hydrated species exhibiting sizable permanent dipole moments cannot be expected to be computed correctly as free species (in the gas phase).[32−34,103,141,144,145] This is manifested in the calculated activation energies for the ammonia substitution that, in several cases (Table 3), are only slightly higher than those for chloride substitution, although the latter reaction is much more facile in aqueous solution. Despite the numerous investigated reactions, those of *cis/trans*-$Pt(NH_3)_2(OH_2)Cl^+$ were not considered. The $\Delta\sum$ values were computed on the basis of the data in Table 1 of ref 139. Since all of these values are negative, the activation is associative. Due to the absence of any intermediate on the reaction path, the $\boldsymbol{I_a}$ mechanism is attributed to all of these reactions.

The hydrolysis of $Pt(en)Cl_2$ was investigated by Costa et al.[147] with HF, DFT, and MP2 methods on the basis of the gas-phase model. Also these authors did not seem to know the older related literature. It is interesting to note that, for both reactions, the hydrolysis of the first and the second chloride, all of the applied computational techniques supplied similar results (only the MP2 data are reported in Table 3). Due to the neglect of hydration effects, the activation energy for the second hydration step is too high by almost 50 kJ/mol. This discrepancy motivated the authors to reinvestigate the second reaction by taking into account hydration.[148] The activation energies that were, however, based on the corresponding inadequate[144,145] gas-phase geometries were computed with the PCM and SCRF model, whereby for the latter, dipole, quadrupole, and octupole terms were included. The MP2-PCM energies (Table 3) are closest to experiment. It should be noted that all of the investigated species exhibit permanent dipole moments and that, therefore, the gas-phase geometries are expected to be significantly different[33,34,144,145] from those in aqueous solution. In general, hydration needs to be included for the geometry optimization of such compounds.

In a study on the H-bonding characteristics of "cisplatin" as an antitumor drug, Robertazzi et al.[145] reinvestigated the first hydrolysis step of *cis*-Pt-$(NH_3)_2Cl_2$ using the mPW1 functional[151] and two CMs involving one and ten H_2O molecules (Table 3). Their calculations on the two free clusters in the gas phase showed that the geometries of all of the species, in particular that of the transition state, are very sensitive to hydration. In contrast, hydration had a small effect on the activation and reaction energies, most likely because of a fortuitous cancellation of errors which is absent in the second hydrolysis step.[144,148]

Toraishi et al.[150] investigated the substitution (reaction 5) in aqueous solution

$$UO_2(OH_2)_5^{2+} + HF \rightarrow UO_2F(OH_2)_4^{+} + H_3O^{+} \quad (5)$$

theoretically by decomposing it into three steps (reactions 6−8).

$$UO_2(OH_2)_5^{2+} + FH(OH_2)_n \rightarrow [UO_2(OH_2)_5 \cdot FH(OH_2)_n]^{2+} \quad (n = 1 \text{ or } 2) \quad (6)$$

$$[UO_2(OH_2)_5 \cdot FH(OH_2)_n]^{2+} \rightarrow [UO_2F(OH_2)_4 \cdot H_3O(OH_2)_n]^{2+} \quad (7)$$

$$[UO_2F(OH_2)_4 \cdot H_3O(OH_2)_n]^{2+} \rightarrow UO_2F(OH_2)_4^{+} + H_3O(OH_2)_n^{+} \quad (8)$$

The equilibrium constants of reactions 6 and 8 were estimated on the basis of the Fuoss equation,[153] and reaction 7 was investigated quantum chemically. The geometry was optimized for the free ions (in the gas phase) with the B3LYP functional, and the electronic energy was computed with the MP2 and B3LYP functionals by treating hydration with the CPCM.

The thermal corrections were based on gas-phase B3LYP Hessians.

The calculated free energy ($\Delta G°$) for reaction 5 disagrees considerably with experiment; it is too low (too exergonic) by more than ~40 kJ/mol. This deviation most likely arises from the inappropriate gas-phase geometries and the neglect of static electron correlation (section 4.2.2). For aqua ions, B3LYP favors the lower coordination number and, therefore, the dissociative pathway, whereby the associative mechanism is disfavored (section 2.3).[10] Thus, the adequacy of B3LYP for the present systems needs to be demonstrated. As already mentioned (section 4.2.2), MP2 is inadequate because of the presence of static electron correlation. The reactant and product of reaction 7 exhibit permanent dipole moments. Therefore, the geometries should be optimized by taking into account hydration (or the validity of the gas-phase geometry has to be assessed; for such systems, this has not been done so far). B3LYP is expected to yield acceptable U=O and U−OH_2 bond lengths but inaccurate H-bonds,[10] whereas, with HF (SCF) methods, too short U=O bond lengths but acceptable H-bonds are obtained.[10] The computed reaction entropy is affected by the inaccurate gas-phase geometries and the neglect of the strong solute−solvent interactions, the H-bonds. While an accurate reaction entropy cannot be calculated on the basis of the present CM[141] (in which, for example, solute−solvent interactions are neglected), it is possible to obtain better geometries and energies (ΔE) for reaction 7.[10]

The authors were unable to locate the transition state for reaction 7 via Eigenmode following. Laudably, they gave a description of their attempts, which failed for $n = 1$, but for $n = 2$, they were able to find an energy maximum by decreasing progressively the U−F distance, which was kept fixed, from 3.96 to 2.60 Å, while all of the other bond parameters were optimized. The same procedure was also executed for the increase of U−F from 2.26 to 2.35 Å. Below 2.60 Å and above 2.35 Å, the calculations failed. Hence, they concluded that reaction 7 may not be an elementary reaction and estimated the activation energy from the maximum (Table 3).

This is a situation we encountered also for certain reactions, and I would like to show possibilities for how the transition state nevertheless could eventually be located using the example of the $Co(NH_3)_5SCN^{2+}$ S → N isomerization (section 4.6.1).[33] We attempted to locate this transition state by elongating progressively the (fixed) Co−S distance, expecting that, at the energy maximum, we would find the transition state. Initially, the energy increased smoothly, while the Co−S distance was increased until, *suddenly*, the energy dropped, and a species resembling the product, $Co(NH_3)_5NCS^{2+}$, was obtained. Along the geometry optimization with the fixed Co−S at which the "sudden" change occurred, there were geometries at which the gradient was (relatively) small. There, the frequencies were computed, whereby a few of them were imaginary. The transition state could then be located in a straightforward manner by following of the appropriate imaginary mode (whereby, for the converged transition state, a single imaginary frequency was calculated). To obtain a geometry that is suitable for the beginning of the transition state search via Eigenmode following, it might be helpful to limit the maximum step size for the geometry optimization during which the "sudden" change occurs. Other possibilities for the location of the transition state of reaction 7 would be to change the "manual reaction coordinate" at the critical point: instead of reducing U−F below 2.60 Å, the corresponding **U**−**O**H_2 or F−H bond could be elongated progressively. Likewise, instead of stretching the U−F bond beyond 2.35 Å, the F−H or the appropriate **U**−**O**H_2 bond could be reduced.

It is an open question whether reaction 7 proceeds in a single step or not.

4.6. Rearrangements

4.6.1. Linkage Isomerization Reactions

The S → N and O → N isomerization reactions of $Co(NH_3)_5SCN^{2+}$ and $Co(NH_3)_5ONO^{2+}$ (Table 4), respectively, were studied[154,155,159,160] extensively with the aim of obtaining information on the existence or nonexistence of the pentacoordinated intermediate $Co(NH_3)_5^{3+}$ in the course of substitution reactions of amine complexes of cobalt(III). In these isomerizations, the nucleophile is present in the leaving group itself. The computations[33,34] on both reactions showed clearly that these reactions are concerted, whereby the isomerizing ligand is not released from the first coordination sphere and, therefore, no $Co(NH_3)_5^{3+}$ intermediate is formed.

The computations on the S → N isomerization reaction of $Co(NH_3)_5SCN^{2+}$ were performed for the free ions in the gas phase and for the hydrated ions (Table 4), for which the geometries are considerably different: according to the calculations on the free ions, the $\boldsymbol{I_a}$ mechanism would operate (because of the negative $\Delta\Sigma$) whereas, for the hydrated ions, it is $\boldsymbol{I}$ (since $\Delta\Sigma$ is close to 0). An additional water molecule in the second coordination sphere has no effect on the results. The aquation of $Co(NH_3)_5SCN^{2+}$ as a side reaction is less favorable via the $\boldsymbol{D}$ than via the $\boldsymbol{I_d}$ pathway (section 4.5). The activation energies are considerably higher for the free than for the hydrated ions. Electron correlation was neglected in these studies because the activation energies agreed with experiment. The geometry of the T-shaped transition state $[Co(NH_3)_5\cdots CNS^{2+}]^{‡}$ was shown to be insensitive to static correlation.

For the O → N isomerization reaction of $Co(NH_3)_5ONO^{2+}$, the experimentalists considered three structures[160] for the transition state. In the first one, the NO_2^- ligand is bound in the η^2 mode, whereby nitrogen and one oxygen act as donor atoms. The second structure is the transition state leading to the pentacoordinated tight ion pair $Co(NH_3)_5\cdot NO_2^{2+}$, and in the third structure, NO_2^- is bound in the η^3 mode. The geometries were optimized for the solvated (with CPCM) and the free ions with B3LYP using basis sets without polarization functions (Table 4). The computed N−O bond lengths (for both the solvated and

the free ions) in the NO_2^- ligand deviate considerably, by more than 0.1 Å, from those in the corresponding crystal structures. The authors attributed this difference, being present in both linkage isomers, to inaccuracies in the X-ray crystal structures arising from disorder. However, it should be noted that reliable geometries of the coordinated NO_2^- anion, exhibiting furthermore π bonds, would have required at least polarization functions on its three atoms. For the computations of the energy, polarization functions were added on the metal and the first row elements.

The transition state with η^2-coordinated NO_2^- was calculated and claimed to be the only species connecting the reactant with the product. However, the transition state or at least the pentacoordinated intermediate representing the tight ion pair could have been investigated as for the reactions of $Co(NH_3)_5SCN^{2+}$ (Table 4).

The common feature of the transition states of these two reactions is the quite strong bond of the isomerizing ligand with the (low-spin) d^6 cobalt(III) center. This is manifested in the negative or nearly zero $\Delta\sum$ values.

Vallet et al.[157] computed the stability of isomers of dioxouranium(VI) oxalato complexes in aqueous solution. They furthermore investigated the intramolecular ligand exchange in $UO_2F_3(C_2O_4)^{3-}$ and $UO_2(\eta^2\text{-}C_2O_4)_2(\eta^1\text{-}C_2O_4)^{4-}$ (Table 4). In these two linkage isomerization reactions, the reactant and the product are identical (reactions 9 and 10).

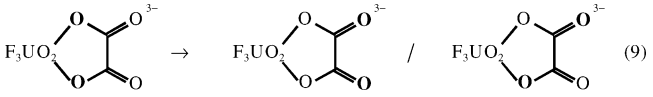

(9)

$$UO_2(\eta^2\text{-}C_2O_4)_2(\eta^1\text{-}\mathbf{C_2O_4})^{4-} \rightarrow UO_2(\eta^2\text{-}C_2O_4)(\eta^2\text{-}\mathbf{C_2O_4})(\eta^1\text{-}C_2O_4)^{4-} \quad (10)$$

The rate-determining step for reaction 9 is ring opening leading to the $UO_2F_3(\eta^1\text{-}C_2O_4)^{3-}$ intermediate, in which the two CO_2^- groups of the partially released $C_2O_4^{2-}$ are perpendicular to each other. Reclosing of the ring may regenerate the reactant with one or no oxygen (of $C_2O_4^{2-}$) exchanged. Alternatively, the ring may be closed by the other oxygen of the bound CO_2^- group, which would yield $UO_2F_3(\eta^2\text{-}C_2O_4)^{3-}$ with a *four-membered* ring. Also in this intermediate, the two CO_2^- groups are perpendicular to each-other. Reopening of this ring, followed by the formation of the $UO_2F_3(\eta^1\text{-}C_2O_4)^{3-}$ intermediate and the reactant, may result in the exchange of one or two O atoms. Since the step with the highest activation energy is bond breaking in $UO_2F_3(\eta^2\text{-}C_2O_4)^{3-}$, reaction 9 proceeds via the $\boldsymbol{I_d}$ mechanism.

In the most stable isomer of $UO_2(C_2O_4)_3^{4-}$, two $C_2O_4^{2-}$ ligands form five-membered chelating rings, and the third $C_2O_4^{2-}$ is coordinated via one O atom. Also in this $\eta^1\text{-}C_2O_4^{2-}$ ligand, the two CO_2^- groups are perpendicular to each other. The most favorable pathway of reaction 10 involves the intermediate, in which all three $C_2O_4^{2-}$ ligands form five-membered chelating rings. For this pathway (mechanism B in ref 157), the geometries were optimized for the free and the hydrated ions. An alternative pathway (mechanism C in ref 157), proceeding via an intermediate with two five-membered rings and one four-membered rings, followed by another intermediate with one four-membered ring, one five-membered ring, and one monodentate $C_2O_4^{2-}$ ion, has activation energies of 16, 25, and 1 kJ/mol for the first, second, and third steps, respectively. The total activation energy for mechanism C, which was based on gas-phase geometries, is higher (by ~11 kJ/mol) than that of mechanism B, based on gas-phase geometries as well. Also in this study, static electron correlation was neglected in the computation of the geometry and the energy, and the corresponding consequences have not been assessed.

Mechanism B would follow the $\boldsymbol{I_a}$ mechanism because the activation involves bond formation. In mechanism C, bond formation is followed by bond breaking and again bond making. Thus, the attribution of a mechanism for this latter pathway is not straightforward; the rate-determining, second, step is bond breaking. Mechanism A (in ref 157), being energetically unfavorable, would proceed via the $\boldsymbol{I_d}$ pathway, since it involves bond breaking to form the $UO_2(\eta^2\text{-}C_2O_4)(\eta^1\text{-}C_2O_4)_2^{4-}$ intermediate.

4.6.2. Square-Planar Complexes

Tautermann et al.[158] investigated the cis−trans isomerization mechanism of square-planar bis(glycinato)copper(II). The quantum chemical calculations were performed for the free species in the gas phase with a modified[158] G3[161,162] method (Table 4). They computed the minimum-energy path at 100−400 K using the variational transition state theory. The transition state is distorted trigonal pyramidal, whereby the apical N donor forms the longest Cu−N bond (of ~2.30 Å), and the two trans O donors, together with the remaining amine, form the T-shaped base of the pyramid. The pathway involving breaking of a Cu−N bond has a higher activation energy. As the authors point out, the computed gas-phase rate constants cannot be compared with the experimental data of the solid-state reaction, but the mechanism derived from the gas-phase model is supposed to operate also in the solid state because it requires less space than ring opening.

4.6.3. Octahedral Complexes

More than 20 years ago, Vanquickenborne and Pierloot[163,164] investigated, among other reactions, the rearrangements of octahedral low-spin d^6 complexes on the basis of ligand field (LF) theory.[165] They showed that stereomobility, for example, racemizations or isomerizations, in octahedral complexes can only occur if a spin-multiplicity change takes place along the reaction coordinate. For this to happen, the gap between the lowest quintet state and the singlet ground state of the (pseudo-) octahedral complex must be sufficiently small. The activation energy for the rearrangement, which may take place via the Bailar or the Ray−Dutt twist, corresponds approximately to this singlet−quintet energy difference. (For other metal centers or ligands, the lowest excited

state may be a triplet.) Thus, they were able to explain why compounds with a low-spin d^6 CoO_6 or FeN_6 chromophore are stereomobile, in contrast to CoN_6 chromophores and octahedral complexes of Rh^{III} and Ir^{III}.

Alternatively, rearrangements may take place in the course of substitution reactions, for example, in the experimentally extensively studied base-catalyzed or spontaneous reactions of amine complexes of cobalt(III). The substitution mechanism is dissociative (***D*** or $\boldsymbol{I_d}$), and therefore, the reactions proceed via pentacoordinated intermediates or pseudo-pentacoordinated transition states (see below). The steric course of the aquations of *cis*- and *trans*-Co(en)$_2$A X^{n+} complexes was also investigated by Vanquickenborne and co-workers[163,164] with LF theory.[165] Their results will be presented in the following section (section 4.6.4).

4.6.4. Pentacoordinated Intermediates

Dissociatively activated substitution reactions, proceeding via the ***D*** mechanism, involve a pentacoordinated intermediate by definition (section 3.1). Today, for many reactions, it is still an open question whether the ***D*** or the $\boldsymbol{I_d}$ mechanism operates. The latter proceeds via a pseudo-pentacoordinated transition state exhibiting five normal metal−ligand (M−L) bonds and two longer bonds, those of the exchanging ligands.[33,84,122,135] Similar transition states exist also for the ***I*** and the $\boldsymbol{I_a}$ mechanisms, whereby the bonds of their exchanging ligands are shorter. Two types of transition states for the $\boldsymbol{I_d}$ mechanism, and also the ***I*** and $\boldsymbol{I_a}$ mechanisms, exist: the first one is square pyramidal with the two exchanging ligands at roughly the position of the ligand having left (such as the species in Figure 5a with, however, longer M···L bonds), and the second one is a trigonal bipyramid to which the two exchanging ligands are added in the trigonal plane such that they are opposite to each other (such as the species in Figure 5b, but also with longer M···L bonds). The first type of transition state gives rise to retention of the configuration, and the second type gives rise to stereomobility. It is important to note that these two kinds of transition states for $\boldsymbol{I_d}$ can be considered as a square pyramid or a trigonal bipyramid being perturbed by the two weakly bound exchanging ligands. Thus, the conclusions drawn by Vanquickenborne et al. for the stereomobility of pentacoordinated intermediates are also valid for the corresponding transition states for the $\boldsymbol{I_d}$ mechanism. The application of their results to the latter will be discussed in detail in the Electronic Structure−Reactivity Relationships section (section 5). I wish to anticipate that, on the basis of the experimental observation of stereomobility, it cannot be concluded that the substitution reaction proceeds necessarily via the ***D*** mechanism (section 5.4).

In two articles, Vanquickenborne and Pierloot elaborated the conditions for the stereomobility of pentacoordinated intermediates[163] and the steric course of the extensively studied thermal substitution reactions of low-spin complexes of cobalt(III).[164] They found, again on the basis of LF theory, that stereomobility of low-spin d^6 systems is not possible in the singlet ground state because of the high singlet energy of the trigonal bipyramid, which is, however, considerably lower for the quintet or triplet states. A rearrangement can only occur if the energy of the trigonal bipyramid is approximately equal to or lower than that of the square pyramid in the singlet ground state. Otherwise, the formation of the trigonal bipyramid cannot compete with the addition of a nucleophile or solvent to the square pyramid. Hence, the observation of stereomobility implies that a spin-multiplicity change occurred along the reaction coordinate.

In their following article,[164] Vanquickenborne and Pierloot investigated the spontaneous and induced aquations of Λ-Co(en)$_2$A X^{n+} and *trans*-Co(en)$_2$A X^{n+} complexes using LF theory.[165] X is the leaving group, and A is either OH^-, a strong π donor, or CN^-, a strong π acceptor. These two ligands represent the prototypes for stereomobility or stereoretention. The Λ- and *trans*-Co(en)$_2$(CN)X^{n+} complexes, for example, aquate with full retention of the configuration, whereas the Λ-Co(en)$_2$A X^{n+} complexes with A = OH^- or H_2O, for example, isomerize as a minor reaction producing <40% of *trans*-Co(en)$_2$A OH_2^{n+}. The major product (>60%) is Λ-Co(en)$_2$A OH_2^{n+}, whereby no racemization takes place (no Δ product is formed). Likewise, from *trans*-Co(en)$_2$A X^{n+}, >60% *trans*-Co(en)$_2$A OH_2^{n+} is obtained together with <40% *rac-cis*-Co(en)$_2$A OH_2^{n+}. The stereochemical product ratio is independent of the nature of the leaving group (X); it is determined exclusively by the nature and the position (cis or trans) of the A ligand. Obviously, the aquations of the cis and trans reactants do not involve a common intermediate, characterized by a well-defined stereochemistry.[164]

To make the model as simple as possible, Vanquickenborne and Pierloot applied their LF computations to the pure ***D*** mechanism. Thus, in the reactant, either Λ-Co(en)$_2$A X^{n+} or *trans*-Co(en)$_2$A X^{n+}, X is eliminated, and square pyramids with A in the basal or apical position are formed. They exhibit singlet ground states and may react with a nucleophile or rearrange. *apical*-Co(en)$_2$A^{n+} can transform exclusively into trigonal bipyramidal *eq*-Co(en)$_2$A^{n+}, whereas, from *basal*-Co(en)$_2$A^{n+}, the trigonal bipyramids *eq*-Co(en)$_2$A^{n+} and *ax*-Co(en)$_2$A^{n+} could be formed. For A = OH^-, both trigonal bipyramids exhibit a quintet ground state, whereas, for A = CN^-, their ground state is a triplet. The latter are much higher than the singlet ground state of the square pyramids. This is the reason why Λ-Co(en)$_2$(CN)X^{n+} and *trans*-Co(en)$_2$(CN)X^{n+} complexes react with retention of the configuration. The quintet state of *ax*-Co(en)$_2$(OH)$^{2+}$ is also too high to be accessible in competition with nucleophile addition to the square pyramid. The direct racemization cannot take place because it would proceed via this *ax*-Co(en)$_2$(OH)$^{2+}$ species, having an activation energy of ∼84 kJ/mol for A = CN^- and OH^-. Hence, racemization would be a two step process: in the first one, a trans product would be formed which would isomerize subsequently to the racemic cis product.

The important result of Vanquickenborne and Pierloot's LF studies[163,164] is that stereomobility can only take place via the *eq*-Co(en)$_2$A^{n+} trigonal bipyramidal species in its quintet ground state, provided that its energy, which depends on the nature of the A ligand, is not too high.

The putative pentacoordinated intermediate Cr(NH$_3$)$_5^{3+}$ is square pyramidal with a quartet electronic ground state.[84] Its rearrangement (reaction 11)

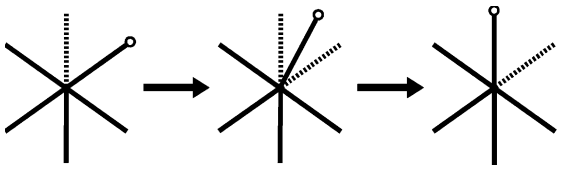

(11)

proceeds via a trigonal bipyramidal transition state, also with a quartet state (Table 4). The reaction via a trigonal bipyramid in its lowest doublet state would have an insurmountably high barrier. Interestingly, the activation energy for the rearrangement of Cr(NH$_2$CH$_3$)$_5^{3+}$ is virtually equal. Although, for both amine complexes, the activation energy for reaction 11 is relatively low, the rearrangement could not compete with nucleophile or solvent addition to the square pyramidal intermediate. Hence, substitutions of chromium(III) complexes by either a concerted ***I*$_a$**, ***I***, or ***I*$_d$** mechanism or the ***D*** mechanism proceed with retention of the configuration.[84]

In CPMD simulations of the Cu^{2+} ion in aqueous solution (Table 4),[77] reaction 11 was also observed. The square pyramidal Cu(OH$_2$)$_5^{2+}$ species was converted into the trigonal bipyramidal one after ~9 ps and remained so until the end of the simulation (~8 ps). It should be remembered that the coordination number of Cu^{2+} in aqueous solution is not established.[10] After the publication of this CPMD study, the coordination number of Cu^{2+} was reported to be 6 on the basis of an EXAFS and large angle X-ray scattering study,[78] whereas 5 was obtained in a X-ray absorption study,[82] according to which Cu(OH$_2$)$_5^{2+}$ would have a distorted square pyramidal structure with four equatorial Cu−O bonds of 1.956 Å and a longer apical Cu−O bond of 2.36 Å. A coordination number of 6 was found in two QM/MM simulations,[79,80] and one of 5.7 was found in the most recent CPMD study,[81] which was also based on the BLYP functional.

5. Electronic Structure–Reactivity Relationships

5.1. Geometry of Pentacoordinated Species

They can adopt a square pyramidal or a trigonal bipyramidal structure, whereby, in the latter, the ligand−ligand repulsions are weaker. In transition metal complexes, the geometry is determined by these steric factors and the population of the d shell as well (Table 5). The trigonal bipyramid is destabilized, if the d_{xy} and the $d_{x^2-y^2}$ MOs, that are degenerate or nearly so, have unequal occupations, since the d_{xy} MO has a lower energy in the square pyramid (Scheme 6[163]).

It should be noted that, apart from the exception of Ni^{II}, the transition metal centers with a preference

Scheme 6[a]

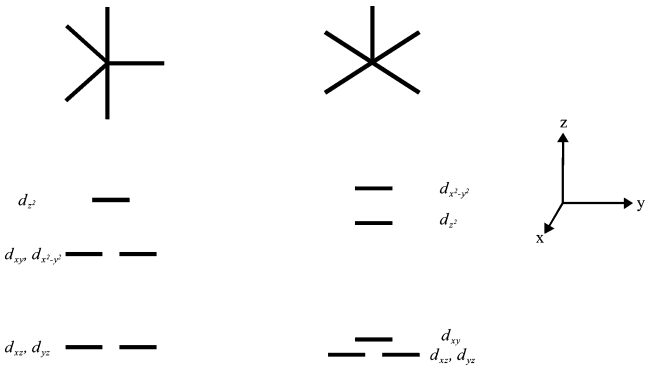

[a] Data are from ref 163.

Scheme 7

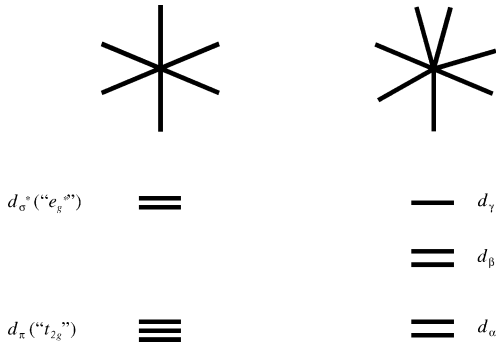

for the square pyramidal structure (Table 5) are precisely those whose (pseudo-) octahedral complexes are inert. Those of high-spin Ni^{II} are more reactive because each of their antibonding d_{σ^*} ("e_g*") MOs is occupied by one electron.

5.2. Nature and Existence of Heptacoordinated Species

In contrast to hexa- and pentacoordinated complexes which, at least theoretically, exist for all the di- and trivalent transition metal ions, heptacoordinated species do not exist for every electron configuration, and if they do so, they can be either intermediates (for the ***A*** mechanism) or transition states (for the ***I*$_a$**, ***I***, or ***I*$_d$** mechanism). They are distorted pentagonal bipyramidal, and as transition states, they usually exhibit two elongated bonds which are those of the ligands involved in the substitution reaction (Figure 5).

In hexacoordinated complexes, there are three nonbonding (d_π) and two antibonding (d_{σ^*}) MOs (Scheme 7).[54] The addition of a seventh ligand destabilizes one of the nonbonding MOs, whereby, for a regular pentagonal bipyramid, the d levels split into two nonbonding degenerate MOs (d_α), two moderately antibonding, also degenerate MOs (d_β), and one strongly antibonding MO (d_γ). Upon distortion of the pentagonal bipyramid, the degeneracy is removed, which causes the splitting of the d_α and d_β levels.

All of the computed transition metal heptaaqua ions are listed in Table 6. It is obvious that they are intermediates, if the antibonding d_β and d_γ MOs are empty. Interestingly, if each of the antibonding MOs is populated by a single electron, giving rise to the $d_\beta^2 d_\gamma^1$ electron configuration, and if the d_α MOs are

Table 6. Nature and Electronic Structure of Heptaaqua Ions

metal ion	electron config	nature of the heptacoordinated species[a]	remarks[b]	ref
Sc^{III}	$3d^0$, $d_\alpha{}^0d_\beta{}^0d_\gamma{}^0$	intermediate		54, 166
Ti^{III}	$3d^1$, $d_\alpha{}^1d_\beta{}^0d_\gamma{}^0$	intermediate		53, 83, 166
V^{III}	high-spin $3d^2$, $d_\alpha{}^2d_\beta{}^0d_\gamma{}^0$	intermediate		54, 166
V^{II}	high-spin $3d^3$, $d_\alpha{}^2d_\beta{}^1d_\gamma{}^0$	transition state	adjacent/remote; stereoretention is favorable	23, 53
Cr^{III}	high-spin $3d^3$, $d_\alpha{}^2d_\beta{}^1d_\gamma{}^0$	transition state	adjacent/remote; stereoretention is favorable	54, 84, 166
Cr^{II}	high-spin $3d^4$, $d_\alpha{}^2d_\beta{}^2d_\gamma{}^0$	transition state	remote	54
Mn^{III}	high-spin $3d^4$, $d_\alpha{}^2d_\beta{}^2d_\gamma{}^0$	transition state	remote	54, 166
Mn^{II}	high-spin $3d^5$, $d_\alpha{}^2d_\beta{}^2d_\gamma{}^1$	intermediate		23, 54
Fe^{III}	high-spin $3d^5$, $d_\alpha{}^2d_\beta{}^2d_\gamma{}^1$	intermediate		54, 166
Fe^{II}	high-spin $3d^6$, $d_\alpha{}^3d_\beta{}^2d_\gamma{}^1$	transition state	adjacent/remote	23, 54
Co^{III}	high-spin $3d^6$, $d_\alpha{}^3d_\beta{}^2d_\gamma{}^1$	transition state		166
Ru^{III}	low-spin $4d^5$, $d_\alpha{}^4d_\beta{}^1d_\gamma{}^0$	transition state	adjacent	84
Rh^{III}	low-spin $4d^6$, $d_\alpha{}^4d_\beta{}^2d_\gamma{}^0$	transition state	adjacent	85
Ir^{III}	low-spin $5d^6$, $d_\alpha{}^4d_\beta{}^2d_\gamma{}^0$	transition state	adjacent	58
Co^{II}	high-spin $3d^7$, $d_\alpha{}^4d_\beta{}^2d_\gamma{}^1$	intermediate		54

[a] All of these transition states and intermediates exhibit C_2 symmetry. [b] "adjacent" means exchanging ligands are adjacent to each other (as in Figure 5a), giving rise to stereoretention; "remote" means exchanging ligands are remote to each other (as in Figure 5b), giving rise to stereomobility; "adjacent/remote" means exchanging ligands can be adjacent (as in Figure 5a) or remote (as in Figure 5b) to each other, giving rise to stereoretention or stereomobility, respectively.

occupied *symmetrically*, with either a $d_\alpha{}^2$ or a $d_\alpha{}^4$ electron configuration, the heptacoordinated species is also an intermediate. For occupations of the d_β and d_γ levels exceeding three, as in Ni^{II}, Cu^{II}, and Zn^{II}, it was impossible to compute a heptacoordinated species on the basis of the cluster model with seven H_2O molecules.[53,54,63]

The heptacoordinated species is a transition state, if the d_γ MO is empty and if the two d_β MOs are occupied by one (as in V^{II}, Cr^{III}, and Ru^{III}) or two electrons in the high- or low-spin configuration (as in Cr^{II} and Mn^{III} or Co^{III}, Rh^{III}, and Ir^{III}, respectively). Furthermore, the high-spin d^6 ions (Fe^{II} and Co^{III}), exhibiting an asymmetric occupation of the d_α shell, are also transition states. Whether the water exchange reaction of (low-spin) $Co(OH_2)_6{}^{3+}$ proceeds via a high- or a low-spin transition state is still an open question.[167]

5.3. Electronic Structure–Substitution Mechanisms Relationships

The ***D*** mechanism is, at least theoretically, always feasible for substitutions of hexacoordinated di- and trivalent transition metal complexes because the corresponding pentacoordinated species are available computationally.[53,54] It is the preferred pathway for the metals on the right side of the periodic table. In contrast, the ***A*** and $\boldsymbol{I_a}$ and also the ***I*** and $\boldsymbol{I_d}$ mechanisms are possible only for those electron configurations for which the corresponding heptacoordinated species exist (Table 6). ***A*** is advantageous for the metals on the left side of the periodic table, which are the d^0, d^1, and d^2 ions exhibiting empty antibonding d_β and d_γ MOs. For the metal ions in the middle of the periodic table, the substitution mechanisms may be associative (***A*** or $\boldsymbol{I_a}$), concerted (***I***), or dissociative (***D*** or $\boldsymbol{I_d}$), since activation energies for two mechanisms are available: for the hexaaqua ions of V^{II}, Mn^{III}, and Fe^{II}, the activation energies for $\boldsymbol{I_a}$ and ***D*** are close, whereas, for Mn^{II} and Co^{II}, they are so for ***A*** and ***D*** (Table 1). For other ions, such as, for example, Cr^{II}, Cr^{III}, and Fe^{III}, two mechanisms are also possible, but for the water exchange on these hexaaqua ions, there is a pronounced preference for the ***D***, $\boldsymbol{I_a}$, and ***A*** mechanisms (Table 1). The ***D*** mechanism as well as a concerted ($\boldsymbol{I_a}$, ***I***, or $\boldsymbol{I_d}$) mechanism is feasible for the water exchange reaction on aqua–amine complexes of Cr^{III}, Ru^{III}, and Rh^{III} (Table 2). For Cr^{III}, the entire $\boldsymbol{I_a}$ ... ***I*** ... $\boldsymbol{I_d}$ continuum was observed,[84] whereby the dissociative character of the exchange reaction increases with increasing basicity of the nonexchanging ("spectator") ligands. The nature of the concerted mechanism depends on both the ligands and the electronic structure of the metal ion. In general, an increase in the donor strength (basicity) of nonexchanging ("spectator") ligands augments the dissociative character of the concerted pathway, and at the same time, it lowers the activation energy for the ***D*** mechanism. The pH dependence of the water exchange reaction of $Fe(OH_2)_6{}^{3+}$ is a representative example: the deprotonation of an aqua ligand gives rise to a mechanistic change from associative to dissociative.[168,169]

The water exchange mechanism on the hexaaqua ions of Mn^{III} and Co^{III} is not known experimentally, and as already mentioned, it is an open question whether the reaction of Co^{III} proceeds via a spin-multiplicity change.[167] Computations on species in several spin states are very demanding because accurate geometries and energies are needed to get correct relative energies of the states corresponding to the $d_\pi{}^n d_\sigma{}^{*0}$, $d_\pi{}^{n-1} d_\sigma{}^{*1}$, and $d_\pi{}^{n-2} d_\sigma{}^{*2}$ electron configurations. H-bonding, hydration, and electron correlation have to be treated at a high level.

For the two-step mechanisms ***A*** and ***D***, the energy difference between the transition state and the intermediate may be so small that the lifetime of the latter is shorter than ~0.2 ps, the approximate duration of a metal–ligand stretching vibration. In such cases, it would be more appropriate to designate the mechanisms $\boldsymbol{I_a}$ or $\boldsymbol{I_d}$.

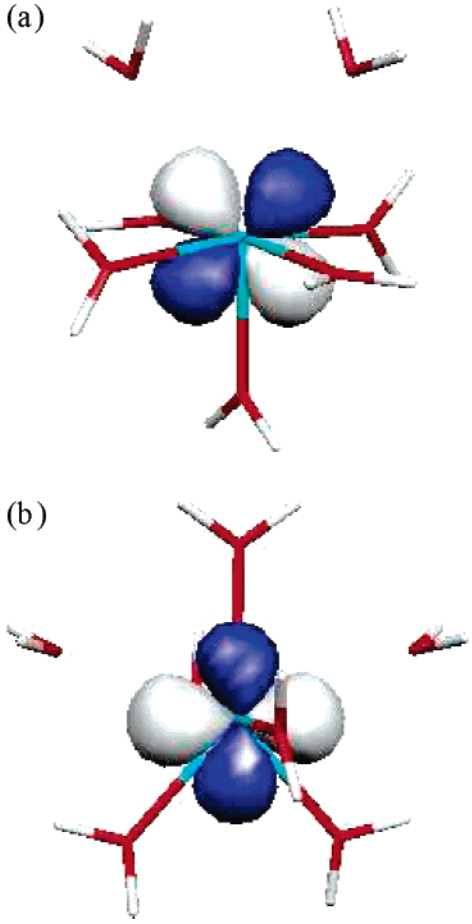

Figure 8. Singly occupied antibonding d_β MO of the transition states for the I_a mechanism, [*cis*-$V(OH_2)_5\cdots(OH_2)_2^{2+}]^\ddagger$ (a) and $[V(OH_2)_5\cdots(OH_2)_2^{2+}]^\ddagger$ (b).[170]

The occupancy of the moderately antibonding d_β levels in the transition state (Scheme 7) determines the length of the M···L bonds, which increases with an increasing number of d_β electrons. The I_a mechanism is preferred, if one d_β MO, with either *b* or *a* symmetry (Figure 8),[170] is singly occupied, such as for the water exchange of $V(OH_2)_6^{2+}$, $Cr(OH_2)_6^{3+}$, $Cr(NH_3)_5OH_2^{3+}$, and $Ru(NH_3)_5OH_2^{3+}$ (Tables 1 and 2). The M···L bonds are longer, when each of the two d_β MOs is singly occupied, such as for the less favorable water exchange pathway of $Cr(OH_2)_6^{2+}$ (Table 1). In amine complexes of Co^{III}, the d_β MO with *b* symmetry (Figure 8a) is doubly occupied, which gives rise to relatively long Co···L bonds in the transition state, and therefore, the mechanism is I_d. This is the rational explanation why the aquation (substitution by water) of $Cr(NH_3)_5Cl^{2+}$ proceeds via the I_a mechanism, whereas that of $Co(NH_3)_5Cl^{2+}$ follows the I_d pathway.[135] In the Co^{III} valence–isoelectronic amine and aqua complexes of Rh^{III} (Tables 1 and 2), the Rh···L bonds are shorter. Hence, the water exchange reactions on $Rh(NH_3)_5OH_2^{3+}$ and $Rh(OH_2)_6^{3+}$, respectively, follow the *I* and I_a mechanisms, whereby the transition state structures [*cis*-$Ir(OH_2)_5\cdots(OH_2)_2^{3+}]^\ddagger$ and [*cis*-$Rh(OH_2)_5\cdots(OH_2)_2^{3+}]^\ddagger$ are almost equal. The similarity of the transition state structures of (high-spin d^3) Cr^{III} and (low-spin d^5) Ru^{III} complexes arises also from the population of the d_β MO, which, for both metal ions, is singly occupied in the transition state for the I_a mechanism.[84] The two additional d electrons in Ru^{III} occupy the nonbonding d_α levels, whose population has a weak effect on the transition state structure.

5.4. Steric Course of Substitution Reactions

5.4.1. Associative Mechanisms

In general, the substitution reactions following the *A* mechanism are expected to proceed with stereomobility because, in the heptacoordinated intermediate, the seven metal–ligand bond lengths are similar.[53,54,83] Therefore, the bonds can rearrange rapidly in the intermediate, and any ligand could leave to form the product.

Two structures (Figure 5) exist for the transition state for the I_a (and also the *I*) mechanism. In the first one (Figure 5a), the exchanging ligands are adjacent to each other. This pathway leads to stereoretention because the incoming ligand takes the place of the leaving ligand. In the second structure (Figure 5b), the exchanging ligands are remote from each other. The entering ligand attacks adjacent to the ligand which is trans to the leaving one, and one of the ligands cis to the leaving ligand takes its place. (The course of these reactions is the same for the I_d mechanism, which is illustrated in more detail in the next section, section 5.4.2.) Both types of transition states for the water exchange reaction on $V(OH_2)_6^{2+}$ exhibit C_2 symmetry. In the species giving rise to stereoretention, the (antibonding) d_β MO with *b* symmetry (Figure 8a) is occupied (by a single electron), whereas, in that for stereomobility, it is the d_β MO with *a* symmetry (Figure 8b).

For the water exchange reactions of $V(OH_2)_6^{2+}$, $Cr(NH_3)_5OH_2^{3+}$, and $Ru(NH_3)_5OH_2^{3+}$, both types of I_a pathways have been calculated,[32,53,84] and in all of these cases, the mechanism giving rise to stereoretention is most favorable. The common feature of all these reactions is that the d_β MO is occupied by a single electron. In the transition state for stereoretention, the nonexchanging ligands with normal metal–ligand bond lengths form a slightly distorted square pyramid (Figures 5a and 8a), whereas, in the transition state giving rise to stereomobility, they form a trigonal bipyramid (Figures 5b and 8b). It was shown (section 5.1) that substitutions on high-spin d^3 systems via the *D* mechanism occur preferentially with stereoretention because the square pyramid is more stable than the trigonal bipyramid (Table 5 and Scheme 6). Also, the rearrangement of square pyramidal $Cr(NH_3)_5^{3+}$ and $Cr(NH_2CH_3)_5^{3+}$ (reaction 11), which proceeds via a trigonal bipyramidal transition state (Table 4), shows the higher stability of the square pyramid. Thus, not only for the *D* but also for the I_a and, of course, the *I* and I_d mechanisms, the higher stability of the square pyramid is the origin for the preference of stereoretention. This holds also for low-spin d^6 complexes of Rh^{III} and Ir^{III}, in which the d_β MO with *b* symmetry is populated by two electrons.

The water exchange reaction on the hexaaqua ions of Cr^{II} and Mn^{III} proceeds via the *D* mechanism (Table 1). For both of these high-spin d^4 ions, the

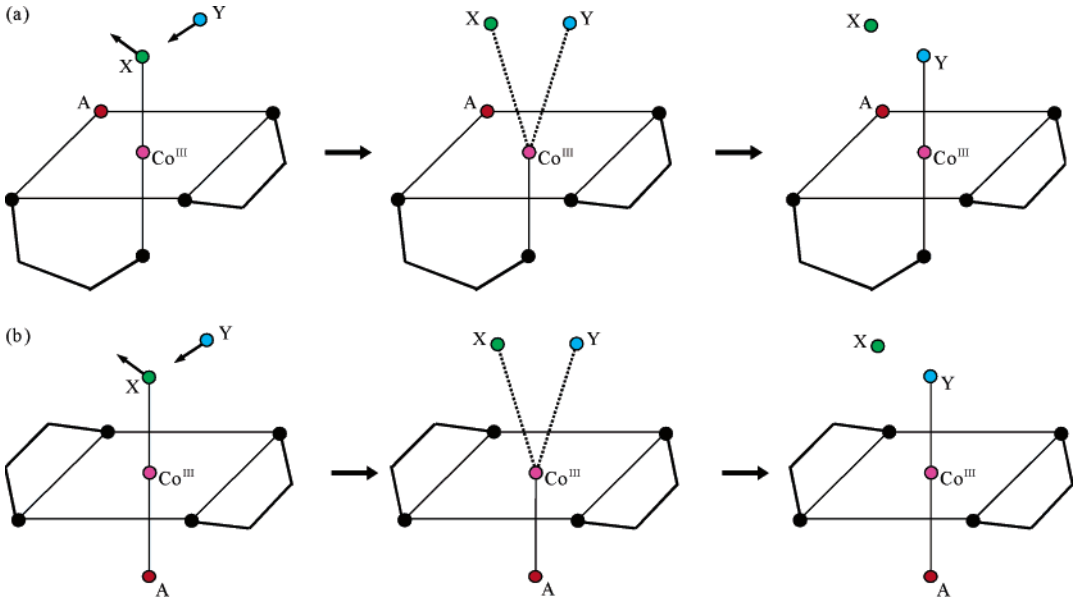

Figure 9. Course of the substitution reaction of Λ-Co(en)$_2$A X^{n+} (a) and *trans*-Co(en)$_2$A X^{n+} (b) via the $\boldsymbol{I_d}$ mechanism and retention of the configuration (X = leaving group; Y = entering group).

stereomobile $\boldsymbol{I_a}$ pathway exists as well, but the computation of the corresponding transition states for stereoretention was not possible.[171] For pentacoordinated high-spin d^4 ions, the trigonal bipyramid is more stable than the square pyramid (Table 5 and Scheme 6) and, obviously, the advantage for the stereomobile pathway is due to the higher stability of the trigonal bipyramid.

The steric course of exchange reactions of high-spin d^3 and d^4 as well as low-spin d^5 and d^6 complexes via the $\boldsymbol{I_a}$ or $\boldsymbol{I}$ mechanism is determined by the stability of the pentacoordinated species involving the five ligands remaining on the metal center. This observation can be generalized for any electron configuration by decomposing conceptually the transition states into pentacoordinated species, to which the exchanging ligands are added as a perturbation. In the following, this concept will be termed the "perturbed pentacoordinated species" (PPCS) model. On the basis of the presently available data, this perturbation is modest because the bond lengths of the exchanging ligands are, in general, considerably longer than those in the pentacoordinated fragment. Thus, it is concluded that the *steric course* of substitution reactions of hexacoordinated complexes via the $\boldsymbol{I_a}$, $\boldsymbol{I}$, $\boldsymbol{I_d}$, and $\boldsymbol{D}$ mechanisms is insensitive to the mechanism but dependent on the electronic structure: stereoretention is preferred for systems for which the square pyramid is more stable, whereas stereomobility takes place in cases where the trigonal bipyramid is more stable. Of course, the lowest electronic state of each species, square pyramidal and trigonal bipyramidal, is relevant, as shown by Vanquickenborne and Pierloot.[163,164] For certain electron configurations, it might be necessary to investigate spin-multiplicity changes in the course of the reaction.

5.4.2. Dissociative Mechanisms

The steric course of substitution reactions proceeding via the $\boldsymbol{D}$ mechanism has already been discussed implicitly (section 5.1). They proceed with stereoretention, if the square pyramidal intermediate is more stable than the trigonal bipyramidal one, and if the latter is more stable, the reactions are stereomobile. Thus, stereoretention is expected only for the metal ions listed in Table 5 whereby, as found by Vanquickenborne and Pierloot,[163,164] stereomobility can take place for low-spin d^5 and d^6 ions with a weak ligand field (section 4.6.4). For all the other electron configurations, stereomobility is possible, whereby the trigonal bipyramid is formed concerted with the departure of the leaving group (Figure 4b).

Vanquickenborne and Pierloot[163,164] studied the steric course of the aquations of Λ-Co(en)$_2$A X^{n+} and *trans*-Co(en)$_2$A X^{n+} complexes on the basis of the $\boldsymbol{D}$ mechanism, since the application of LF theory to pentacoordinated species is straightforward. Their conclusions are, however, also valid for the $\boldsymbol{I_d}$ and the $\boldsymbol{I}$ and $\boldsymbol{I_a}$ mechanisms. For the $\boldsymbol{I_d}$ mechanism, the PPCS model (section 5.4.1) is a good approximation because the bonds of the exchanging ligands are long,[33,84,122,135] typically longer than 2.8 Å, and, therefore, they exert a weak perturbation onto the pentacoordinated fragment.

The aquation of Λ-Co(en)$_2$A X^{n+} and *trans*-Co(en)$_2$-A X^{n+} via the $\boldsymbol{I_d}$ mechanism and retention of the configuration is illustrated schematically in Figure 9. The incoming ligand (Y) attacks adjacent to the leaving group (X). This kind of transition states was reported for the aquation of the similar complexes Co(NH$_3$)$_5$Cl^{2+}, Co(NH$_3$)$_5$SCN^{2+}, and Co(NH$_3$)$_5$NCS^{2+} (Table 3) and for the water exchange of Cr(NH$_2$CH$_3$)$_5$-OH$_2^{3+}$ and Rh(NH$_2$CH$_3$)$_5$OH$_2^{3+}$ (Table 2). All of these $\boldsymbol{I_d}$ transition states (Figure 10) have the perturbed square pyramidal structure.

The aquation with stereochemical changes requires the attack of the incoming ligand (Y) adjacent to the ligand which is trans to the leaving group (X). In *cis*-Co(en)$_2$A X^{n+} complexes, there are three sites for such a remote attack: two inequivalent N−N edges and one N−A edge (Figure 11). The attack onto the

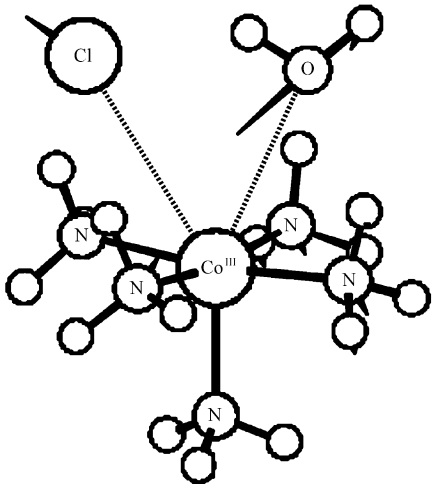

Figure 10. Transition state for the aquation of $Co(NH_3)_5Cl^{2+}$ via the I_d mechanism.[33]

remote N−A edge leads to stereoretention via, however, a trigonal bipyramidal transition state with A in the equatorial plane instead of the above-described square pyramid (Figures 9 and 10).

The attack of the incoming ligand (Y) onto the N−N edge with one NH_2 group cis and the other one trans to A gives rise to the cis−trans isomerization (Figure 11a). The axial NH_2 donors in Λ-$Co(en)_2A\ X^{n+}$, linked together with a dashed orange line, keep their positions. The trigonal bipyramidal transition state with A in the equatorial position (Figure 11a) is formed via the attack of Y onto the N−N edge of the orange square, the concerted migration of the NH_2 group trans to A, and the elongation of the Co−X bond. Y and X are also located in the equatorial plane and weakly bound. The $Co(en)_2A$ fragment is chiral, since it exhibits (approximately) C_2 symmetry. The trans product is formed by the loss of X, which takes place concerted with the continued migration of the NH_2 group.

The direct conversion of Λ-$Co(en)_2A\ X^{n+}$ into the Δ product in a single step would proceed via the attack of Y onto the other N−N edge (Figure 11b), having both NH_2 groups cis to A. This pathway involves the trigonal bipyramidal transition state with A in an axial position. The weakly bound X and Y ligands are in the equatorial plane, whereby the $Co(en)_2A$ fragment is achiral due to its mirror plane (the conformational changes of the en rings are assumed to be fast).

The transformation of *trans*-$Co(en)_2A\ X^{n+}$ into racemic *cis*-$Co(en)_2A\ X^{n+}$ (Figure 11c) proceeds, of course, via the same transition state as the cis−trans

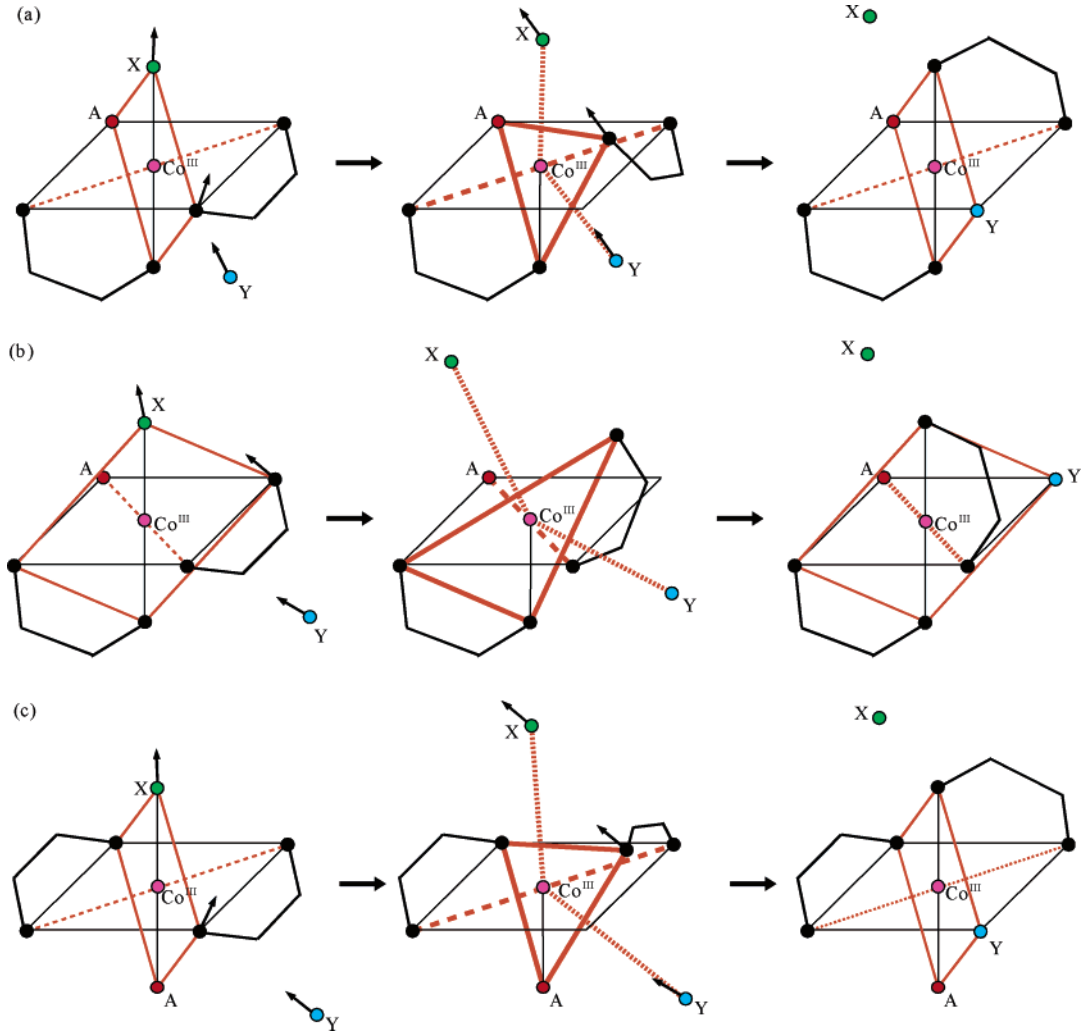

Figure 11. Course of the stereomobile substitution reaction of Λ-$Co(en)_2A\ X^{n+}$ and *trans*-$Co(en)_2A\ X^{n+}$ via the I_d mechanism yielding the trans (a), the Δ (b), and the cis (c) isomers (X = leaving group; Y = entering group).

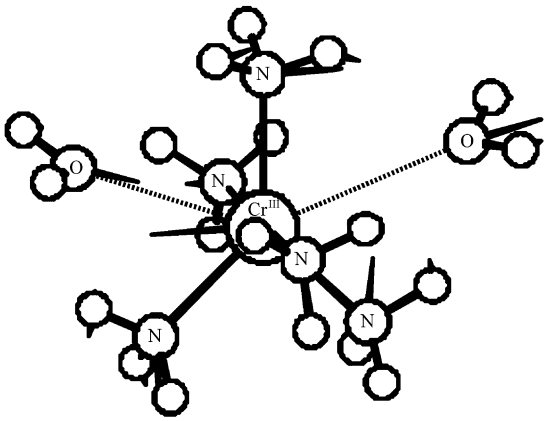

Figure 12. Perturbed trigonal bipyramidal transition state (for the water exchange of $Cr(NH_3)_5OH_2^{3+}$ via the unfavorable stereomobile pathway).[84]

isomerization (Figure 11a). In *trans*-$Co(en)_2A\ X^{n+}$, there are four remote, symmetry-equivalent, A−N edges. The Δ product is formed via the attack onto either of the two A−N edges of the orange square (Figure 11c), whereas the Λ product would be obtained if the attack takes place onto one of the other two A−N edges.

As already mentioned, the results of Vanquickenborne and Pierloot[163,164] are also valid for the ***I_d*** mechanism. According to their LF calculations, the direct conversion of Λ-$Co(en)_2A\ X^{n+}$ into Δ-$Co(en)_2A\ X^{n+}$ (Figure 11b) is not competitive with the other reactions, since this pathway involves the trigonal bipyramid with A in an axial position: its energy is considerably higher than that with equatorial A.[164] Hence, if the reaction is stereomobile, it takes place via the Δ → trans, Λ → trans, and trans → rac-cis pathways, which all proceed via the same (trigonal bipyramidal) transition state, Δ- or Λ-$Co(en)_2A\cdots(X)(Y)^{n+}$. For substitution reactions of amine complexes of Co^{III}, computations on such transition states have not been published thus far, presumably because of the high computational demand of this task, which requires accurate geometries and energies by taking into account H-bonding, hydration, and static and dynamic electron correlation. Transition states exhibiting the perturbed trigonal bipyramidal structure (Figure 12) have been reported (Table 2) for the stereomobile pathway of the water exchange reactions on $Ru(NH_3)_5OH_2^{3+}$ and $Cr(NH_3)_5OH_2^{3+}$ via the ***I_a*** mechanism, which is, however, not competitive with the pathway with retention of the configuration. For Cr^{III} and Ru^{III}, the transition state structures are virtually equal because, in both species, the d_β MO is occupied by a single electron.

The above-described application of the PPCS model to the aquation of amine complexes of cobalt(III) shows that, in general, observed stereomobility cannot be used to distinguish the ***D*** from ***I_d*** the mechanism.

5.5. Distinction of the Stepwise from the Corresponding Concerted Mechanism

Only in the few previously discussed cases (section 3.1) was experimental evidence for the existence or the nonexistence of pentacoordinated intermediates in dissociatively activated substitution reactions found. The experimental as well as the theoretical differentiation between the two-step ***A/D*** mechanisms and their corresponding concerted ***I_a/I_d*** analogues (Schemes 1−3) remains a very difficult task.

The ***A*** and the ***D*** mechanisms are equal in the sense that a species with a higher coordination number is converted in one step, via a single transition state, into a species with a lower coordination number or vice versa (reaction 12).

$$M(OH_2)_n^{m+} \rightleftarrows [M(OH_2)_{n-1}\cdots OH_2^{m+}]^{\ddagger} \rightleftarrows M(OH_2)_{n-1}^{m+} + H_2O \quad (12)$$

In both mechanisms, the imaginary mode (Figures 3 and 4) describes the motion of a single ligand, the bond-making or the bond-breaking process. The difference is that, for ***A***, the species with the lower coordination number is more stable, whereas, for ***D***, it is that with the higher coordination number. Consequently, for ***D*** (with $n = 6$) and ***A*** (with $n = 7$), respectively, the higher barrier is in the forward and backward direction of reaction 12. Thus, certain features of ***A*** are also valid for ***D*** and vice versa. It is interesting to note that for the hexaaqua ions of In^{III}, Mn^{II}, and Co^{II}, for which both mechanisms were computed, the M···O bond in the transition state is shorter for the ***A*** than for the ***D*** mechanism (Table 1). This ascertainment is in perfect agreement with Hammond's postulate:[172] in the transition state for ***A***, the M···O bond is relatively short because it is close to the corresponding M−O bond in the heptacoordinated intermediate, whereas, in the transition state for ***D***, the M···O bond is long and resembles that of the (lost) water ligand in the second coordination sphere of the pentacoordinated intermediate.

It is well-known that, for almost all the substitution reactions, neither the existence nor the nonexistence of intermediates can be proved experimentally despite the large number of reactions for which the activation parameters $\Delta H^{\ddagger}$, $\Delta S^{\ddagger}$, $\Delta G^{\ddagger}$, and $\Delta V^{\ddagger}$ are available.[4,7] From temperature-dependent kinetic measurements, the product $\kappa e^{\Delta S^{\ddagger}/R}$ is determined. Hence, the experimental $\Delta S^{\ddagger}$ values represent a lower limit because, in general, the transition probability κ is assumed to be 1. In cases where κ is smaller than 1, $\Delta S^{\ddagger}$ is larger than $\Delta S^{\ddagger}$ based on $\kappa = 1$. Therefore, the assignment of mechanisms on the basis of $\Delta S^{\ddagger}$ has to be made with care. Furthermore, even if $\Delta S^{\ddagger}$ is known exactly (and not as a lower limit), it does not provide in a direct manner information on the transition state, in particular its structure. As already discussed (section 3.1), $\Delta V^{\ddagger}$ supplies information on the size of the transition state for solvent exchange reactions, and it allows one to distinguish in a straightforward manner associative from dissociative activations.[48] The distinction of the two-step from the concerted mechanism on the basis of $\Delta V^{\ddagger}$ is not possible because the volume of the transition state is smaller or larger than that of the corresponding penta- or heptacoordinated intermediate.[55] Hence, the observed $|\Delta V^{\ddagger}|$ is smaller than the limiting $|V_S°|$ value,[50,51] which is based on the *inter-*

mediate for the ***A*** or the ***D*** mechanism. Therefore, even for reactions proceeding via the ***A*** or the ***D*** mechanism, the limiting $V_S°$ values cannot be expected to be observed experimentally.

For the quantum chemical methods, the problem is equally complex: although it was possible to compute the I_d and the ***D*** pathways for a few water exchange and aquation reactions of chromium(III), rhodium(III), and cobalt(III) (Tables 2 and 3), a differentiation of these two mechanisms was not possible. The differences in the calculated activation energies ($\Delta E^{‡}$) are insignificant because of the limitations and approximations in the model and the computational methods (section 2). Also, the lifetime of the intermediate is affected by these limitations. The parameter $\Delta\Sigma$ cannot be correlated in a quantitative manner to $\Delta V^{‡}$ or $\Delta V_{int}^{‡}$. In the transition state, the metal−leaving group bond is shorter by more than 0.2 Å for I_d compared with ***D***, but this property has not been correlated with $\Delta V^{‡}$ or $\Delta V_{int}^{‡}$ so far.

A pronounced difference between ***D*** and I_d can be seen in their imaginary modes which describe either the motion of a single ligand (Figure 4) or the concerted motion of the incoming and leaving ligand (Figure 10), but this feature cannot be detected experimentally. It is imaginable that the nature of the dissociative mechanism, I_d or ***D***, depends on the bond strengths of the two ligands involved in the exchange reaction.

The difference between the I_d and the ***D*** mechanisms may be very subtle. In the I_a ... ***I*** ... I_d mechanistic continuum, the two M···L bonds in the transition state become weaker with increasing dissociative character. The two weak M···L bonds in the I_d mechanism might be at the origin of a weak coupling of the motions of the incoming and the leaving ligands: the weaker this coupling, the more the motions of the exchanging ligands become independent, and the stronger the ***D*** character of the reaction. (In solution, this weak coupling could, furthermore, be lost in the interactions of the exchanging ligands with the solvent.) In the I_a mechanism, for example, the activation energy for bond breaking is reduced by the concerted bond-formation process. In the I_d mechanism, the influence of bond formation on the transition state energy is weak; it occurs at a late stage of the activation, when the bond of the leaving group is largely broken. If the M···L bonds are appreciably strong, as in the aquation reactions of $Co(NH_3)_5X^{2+}$ (X = Cl, **S**CN, **N**CS), the I_d mechanism is favored energetically over ***D*** (Table 3), and the two mechanisms can be distinguished. This is, however, difficult in cases where the M···L bonds are weak, as in the water exchange reactions on aqua pentakis-methylamine complexes of Cr^{III} and Rh^{III} (Table 2).

The question whether, for dissociative activations, the concerted mechanism can be distinguished from the stepwise one can, in general, be answered neither experimentally nor via computations based on the CM including the first coordination sphere. The method[55] for the estimation of $\Delta V^{‡}$ that was applied[55,58] successfully to the water exchange reactions of the hexaaqua ions of Al^{III}, Ga^{III}, In^{III}, Rh^{III}, and Ir^{III} does not yield correct results for all of the transition metal hexaaqua ions.[173] An answer to this difficult question could eventually be obtained via the comparison of experimental and calculated $\Delta S^{‡}$ and especially $\Delta V^{‡}$ data, whereby, for the computations on the I_d and the ***D*** mechanisms, a CM including at least a quantum chemically described second coordination sphere is required.

As already mentioned, no heptacoordinated species could be computed for aqua ions exhibiting more than three electrons in the d_β/d_γ MOs (Table 6). If, nevertheless, such species would exist with a structure such as, for example, that of a transition state for the I_d mechanism, the M···L bonds would be very weak and, therefore, the motions of the two M···L bonds would be, if at all, coupled very weakly, whereby this weak coupling is likely to be lost through coupling with the solvent. If the motions of the incoming and the leaving ligands are not coupled, the mechanism cannot be of the interchange type. Therefore, the I_d mechanism is unlikely to be feasible for such systems (with more than three electrons in the d_β/d_γ MOs), but not so the ***D*** pathway. According to these considerations, the water exchange reactions on Ni^{II}, Cu^{II}, and Zn^{II} would follow the ***D*** mechanism, whereas, for those of Co^{II} and Fe^{II} both, the I_d and the ***D*** mechanisms could operate.

6. Summary

(i) A critical discussion of published computational work on substitution and rearrangement reactions was presented. It has been shown that uncertain and/or incorrect conclusions can arise from too small basis sets for the metal and/or the ligands, in particular when the latter carry a negative charge and/or exhibit π bonds. Also, inadequate computational methods treating electron correlation and/or H-bonding in an inappropriate manner may be at the origin of discrepancies. The validity of approximations or simplifications, which are usually unavoidable, needs to be assessed.

(ii) The thus far published computations complement the knowledge obtained from the experimental studies and offer a deeper insight into substitution reactions. The classification of mechanisms as ***A***, I_a/***I***/I_d, and ***D***, which was done empirically on the basis of rate laws, the dependence of the rate constant on the entering and the leaving ligands, product distributions, and activation parameters, in particular the activation volume (without knowledge of any structure!), very likely reflects the reality. The relative stability, geometry, lifetime, and stereochemical behavior of penta- and heptacoordinated intermediates can be estimated, and the nature (intermediate or transition state) of the heptacoordinated species can be elucidated.

(iii) According to the presently introduced "perturbed pentacoordinated species" (PPCS) model, the steric course of substitution reactions is determined mainly by the electronic structure of the metal center (which depends on the ligands) but not by the reaction mechanism.

7. References and Notes

(1) Asano, T.; Le Noble, W. J. *Chem. Rev.* **1978**, *78*, 407.
(2) Van Eldik, R.; Asano, T.; Le Noble, W. J. *Chem. Rev.* **1989**, *89*, 549.
(3) Lincoln, S. F.; Merbach, A. E. *Adv. Inorg. Chem.* **1995**, *42*, 1.
(4) Drljaca, A.; Hubbard, C. D.; Van Eldik, R.; Asano, T.; Basilevsky, M. V.; Le Noble, W. *Chem. Rev.* **1998**, *98*, 2167.
(5) Tobe, M. L.; Burgess, J. *Inorganic Reaction Mechanisms*; Addison-Wesley Longman: New York, 1999.
(6) Richens, D. T. *The Chemistry of Aqua Ions*; Wiley & Sons: New York, 1997.
(7) Dunand, F. A.; Helm, L.; Merbach, A. E. *Adv. Inorg. Chem.* **2003**, *54*, 1.
(8) Helm, L.; Merbach, A. E. *Coord. Chem. Rev.* **1999**, *187*, 151.
(9) Erras-Hanauer, H.; Clark, T.; van Eldik, R. *Coord. Chem. Rev.* **2003**, *238–239*, 233.
(10) Rotzinger, F. P. *J. Phys. Chem. B* **2005**, *109*, 1510.
(11) Spångberg, D.; Rey, R.; Hynes, J. T.; Hermansson, K. *J. Phys. Chem. B* **2003**, *107*, 4470.
(12) Day, P. N.; Jensen, J. H.; Gordon, M. S.; Webb, S. P.; Stevens, W. J.; Krauss, M.; Garmer, D.; Basch, H.; Cohen, D. *J. Chem. Phys.* **1996**, *105*, 1968.
(13) Gordon, M. S.; Freitag, M. A.; Bandyopadhyay, P.; Jensen, J. H.; Kairys, V.; Stevens, W. J. *J. Phys. Chem. A* **2001**, *105*, 293.
(14) Car, R.; Parrinello, M. *Phys. Rev. Lett.* **1985**, *55*, 2471.
(15) Carter, E. A.; Ciccotti, G.; Hynes, J. T.; Kapral, R. *Chem. Phys. Lett.* **1989**, *156*, 472.
(16) Curioni, A.; Sprik, M.; Andreoni, W.; Schiffer, H.; Hutter, J.; Parrinello, M. *J. Am. Chem. Soc.* **1997**, *119*, 7218.
(17) Kirkwood, J. G. *J. Chem. Phys.* **1934**, *2*, 351.
(18) Onsager, L. *J. Am. Chem. Soc.* **1936**, *58*, 1486.
(19) Szafran, M.; Karelson, M. M.; Katritzky, A. R.; Koput, J.; Zerner, M. C. *J. Comput. Chem.* **1993**, *14*, 371.
(20) Tomasi, J.; Persico, M. *Chem. Rev.* **1994**, *94*, 2027.
(21) Klamt, A.; Schüürmann, G. *J. Chem. Soc., Perkin Trans.* **1993**, *2*, 799.
(22) Infante, I.; Visscher, L. *J. Comput. Chem.* **2004**, *25*, 386.
(23) Rotzinger, F. P. *Helv. Chim. Acta* **2000**, *83*, 3006.
(24) Ivanic, J. *J. Chem. Phys.* **2003**, *119*, 9364.
(25) Bender, C. F.; Davidson, E. R. *J. Phys. Chem.* **1966**, *70*, 2675.
(26) Andersson, K.; Malmqvist, P. Å.; Roos, B. O.; Sadley, A. J.; Wolinski, K. *J. Phys. Chem.* **1990**, *94*, 5483.
(27) Andersson, K.; Malmqvist, P. Å.; Roos, B. O. *J. Chem. Phys.* **1992**, *96*, 1218.
(28) Nakano, H. *J. Chem. Phys.* **1993**, *99*, 7983.
(29) Nakano, H. *Chem. Phys. Lett.* **1993**, *207*, 372.
(30) Shadhukhan, S.; Munoz, D.; Adamo, C.; Scuseria, G. E. *Chem. Phys. Lett.* **1999**, *306*, 83.
(31) Pavese, M.; Chawla, S.; Lu, D.; Lobaugh, J.; Voth, G. A. *J. Chem. Phys.* **1997**, *107*, 7428.
(32) Rotzinger, F. P. *J. Phys. Chem. A* **1999**, *103*, 9345.
(33) Rotzinger, F. P.; Benoit, D. M. *Inorg. Chem.* **2000**, *39*, 944.
(34) Ciofini, I.; Adamo, C. *J. Phys. Chem. A* **2001**, *105*, 1086.
(35) Rotzinger, F. P. *J. Chem. Soc., Dalton Trans.* **2002**, 719.
(36) Langford, C. H.; Gray, H. B. *Ligand Substitution Dynamics*; Benjamin: New York, 1965.
(37) Toma, H. E.; Malin, J. M. *Inorg. Chem.* **1973**, *12*, 1039.
(38) Toma, H. E.; Malin, J. M. *Inorg. Chem.* **1974**, *13*, 1772.
(39) Reddy, K. B.; van Eldik, R. *Inorg. Chem.* **1991**, *30*, 596.
(40) Tobe, M. L. In *Advances in Inorganic and Bioinorganic Mechanisms*; Sykes, A. G., Ed; Academic Press: New York, 1983; Vol. 2, p 1.
(41) Jackson, W. G. *Inorg. React. Mech.* **2002**, *4*, 1.
(42) Rotzinger, F. P. *Inorg. Chem.* **1988**, *27*, 768.
(43) Rotzinger, F. P. *Inorg. Chem.* **1988**, *27*, 772.
(44) Rotzinger, F. P. *Inorg. Chem.* **1991**, *30*, 2763.
(45) Rotzinger, F. P.; Weber, J.; Daul, C. *Helv. Chim. Acta* **1991**, *74*, 1247.
(46) Comba, P. C.; Jackson, W. G.; Marty, W.; Stöeckli-Evans, H.; Zipper, L. *Helv. Chim. Acta* **1992**, *75*, 1130.
(47) Comba, P. C.; Jackson, W. G.; Marty, W.; Stöeckli-Evans, H.; Zipper, L. *Helv. Chim. Acta* **1992**, *75*, 1172.
(48) Merbach, A. E. *Pure Appl. Chem.* **1982**, *54*, 1479.
(49) Swaddle, T. W. *Coord. Chem. Rev.* **1974**, *14*, 217.
(50) Swaddle, T. W.; Mak, M. K. S. *Can. J. Chem.* **1983**, *61*, 473.
(51) Swaddle, T. W. *Adv. Inorg. Bioinorg. Mech.* **1983**, *2*, 95.
(52) Hugi, A. D.; Helm, L.; Merbach, A. E. *Inorg. Chem.* **1987**, *26*, 1763.
(53) Rotzinger, F. P. *J. Am. Chem. Soc.* **1996**, *118*, 6760.
(54) Rotzinger, F. P. *J. Am. Chem. Soc.* **1997**, *119*, 5230.
(55) Kowall, Th.; Caravan, P.; Bourgeois, H.; Helm, L.; Rotzinger, F. P.; Merbach, A. E. *J. Am. Chem. Soc.* **1998**, *120*, 6569.
(56) Ducommun, Y.; Merbach, A. E. In *Studies in Inorganic Chemistry 7: Inorganic High-Pressure Chemistry, Kinetics and Measurements*; van Eldik, R., Ed.; Elsevier: Amsterdam, 1986.
(57) Connolly, M. L. *Science* **1983**, *221*, 709.
(58) De Vito, D.; Weber, J.; Merbach, A. E. *Inorg. Chem.* **2004**, *43*, 858.
(59) Vallet, V.; Wahlgren, U.; Schimmelpfennig, B.; Szabó, Z.; Grenthe, I. *J. Am. Chem. Soc.* **2001**, *123*, 11999.
(60) Barone, V.; Cossi, M. *J. Phys. Chem. A* **1998**, *102*, 1995.
(61) Cossi, M.; Rega, N.; Scalmani, G.; Barone, V. *J. Comput. Chem.* **2003**, *24*, 669.
(62) Benmelouka, M.; Messaoudi, S.; Furet, E.; Gauthier, R.; Le Fur, E.; Pivan, J.-Y. *J. Phys. Chem. A* **2003**, *107*, 4122.
(63) Hartmann, M.; Clark, T.; van Eldik, R. *J. Am. Chem. Soc.* **1997**, *119*, 7843.
(64) Marx, D.; Sprik, M.; Parrinello, M. *Chem. Phys. Lett.* **1997**, *273*, 360.
(65) Carloni, P.; Sprik, M.; Andreoni, W. *J. Phys. Chem. B* **2000**, *104*, 823.
(66) Naor, M. M.; Nostrand, K. V.; Dellago C. *Chem. Phys. Lett.* **2003**, *369*, 159.
(67) Harris, D. J.; Brodholt, J. P.; Sherman, D. M. *J. Phys. Chem. B* **2003**, *107*, 9056.
(68) Armunanto, R.; Schwenk, C. F.; Rode, B. M. *J. Phys. Chem. A* **2003**, *107*, 3132.
(69) Ohtaki, H.; Radnai, T. *Chem. Rev.* **1993**, *93*, 1157.
(70) Carrillo-Tripp, M.; Saint-Martin, H.; Ortega-Blake, I. *J. Chem. Phys.* **2003**, *118*, 7062.
(71) Fulton, J. L.; Heald, S. M.; Badyal, Y. S.; Simonson, J. M. *J. Phys. Chem. A* **2003**, *107*, 4688.
(72) Bakó, I.; Hutter, J.; Pálinkás, G. *J. Chem. Phys.* **2002**, *117*, 9838.
(73) Dang, L. X.; Schenter, G. K.; Fulton, J. L. *J. Phys. Chem. B* **2003**, *107*, 14119.
(74) Smirnov, P.; Wakita, H.; Yamaguchi, T. *J. Phys. Chem. B* **1998**, *102*, 4802.
(75) Rudolph, W. W.; Pye, C. C. *J. Phys. Chem. A* **2000**, *104*, 1627.
(76) Tsushima, S.; Yang, T.; Mochizuki, Y.; Okamoto, Y. *Chem. Phys. Lett.* **2003**, *375*, 204.
(77) Pasquarello, A.; Petri, I.; Salmon, P. S.; Parisel, O.; Car, R.; Tóth, É.; Powell, D. H.; Fischer, H. E.; Helm, L.; Merbach, A. E. *Science* **2001**, *291*, 856.
(78) Persson, I.; Persson, P.; Sandström, M.; Ullström, A.-S. *J. Chem. Soc., Dalton Trans.* **2002**, 1256.
(79) Schwenk, C. F.; Rode, B. M. *ChemPhysChem* **2003**, *4*, 931.
(80) Schwenk, C. F.; Rode, B. M. *J. Chem. Phys.* **2003**, *119*, 9523.
(81) Blumberger, J.; Bernasconi, L.; Tavernelli, I.; Vuilleumier, R.; Sprik, M. *J. Am. Chem. Soc.* **2004**, *126*, 3928.
(82) Benfatto, M.; D'Angelo, P.; Della Longa, S.; Pavel, N. V. *Phys. Rev. B* **2002**, *65*, 174205.
(83) Hartmann, M.; Clark, T.; van Eldik, R. *J. Phys. Chem. A* **1999**, *103*, 9899.
(84) Rotzinger, F. P. *J. Phys. Chem. A* **2000**, *104*, 8787.
(85) De Vito, D.; Sidorenkova, H.; Rotzinger, F. P.; Weber, J.; Merbach, A. E. *Inorg. Chem.* **2000**, *39*, 5547.
(86) Armunanto, R.; Schwenk, C. F.; Hung, T. T.; Rode, B. M. *J. Am. Chem. Soc.* **2004**, *126*, 2582.
(87) Yang, T.; Tsushima, S.; Suzuki, A. *J. Solid State Chem.* **2003**, *171*, 235.
(88) Van Eldik, R.; Gaede, W.; Cohen, H.; Meyerstein, D. *Inorg. Chem.* **1992**, *31*, 3695.
(89) Slater, J. C. *Phys. Rev.* **1951**, *81*, 385.
(90) Vosko, S. H.; Wilk, L.; Nusair, M. *Can. J. Phys.* **1980**, *58*, 1200.
(91) Becke, A. D. *Phys. Rev. A* **1988**, *38*, 3098.
(92) Lee, C.; Yang, W.; Parr, R. G. *Phys. Rev. B* **1988**, *37*, 785.
(93) Miehlich, B.; Savin, A.; Stoll, H.; Preuss, H. *Chem. Phys. Lett.* **1989**, *157*, 200.
(94) Becke, A. D. *J. Chem. Phys.* **1993**, *98*, 5648.
(95) Stephens, P. J.; Devlin, F. J.; Chablowski, C. F.; Frisch, M. J. *J. Phys. Chem.* **1994**, *98*, 11623.
(96) Hertwig, R. H.; Koch, W. *Chem. Phys. Lett.* **1997**, *268*, 345.
(97) Becke, A. D. *J. Chem. Phys.* **1986**, *84*, 4524.
(98) Perdew, J. P. *Phys. Rev. B* **1986**, *33*, 8822; **1986**, *34*, 7406.
(99) Perdew, J. P.; Burke, K.; Ernzerhof, M. *Phys. Rev. Lett.* **1996**, *77*, 3865.
(100) Perdew, J. P.; Wang, Y. *Electronic Structure of Solids '91*; Akademie Verlag: Berlin, 1991; p 11.
(101) Åkesson, R.; Pettersson, L. G. M.; Sandström, M.; Wahlgren, U. *J. Am. Chem. Soc.* **1994**, *116*, 8705.
(102) Bockris, J. O'M.; Reddy, A. K. N. *Modern Electrochemistry*; Plenum: New York, 1970; Vol. 1, p 60.
(103) Deeth, R.; Elding, L. I. *Inorg. Chem.* **1996**, *35*, 5019.
(104) Born, M. *Z. Phys.* **1920**, *1*, 45.
(105) Stevens, W. J.; Krauss, M.; Basch, H.; Jasien, P. G. *Can. J. Chem.* **1992**, *70*, 612.
(106) Hehre, W. J.; Ditchfield, R.; Pople, J. A. *J. Chem. Phys.* **1972**, *56*, 2257.
(107) Ditchfield, R.; Hehre, W. J.; Pople, J. A. *J. Chem. Phys.* **1971**, *54*, 724.
(108) Krishnan, R.; Binkley, J. S.; Seeger, R.; Pople, J. A. *J. Chem. Phys.* **1980**, *72*, 650.
(109) Wachters, A. J. H. *J. Chem. Phys.* **1970**, *52*, 1033.
(110) Hay, P. J. *J. Chem. Phys.* **1977**, *66*, 4377.
(111) Schäfer, A.; Horn, H.; Ahlrichs, R. *J. Chem. Phys.* **1992**, *97*, 2571.

(112) Schäfer, A.; Huber, C.; Ahlrichs, R. *J. Chem. Phys.* **1994**, *100*, 5829.
(113) Weigend, F.; Furche, F.; Ahlrichs, R. *J. Chem. Phys.* **2003**, *119*, 12753.
(114) Rassolov, V. A.; Pople, J. A.; Ratner, M. A.; Windus, T. L. *J. Chem. Phys.* **1998**, *109*, 1223.
(115) Moll, H.; Denecke, M. A.; Jalilehvand, F.; Sandström, M.; Grenthe, I. *Inorg. Chem.* **1999**, *38*, 1795.
(116) These calculations were performed using the GAMESS[118] program and the SBKJ/6-31G(d) basis sets[105−107] for Ag/O,H (α_d(O) = 1.20[111]).
(117) At the HF level, all of the computed frequencies of $Ag(OH_2)_6^+$ are real, whereas, at the MP2 (and B3LYP) level, one frequency is imaginary. This indicates that, on the basis of MP2, the coordination number of Ag^+ (in the gas phase) is less than six.
(118) Schmidt, M. W.; Baldridge, K. K.; Boatz, J. A.; Elbert, S. T.; Gordon, M. S.; Jensen, J. H.; Koseki, S.; Matsunaga, N.; Nguyen, K. A.; Su, S. J.; Windus, T. L.; Dupuis, M.; Montgomery, J. A. *J. Comput. Chem.* **1993**, *14*, 1347.
(119) Swaddle, T. W.; Stranks, D. R. *J. Am. Chem. Soc.* **1972**, *94*, 8357.
(120) González, G.; Moullet, B.; Martinez, M.; Merbach, A. E. *Inorg. Chem.* **1994**, *33*, 2330.
(121) Doine, H.; Ishihara, K.; Krouse, H. R.; Swaddle, T. W. *Inorg. Chem.* **1987**, *26*, 3240.
(122) Rotzinger, F. P. *J. Phys. Chem. A* **2000**, *104*, 6439.
(123) Lundberg, M.; Blomberg, M. R. A.; Siegbahn, P. E. M. *Theor. Chem. Acc.* **2003**, *110*, 130.
(124) Alezra, V.; Bernardinelli, G.; Corminboeuf, C.; Frey, U.; Kündig, E. P.; Merbach, A. E.; Saudan, C. M.; Viton, F.; Weber, J. *J. Am. Chem. Soc.* **2004**, *126*, 4843.
(125) Farkas, I.; Bányai, I.; Szabó, Z.; Wahlgren, U.; Grenthe, I. *Inorg. Chem.* **2000**, *39*, 799.
(126) Vallet, V.; Privalov, T.; Wahlgren, U.; Grenthe, I. *J. Am. Chem. Soc.* **2004**, *126*, 7766.
(127) Vallet, V.; Wahlgren, U.; Szabó, Z.; Grenthe, I. *Inorg. Chem.* **2002**, *41*, 5626.
(128) Hay, P. J.; Martin, R. L.; Schreckenbach, G. *J. Phys. Chem. A* **2000**, *104*, 6259.
(129) Schwenk, C. F.; Rode, B. M. *ChemPhysChem* **2004**, *5*, 342.
(130) Armunanto, R.; Schwenk, C. F.; Randolf, B. R.; Rode, B. M. *Chem. Phys. Lett.* **2004**, *388*, 395.
(131) Maeda, M.; Maegava, Y.; Yamaguchi, T.; Ohtaki, H. *Bull. Chem. Soc. Jpn.* **1979**, *52*, 2545.
(132) Yamaguchi, T.; Wakita, H.; Nomura, M. *J. Chem. Soc., Chem. Commun.* **1988**, 433.
(133) Parris, M.; Wallace, W. J. *Can. J. Chem.* **1969**, *47*, 2257.
(134) Guastalla, G.; Swaddle, T. W. *Can. J. Chem.* **1973**, *51*, 821.
(135) Rotzinger, F. P. *Inorg. Chem.* **1999**, *38*, 5730.
(136) Chan, S. C. *J. Chem. Soc. A* **1967**, 291.
(137) Jones, W. E.; Carey, L. R.; Swaddle, T. W. *Can. J. Chem.* **1972**, *50*, 2739.
(138) Buckingham, D. A.; Clark, C. R.; Liddell, G. F. *Inorg. Chem.* **1992**, *31*, 2909.
(139) Burda, J. V.; Zeizinger, M.; Leszczynski, J. *J. Chem. Phys.* **2004**, *120*, 1253.
(140) Coe, J. S. *MTP Int. Rev. Sci.: Inorg. Chem., Ser. 2* **1974**, 45.
(141) Cooper, J.; Ziegler, T. *Inorg. Chem.* **2002**, *41*, 6614.
(142) Miller, S. E.; Gerard, K. J.; House, D. A. *Inorg. Chim. Acta* **1991**, *190*, 135.
(143) Kitamura, Y.; Ida, K. *Inorg. Chim. Acta* **1984**, *88*, 161.
(144) Zhang, Y.; Guo, Z.; You, X.-Z. *J. Am. Chem. Soc.* **2001**, *123*, 9378.
(145) Robertazzi, A.; Platts, J. A. *J. Comput. Chem.* **2004**, *25*, 1060.
(146) Coley, R. F.; Martin, D. S., Jr. *Inorg. Chim. Acta* **1973**, *7*, 573.
(147) Costa, L. A. S.; Rocha, W. R.; De Almeida, W. B.; Dos Santos, H. F. *J. Chem. Phys.* **2003**, *118*, 10584.
(148) Costa, L. A. S.; Rocha, W. R.; De Almeida, W. B.; Dos Santos, H. F. *Chem. Phys. Lett.* **2004**, *387*, 182.
(149) Szabó, Z.; Glaser, J.; Grenthe, I. *Inorg. Chem.* **1996**, *35*, 2036.
(150) Toraishi, T.; Privalov, T.; Schimmelpfennig, B.; Wahlgren, U.; Grenthe, I. *J. Phys. Chem. A* **2003**, *107*, 9456.
(151) Adamo, C.; Barone, V. *J. Chem. Phys.* **1998**, *108*, 664.
(152) Tobe, M. L.; Burgess, J. *Inorganic Reaction Mechanisms*; Longman: Essex, U.K., 1999.
(153) Fuoss, R. M. *J. Am. Chem. Soc.* **1958**, *80*, 5059.
(154) Mares, M.; Palmer, D. A.; Kelm, H. *Inorg. Chim. Acta* **1978**, *27*, 153.
(155) Jackson, W. G.; Lawrance, G. A.; Lay, P. A.; Sargeson, A. M. *Aust. J. Chem.* **1982**, *35*, 1561.
(156) Szabó, Z.; Grenthe, I. *Inorg. Chem.* **1998**, *37*, 6214.
(157) Vallet, V.; Moll, H.; Wahlgren, U.; Szabó, Z.; Grenthe, I. *Inorg. Chem.* **2003**, *42*, 1982.
(158) Tautermann, C. S.; Sabolović, J.; Voegele, A. F.; Liedl, K. R. *J. Phys. Chem. B* **2004**, *108*, 2098.
(159) Buckingham, D. A. *Coord. Chem. Rev.* **1994**, *135*/*136*, 587.
(160) Jackson, W. G.; Lawrance, G. A.; Lay, P. A.; Sargeson, A. M. *Inorg. Chem.* **1980**, *19*, 904.
(161) Curtiss, L. A.; Raghavachari, K.; Redfern, P. C.; Rassolov, V.; Pople, J. A. *J. Chem. Phys.* **1998**, *109*, 7764.
(162) *Quantum-Mechanical Prediction of Thermochemical Data*; Cioslowski, J., Ed.; Understanding Chemical Reactivity Series Vol. 22; Kluwer: Dordrecht, 2001.
(163) Vanquickenborne, L. G.; Pierloot, K. *Inorg. Chem.* **1981**, *20*, 3673.
(164) Vanquickenborne, L. G.; Pierloot, K. *Inorg. Chem.* **1984**, *23*, 1471.
(165) Vanquickenborne, L. G.; Ceulemans, A. *J. Am. Chem. Soc.* **1978**, *100*, 475.
(166) Tsutsui, Y.; Wasada, H.; Funahashi, S. *THEOCHEM* **1999**, *461*−*462*, 379.
(167) Taube, H. *Inorganic Reaction Mechanisms*; Nelson: London, 1972.
(168) Swaddle, T. W.; Merbach, A. E. *Inorg. Chem.* **1981**, *20*, 4212.
(169) Grant, M.; Jordan, R. B. *Inorg. Chem.* **1981**, *20*, 55.
(170) The MOs were plotted using the MOLEKEL progam: Flükiger, P.; Lüthi, H. P.; Portmann, S.; Weber, J. *MOLEKEL 4.0*; Swiss Center for Scientific Computing: Manno (Switzerland), 2000.
(171) These transition states would have, in addition to the elongated bonds of the exchanging ligands, the bond of the ligand trans to the exchanging ligands elongated as well. It was not possible to optimize the geometry of such transition states because, after the removal of the constraints, again the square pyramidal pentacoordinated intermediate with two H_2O molecules in the second coordination sphere was obtained (Figure 6).
(172) Hammond, G. S. *J. Am. Chem. Soc.* **1955**, *77*, 334.
(173) De Vito, D.; Rotzinger, F. P.; Merbach, A. E. Unpublished results.

CR030715V